Spring 2021

In vitro and in vivo response to a novel borophosphate bioactive glass

Nada Abokefa

Department:

IN VITRO AND IN VIVO RESPONSE TO A NOVEL BOROPHOSPHATE BIOACTIVE GLASS

by

NADA AMIN MOHAMED ABDELRAHAMAN ABOKEFA

A THESIS

Presented to the Graduate Faculty of the

MISSOURI UNIVERSITY OF SCIENCE AND TECHNOLOGY

In Partial Fulfillment of the Requirements for the Degree

MASTER OF SCIENCE IN APPLIED AND ENVIRONMENTAL BIOLOGY

2021

Approved by:

Julie Semon, Advisor
Yue-Wern Huang
Katie Shannon

PUBLICATION THESIS OPTION

This thesis consists of the following two articles, which will be submitted for publication as follows and have been formatted in the style used by the Missouri University of Science and Technology:

Paper I, found on pages 20–49, is intended for submission to the Journal of Tissue Engineering and Regenerative Medicine, under the title "Adipose Stem Cell Response to Borophosphate Bioactive Glass".

Paper II, found on pages 50–78, is intended for submission to the Journal of Biomedical Materials Research – Part A under the title of "The Angiogenic Potential of pH Neutral Borophosphate Bioactive Glasses".

ABSTRACT

Bioactive glasses have been widely used in several biomedical and tissue engineering applications since the late 1960s. Numerous families of bioactive glasses have emerged over the years, with each having its own advantage and disadvantage. One concern common to all families is that most bioactive glasses create a basic or acidic environment when degraded and, therefore, are toxic for cells. Recently, there has been an increased interest in borophosphate bioactive glass (BPBGs) because of their neutral pH, release of therapeutic ions, and biodegradable properties. Despite the growing interest, there is little reported on the bioactivity of BPBGs. The biological effects of a novel series of BPBG were investigated in these studies. BPBGs were tested on human adipose stem cells (ASCs) and endothelial cells (ECs) and evaluated for viability, differentiation, migration, secretome activity, and angiogenesis. The results showed that some of the BPBG compositions created a neutral pH environment and thus, showed a high level of cell viability in direct contact under normal static conditions *in vitro*. Moreover, some of the BPBG compositions increased angiogenesis and altered the ASCs secretome. These results indicate that each of the BPBG compositions have a specific therapeutic pattern with a significant potential in the clinical and biomedical applications.

ACKNOWLEDGMENTS

First and foremost, I praise God for giving me this opportunity and the capability to proceed successfully. I would like to express my sincere and deepest gratitude to my advisor, Dr. Julie Semon, for her help, guidance, understanding, and support throughout this research project. She always pushed me to think critically and scientifically and to be a true scientist. She played a tremendously influential role in helping me pursuing my master's degree and to earn it successfully.

I would also like to expand my thanks to my committee members: Prof. Yue-Wern Huang and Dr. Katie Shannon. I appreciate them being on my committee, their valuable time, and for always being so friendly to me during this period. Thanks to my fellow graduate student, Bradley Bromet and all the undergrads for their help and cooperation. I would also like to thank our collaborator, Prof. Richard Brow and his graduate student Rebekah Blatt for providing us with the bioactive glass throughout this study. Additionally, I would like to thank Dr. Terry Wilson and Dr. David Westenberg, for being amazing and insightful GTA advisors, I loved being around them.

Finally, and most importantly, I would like to express my deepest gratitude to my husband, my parents, and my brothers. I could not have survived the duration of this study without their unconditional love, support, and prayers. I am very much grateful and thankful to my husband, Yasser Darwish, for encouraging me to pursue a master's degree in the first place and for always being supportive and encouraging. He was always by my side during my hard and dark days. I am sure that without his love, sacrifices and support, I could not have earned this degree. I cannot ask for a better husband and family.

TABLE OF CONTENTS

SECTION

LIST OF ILLUSTRATIONS

SECTION Page

LIST OF TABLES

NOMENCLATURE

ASCs	Adipose stem cells
B	Boron
BG	Bioactive Glass
BP	Borophosphate
B3	13-93B3
BBG	Borate Bioactive Glass
BPBG	Borophosphate Bioactive Glass
CAM	Chick chorioallantoic membrane
Co	Cobalt
Cu	Copper
CCM	Complete Culture Media
DP	Dissolution product
EC	Endothelial cells
EM	Endothelial medium
ECM	Extracellular matrix
HUVEC	Human umbilical vein endothelial cell
HUMVEC-d	Human dermal microvascular endothelial cells
HA	Hydroxyapatite
PBS	Phosphate Buffer Saline
PBG	Phosphat Bioactive Glass
SBG	Silicate Bioactive Glass
SBF	Simulated Body Fluid
VEGF	Vascular endothelial growth factor
Zn	Zinc

1. INTRODUCTION

1.1. BACKGROUND

In this section, a brief introduction to the main topics of the thesis is described.

1.1.1. Bioactive Glasses. Bioactive glasses (BGs) are a special type of oxide-based ceramics[1]. They can be fabricated by either sol-gel or melting routes to form different shapes and sizes such as powders, fibers, and scaffolds[2].

1.1.1.1. Silicate bioactive glass (Bioglass®). One specific composition of silicate bioactive glass (SBG), known as 45S5 in literature and Bioglass® on the market, is composed of four different oxides (45.0% SiO_2−24.5% Na_2O−24.5% CaO−6.0% P_2O_5). It was the first BG and invented by the pioneer Larry Hench in 1969 when his team discovered the glass bonded to soft and hard tissues after six weeks of implantation in rat femoral bones [3]. The phenomenon of glass bonding to tissues and forming hydroxyapatite on the surface of bone is known as biocompatibility. Before the invention of this novel Bioglass®, all implant materials such as metals and polymers, triggered an immune reaction and encapsulation after implantation rather than forming a stable bond with tissues. Bioglass®, on the other hand, proved to be biocompatible by stimulating a beneficial response in the body, causing tissue regeneration over time [3,4].

Since Bioglass® was invented, several types of BGs have emerged over the years, including borate-based and phosphate-based glasses. In addition to creating different compositions, researchers continue to modify the base compositions by doping them with ions of interest [5].

1.1.1.2. Borate bioactive glass (Miragen). Borate-based glasses (BBG) are another main class of BGs in which silica is replaced with boron. When compared to silicate BGs, BBGs had a faster degradation rate, more hydroxyapatite formation, and a quicker release of ions [6]. Over the years, a wide range of BBGs have emerged [6,8–10]. One BBG composition, known as 13-93B3 in literature and commercially as Mirragen, has contributed to the healing of chronic wounds in the clinic [11]. However, BBGs release boron, increasing the pH to toxic levels in static cell culture conditions [12,13]. To overcome this limitation, Hohenbild et al. pre-reacted the glass in cell culture media, which controlled the pH environment [14]. However, the specific time period and methodology of pre-reacting glass is still unclear. Furthermore, pre-reacting glass is far from ideal in both the clinic and in the laboratory setting. Consequently, there has been a need and interest in creating a BG that provides a neutral pH. One method to do this is by changing the concentrations of boron and phosphate ions [12].

1.1.1.3. Phosphate bioactive glass. Phosphate based glasses (PBG) are another family of BGs but have the silica substituted with phosphate [15,16]. PBGs can control the pH while they are degrading, and they have also been shown to promote angiogenesis [17]. However, the preparation of PBG is challenging due to very high temperature requirements and their tendency to crystallize after thermal treatment [18].

1.1.1.4. Borophosphate bioactive glass. Borophosphate Bioactive Glasses (BPBGs) have emerged recently to provide the beneficial properties of both BBGs and PBGs [19,20]. Figure 1.1 demonstrates the popularity of the BPBGs compared to the other common BG classes obtained from the published data on google scholar over the last ten years. However, there is little reported on the bioactivity of BPBGs. Accordingly, this

thesis evaluated the biological abilities of a novel BPBG series both in vitro and in vivo. A combination of cells was used in these studies: adipose stem cells (ASCs) were used because of their known regenerative capacity, and endothelial cells (ECs) were used to evaluate angiogenesis, rate limiting step in most tissue engineering applications [21]. Angiogenesis was further investigated in vivo using a chick chorioallantoic membrane (CAM) assay.

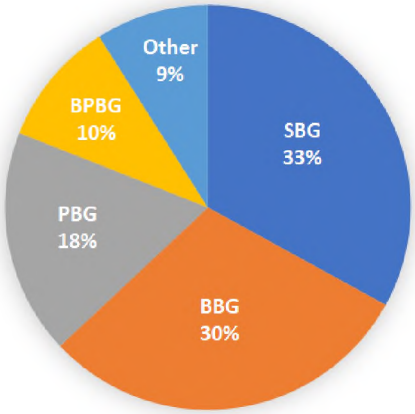

Figure 1.1. Represents the most common classes of BGs in the literature obtained from the published data on google scholar over the last ten years. Silicate bioactive glasses (SBGs) showed the highest popularity among the other types of glasses. The chart represents the need to further investigate the BPBGs.

1.1.2. Adipose Stem Cells. ASCs have been used widely in cell therapy and tissue engineering applications because of their ability to differentiate into multiple cell lineages, as well as their immunomodulatory, angiogenic, migratory, and anti-inflammatory effects both in vitro and in vivo [21,23–26]. Additionally, the exosome and secretome of ASCs are of increasing interest due to their wide-ranging contribution to most tissue regeneration processes, including angiogenesis, extracellular matrix (ECM)

remodeling, and immune cell regulation [27–30]. ASCs are greatly affected by their surrounding environmental "niche" and may change phenotype when exposed to a new biomaterial [31].

1.1.3. Endothelial Cells (ECs). The vascular system is a complex network of blood vessels such as arteries, capillaries, and veins. ECs play an essential role in the development and remodeling of vasculature by proliferating and migrating from pre-existing vasculature in a process called angiogenesis [32]. Achieving vascularization is a major challenge and a rate limiting step in most tissue engineering applications [33]. A number of growth factors and proteins secreted by the ASCs, including vascular endothelial growth factor (VEGF), basic fibroblast growth factor (bFGF), and various members of the transforming growth factor beta (TGFβ) family, are each involved in the angiogenesis process and affects the migration of the endothelial cells. Recently, studies done in vitro and in vivo have shown that BGs stimulate angiogenesis and vascularization, making these cells important to study with our novel BPBG composition[34].

1.2. OBJECTIVES

The objective of the proposed research is to evaluate the bioactivity of a novel borophosphate bioactive glass both *in vitro* and *in vivo*. These BPBGs were designed with a series of boron to phosphate ratios in order to evaluate (1) their dissolution rates; (2) ions released into the solution; (3) their effect on the solution pH; (4) their cytotoxic effects on different types of cells; (5) their effect on cell function, including proliferation, migration, differentiation, and protein expression; and (6) their toxicity *in vivo*.

The following scope of work accomplished these goals:

- Paper I "Adipose Stem Cell Response to Novel Borophosphate Bioactive Glass" demonstrated that each glass composition could influence ASCs in a unique pattern *in vitro* and achieved goals 2-6 listed above.
- Paper II "The Angiogenic Potential of pH Neutral Borophosphate Bioactive Glasses" demonstrated that BPBG had distinct effects on ECs from different sources *in vitro* and was angiogenic both *in vitro* and *in vivo*. This achieved goals 1-4 and 6 listed above.

PAPER

I. ADIPOSE STEM CELL RESPONSE TO BOROPHOSPHATE BIOACTIVE GLASS

Nada Abokefa[1], Bradley Bromet[1], Makenna Pickett[1], Brianna Bentley[1], Emma Nicks[1], Rebekah Blatt[2], Richard Brow[2] and Julie Semon[1].

[1] Deparment of Biological Sciences, Missouri University of Science and Technology, Rolla, MO 65409

[2] Department of Materials Engineering, Missouri University of Science and Technology, Rolla, MO 65409

ABSTRACT

It has been reported previously that silicate and borate bioactive glasses create alkaline solutions by significantly increasing the pH due to the rapid release of the ions when degrade. This alkaline solution affected the cell viability at certain levels. Consequently, adding phosphate ions to the glass composition proved to control the degradation rate of bioactive glasses and create a neutral pH environment. Accordingly, in this study, we evaluated the effect of a series of novel borophosphate bioactive glass (BPBGs) compositions *in vitro*. BPBGs compositions varied based on the borate-to-phosphate ratios. A borate-free, borate-rich and intermediate borate-phosphate glasses were used in this study. Adipose stem cells (ASCs) were used for their known therapeutic uses in various biomedical applications. BPBGs were investigated for their effect on the solution pH, ions released when degraded, ASCs viability, migration, angiogenesis, differentiation, and protein secretions. The intermediate borate-to-phosphate BPBGs

created a physiologically neutral pH in direct contact and in complete culture media after 24 hours. The slightly alkaline borate-free BPBG with the concentration 2.5 mg/ml maintained the highest cell viability in direct contact for 72 hours and promoted the ASCs migration in a 5-hour transwell migration assay. On the other hand, the highly alkaline borate-rich BPBGs showed to be more angiogenic than any of the compositions tested by increasing the secretions of VEGF, TGF β1 and bFGF. Additionally, BPBGs altered the ASCs secretome which were presented in a detailed cytokine array comparison.

1. INTRODUCTION

Bioactive glasses (BGs) are a class of oxide-based ceramics first invented by Larry Hench in the late 1960s [1]. BGs have gained increased interest due to their bioactivity, biocompatibility, ability to bond to hard and soft tissues, and potential to stimulate tissue regeneration [2–5]. They have a versatile nature to be manufactured into different shapes and sizes such as powders, fibers and scaffolds [6,7]. Consequently, several BG families have emerged with different compositions, one of which is borate BGs (BBGs). When compared to the traditional silicate BG, BBGs showed lower chemical durability which increased their degradation rate [8–10], enhanced cell proliferation and differentiation *in vitro* [11] as well as tissue infiltration *in vivo* [12]. Remarkably, BBGs have shown to help in healing chronic wounds and stimulating angiogenesis and vascularization [13–16]. However, BBGs quickly release borate ions creating a basic pH environment [17,18]. This increase in pH has been shown to be toxic to cells under static conditions *in vitro* [15,19]. A recent study conducted by Hohenbild et al. demonstrated that

preconditioning the BGs with cell culture medium will prevent the cytotoxic effects of the BG [20]. However, preconditioning is still unclear in terms of how different pretreating periods can affect the cell viability and characteristics. Hence, prolonged preconditioning times are not ideal in the clinical or in laboratory settings. Another way to control the local pH of BBG is to add phosphate to the glass composition [7,17,21]. A previous study showed that increasing the phosphate content in the BBG can balance the basic borate ions and reduce the local pH without the need of pretreating the glass prior to use [22].

In this respect, a series of borophosphate bioactive glasses (BPBG) were investigated in this study. To evaluate the therapeutic potential of the proposed BPBGs, we tested their effects on adipose stem cells (ASCs). ASCs are therapeutic cells with increased clinical interests due to their ease of attainability, differentiation capacity, immunomodulatory effects and angiogenic abilities. Currently, it is believed that the therapeutic effect of ASCs largely results from their secretome, proteins secreted into the extracellular space [23–28]. Therefore, we also evaluated these novel BPBGs on the secretome of ASCs.

2. MATERIALS AND METHODS

2.1. GLASS PREPARATION

Glasses of the compositional space $16Na_2O$-$24CaO$-XB_2O_3-$(60-X)P_2O_5$ (mol %) system are listed in Table 1. Batch materials were calcined at 300°C for at least 4 hours, and then melted in platinum crucibles from 1000-1150°C, depending on composition. Melts were quenched in graphite molds after one hour and were stirred on the half hour

during melting with a platinum stir rod. Samples were annealed at 350°C for one hour then allowed to cool to room temperature. Glasses were confirmed to be fully amorphous by x-ray diffraction (XRD), using a PANalytical X'Pert Multipurpose diffractometer utilizing a Cu K-α source and a PIXcel Detector. Glasses were broken into 75-150 um particles and stored in a vacuum desiccator until use.

Table 1. Compositions of the BP-BGs used in this study presented in mol percent (wt%).

Glass Designation	Na_2O	CaO	B_2O_3	P_2O_5
X0	16	24	-	60
X40	16	24	40	20
X60	16	24	60	-

2.2. CELL CULTURE

2.2.1. Adipose Stem Cells. ASCs were prepared by thawing frozen vials of approximately 1x106 cells (Obatala Sciences, LLC, New Orleans, LA) into 150 cm2 culture plates (Nunc, Rochester, NY) in 20 ml complete culture media (CCM) consisting of alpha minimum essential media (α-MEM; Sigma; St. Louis, MO), 10% fetal bovine serum (FBS; VWR, Dixon, CA), 1% 100x L-glutamine (Sigma), and 1% 100x antibiotic/antimycotic (Sigma). After 24 hours incubation at 37°C humidified 5% CO2 incubator, media was removed and the adherent, viable cells were washed twice with phosphate buffer solution (PBS; Sigma) and harvested using 0.25% trypsin/1 mM Ethylenediaminetetraacetic acid (EDTA; Sigma). ASCs then were plated at 100 cells/cm2 in CCM. The media was changed every 3–4 days and sub-confluent cells

(≤70% confluent) from three separate donors between passages 2-6 were used for all experiments.

2.2.2. Dermal Microvascular Endothelial Cells. Human dermal microvascular endothelial cells (HMVECs-d, pooled donors) were obtained from Lonza (Walkersville, MA). HMVECs were grown under normal conditions in Endothelial Cell Basal Medium-2 (Lonza). Media was changed every 3-4 days.

2.3. GLASS CHARACTERIZATION

ASCs were cultured at 37°C humidified 5% CO2 incubator until 100% confluent. Approximately 2.5 mg/ml of X0, X40 and X60 glass were dissolved in CCM and added to the cells and incubated under normal static conditions for 5 hours or 24 hours. Media was collected and the pH and ions released from each glass composition were measured. The pH was measured using a pH meter (Sper Scientific, Scottsdale, AZ) at 3 time points (0 time, 5 hours and 24 hours) and was done in triplicates. The ions release rates were measured using Inductively Coupled Plasma – Optical Emission Spectroscopy (ICP-OES) on an Avio 200 Spectrometer (PerkinElmer; Waltham, MA, USA). Media were obtained at 5 hours or 24 hours were diluted using 1% HNO3 to obtain solutions with ion concentrations in the 1-20 ppm range. CCM with no glass was used as a control. Samples were run in triplicate and averages are reported.

2.4. CELL VIABILITY

ASCs were plated in 8-chambered slides (LabTek; ThermoFisher; Rochester, NY) and grown till 70% confluence under normal static conditions. Approximately 2.5 mg/mL

of X0, X40 or X60 glass dissolved in CCM was added to the cells for 24 or 72 hours. After incubation at 37°C humidified 5% CO_2, chambers were gently washed 3-4 times in pre-warmed PBS and stained with live/dead stain (Fisher Scientific, Pittsburg, PA). Micrographs were taken with 10x objective on a Nikon A1R-HD/Ti2 E inverted confocal microscope (Melville, NY) and quantified by Fiji software (Madison, Wisconsin).

2.5. DIFFERENTIATION

ASCs were cultured in 6 well culture plates at 37°C humidified 5% CO_2 incubator until 100% confluent in CCM. A solution of 2.5 mg/ml X0, X40 or X60 glass dissolved in CCM was added to the wells and incubated for 24 hours under static conditions. Media was aspirated, wells were gently washed twice with PBS, and differentiation media was added. Adipogenic induction media (Lonza; Walkersville, MD) consisted of 1 mM Dexamethasone, 0.5 mM methyl-isobutylxanthine, 10 mg/mL insulin, 100 mM indomethacin, and 10% FBS in DMEM (4.5 g/ L glucose). Osteogenic induction media (Lonza) consisted of 50 mM ascorbate-2-phosphate, 10 mM b-glycerolphosphate, and 10^{28}M dexamethasone. Media was changed every 3-4 days for 14 days. Cells were washed gently with PBS and fixed in 10% formalin for 1 hour at room temperature. Cells were stained with 0.5% Oil Red O to visualize fat droplets or with 40 mM Alizarin Red (pH 4.1) to measure calcium deposition. Differentiation was imaged with an inverted microscope (Leica DMi1; Heerbrugg, Switzerland). Data was quantified by Fiji software (Madison, Wisconsin).

2.6. MIGRATION

Cell migration assays were performed in a 96-well transwell with 8μm pore membrane inserts (BD Biosciences, Bedford, MA). To evaluate if ASCs were attracted to BPBG, 5.0 x 10^4 ASCs were suspended in serum-free (SF) media and were added to the top of the transwell inserts. Approximately 2.5 mg/ml X0, X40 or X60 glass were suspended in CCM and were added to the bottom of the transwells. After 5 hours of incubation at 37°C, 5% CO2, the transwell insert was removed and gently placed into trypsin/EDTA (Figure 1A). Cells that had migrated to the bottom of the insert were stained with CyQuant and quantified using a fluorescent microplate reader (Fluostar Omega; BMG Labtech, Cary, NC). Each experiment was performed in triplicate with a minimum of three separate ASC donors.

In order to evaluate if BPBG could increase the angiogenic ability of ASCs, ASCs were treated with 2.5 mg/ml of X0, X40, or X60 glass in CCM for 24 hours. Media was then collected, filtered to remove any remaining glass, and placed in the lower chamber of a transwell. Around 2x10^4 HMVEC-d were added to the top of the inserts and incubated for 5 hours. HMVEC-d that migrated to the bottom of the inserts were stained with CyQuant and read on a plate reader (Figure 1B). Each experiment was performed in triplicate.

2.7. CYTOKINE ARRAY

Subconfluent ASCs were incubated with 2.5 mg/ml of X0, X40, X60, or CCM. After 24 hours of incubation, 200 μl of conditioned media was collected, filtered to remove any remanning glass, and analyzed using the Human Cytokine Quantibody Array

4000 which utilizes a multiplex enzyme-linked immunosorbent assay (ELISA) (RayBiotech, Norcross, GA) following the manufacturer's instructions. This array detected and processed 200 human cytokines. The assessments of the 200 proteins were done by the RayBiotech® Analysis Tool and was used for protein classification. This data was used to examine the differences in the secretion profiles among all the groups tested and the control. Cytokine concentrations data was sorted on Microsoft Excel spreadsheets based on the concentration hierarchy. Proteins that were significant from the control ($p \leq 0.5$) was further evaluated and any proteins that had a negligible expression or unsignificant among all groups were excluded from the comparison. A log base 2 of the ratio of the significant protein concentrations datasets compared to the control was calculated and used in designing the hierarchal clustered heatmaps. These experiments were performed in duplicates on pooled conditioned media from 3 ASC donors.

2.8. STATISTICS

All values are presented as means±standard deviation (SD). The statistical differences among two or more groups were determined by ANOVA, followed by post-hoc Tukey versus the control groups.

(A) ASCs migration

(B) ECs migration

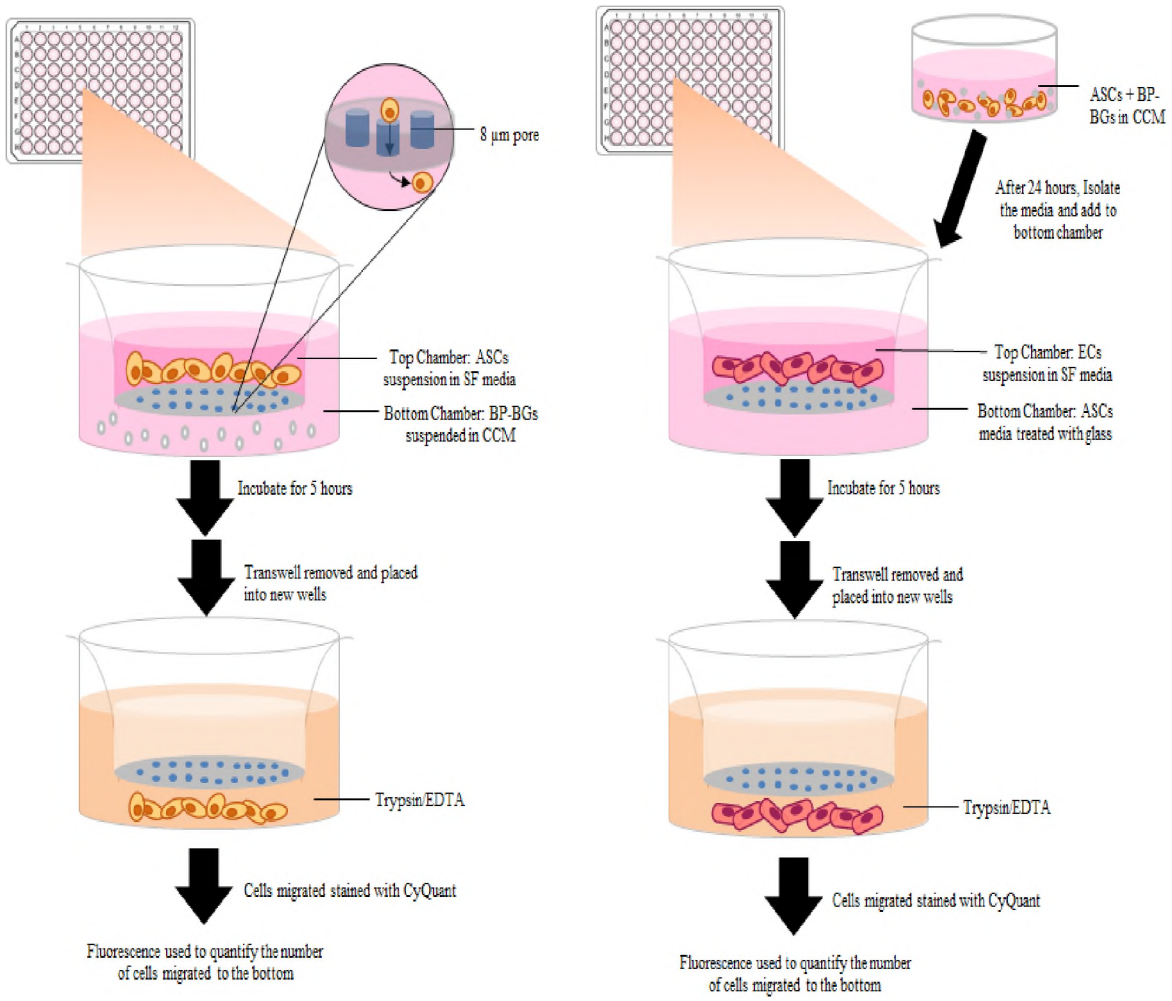

Figure 1. Schematic of the experimental setup for migration assays. (A) ASCs suspended in serum-free media were added to the top of 8mm transwell inserts. Glass solutions at 2.5 mg/ml were added to the bottom of the transwells. After 5 hours, cells that had migrated to the bottom were measured by CyQuant. (B) ASCs were grown under standard conditions until 70% confluent. Glass was added to ASCs at 2.5 mg/ml for 24 hours. The glass-treated conditioned media was then added to the bottom of a transwell. ECs were added to the top of 8mm transwell inserts and incubated for 5 hours. ECs that migrated to the bottom of the inserts were measured by CyQuant.

3. RESULTS

3.1. GLASS PROPERTIES

Borophosphate glasses have shown to dissolve congruently which impacted the pH of the solution. Table 2 demonstrates the pH measurements and the Ions released into the solution at different time points. The phosphate rich X0 glass created a physiologically neutral pH of 7.36 at 5 hours and increased to pH 7.5 creating a slightly alkaline environment after 24 hours. On the other hand, borate rich X60 glass increased the alkalinity to pH 7.78 while the intermediate boron to phosphate X40 glass retained a physiologically pH neutral environment when tested in CCM after 24 hours. Alongside the pH changes, the ions released from each glass composition vary dependently on the boron to phosphate ratios of the glass. At 5 hours, X0 glass showed the lowest release of all ions tested (Ca, and P) while X60 showed the highest among all of those. It is interesting to note that at 24 hours, X0 glass released more ions (Ca, B and P) than X40, which shows the faster degradation of X0 than X40 glass. Furthermore, X40 showed a higher rate of B release while slow-release rate of Ca and P ions between the 5 hours and 24 hours time points. It was observed that the slow release of Ca and P in the X40 glass might be due to the formation of a brushite reaction layer as more glass dissolved, leaving behind a fully reacted particle and a solid precipitate.

3.2. HIGH CONCENTRATION OF BPBGS REDUCED ASCS VIABILITY AT 72 HOURS

According to ISO norm, a decrease in cell viability by 30% indicates a biomaterial is toxic and not biocompatible [29]. To evaluate the cytotoxicity effect of

BPBGs on ASCs, a low and high concentrations (2.5 and 10 mg/ml, respectively) of three glass compositions were directly added to ASCs under normal static conditions (Figure 2). At 24 hours, both the low and high concentration of X0 showed the lowest viability of any of the glass compositions. However, all glass compositions and concentrations were considered viable cultures, per ISO norm. By 72 hours, ASCs treated with a low concentration of X0 maintained its viability while all other glass compositions and concentrations decreased. Additionally, the high concentration of X0 produced a toxic environment to ASCs at 72 hours.

Table 2. Measurements of pH and ions released into cell culture for each BPBG composition. Data presented as Mean±SD. ND represents non-determined values.

			Ions Released (ppm)		
Sample	**Time**	**pH**	**P**	**B**	**Ca**
CCM	5 hours	7.4	34.80 ± 1.45	ND	65.82 ± 2.68
	24 hours	7.84	36.65 ± 0.88	ND	68.41 ± 1.07
X0	5 hours	7.36	72.04 ± 0.47	ND	68.84 ± 2.67
	24 hours	7.57	197.03 ± 5.91	ND	101.28 ± 1.64
X40	5 hours	7.33	121.06 ± 3.61	126.10 ± 1.46	82.36 ± 1.37
	24 hours	7.47	176.01 ± 4.24	217.40 ± 1.06	73.26 ± 1.11
X60	5 hours	7.78	23.27 ± 0.30	249.43 ± 8.00	173.16 ± 3.79
	24 hours	7.75	24.96 ± 0.18	301.26 ± 6.03	201.43 ± 5.03

(A)

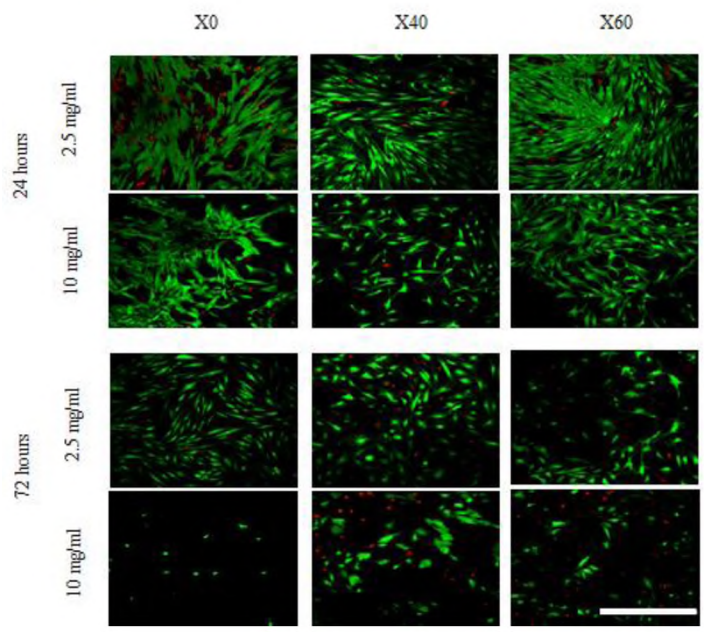

(B)

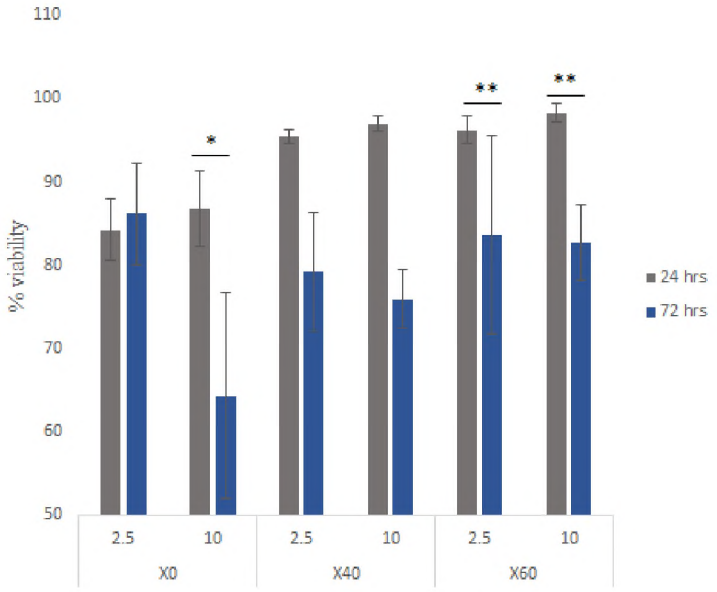

Figure 2. A high concentration of BPBGs reduced ASCs viability at 72 hours under static conditions. Subconfluent ASCs were treated with low or high concentrations of BPBG. (A) Live/dead stain showed ASC viability at 24 and 72 hours. Scale = 500 µm. (B) Viability was quantified with three donors examined in triplicate. Error bars indicate SD (n=9); *$p \leq 0.01$, and ** $p<0.5$

3.3. BPBGS AFFECTS THE ASCS DIFFERENTIATION

ASCs were tested for their differentiation ability with a low concentration of BPBG (Figure 3). Interestingly, Oil Red O staining reveled that basic X60 glass inhibited the adipogenic differentiation of ASCs. On the other hand, X0 glass inhibited the osteogenic differentiation of ASCs. Furthermore, the pH neutral X40 glass did not change the differentiation ability of the ASCs.

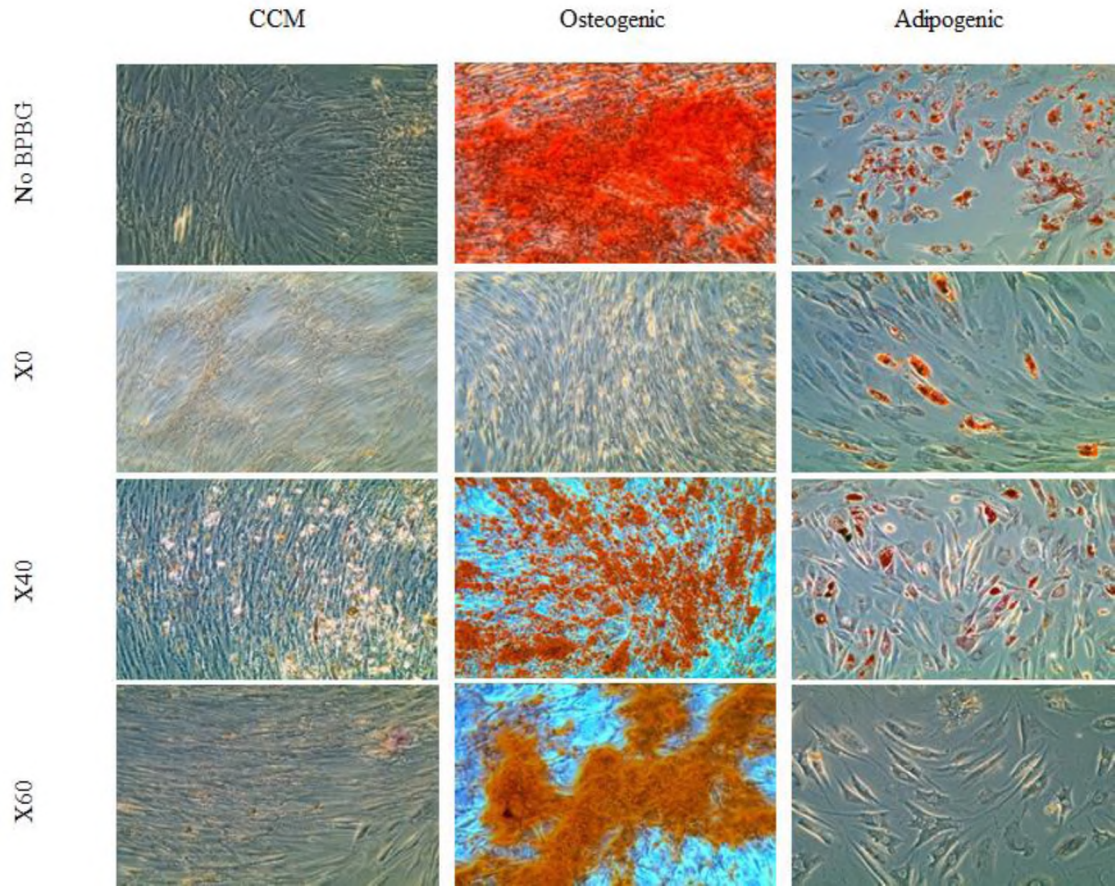

Figure 3. BPBGs influence ASC differentiation. ASCs were induced to differentiate in the absence or presence of BPBG. Representative micrographs of 3 ASC donors are shown. X0 inhibited osteogenic differentiation while X60 inhibited adipogenic differentiation.

3.4. pH-NEUTRAL BPBGS ATTRACT ASCS WHILE ASCS TREATED WITH BASIC BPBGS ATTRACT ECS

ASCs have an inherent ability to migrate into sites of injuries to help in healing and maintaining hemostasis [30]. Furthermore, they also release angiogenic factors that stimulate the vascularization and formation of new blood vessels [26]. Hereby, to test whether the different compositions of BPBGs affected the migration of ASCs, a 5-hour transwell migration assay was used (Figure 1A). X0, which has a neutral pH, increased ASC migration, while X60 with a basic pH had no statistical effect (Figure 4A). As ASCs are not alone *in vivo*, we wanted to determine if priming ASCs with BPBG affected their ability to attract ECs, a step required for angiogenesis. Sub-confluent ASCs were treated with BPBG for 24 hours. The resulting conditioned media was used as an attractant for EC migration (Figure 1B). Interestingly, only X60 significantly increased the ASCs' ability to attract ECs (Figure 4B).

3.5. BPBG ALTERS ASC SECRETOME

To determine if X0, X40 and X60 glasses influenced the ASCs secretory profile, a quantitative sandwich-based ELISA array was performed. Markers tested included 200 cytokines, growth factors, proteases, soluble receptors, and other proteins. After conditioning ASCs with a low concentration of BPBG for 24 hours, the conditioned media was examined for 200 secreted proteins. Of those, 183 proteins were detectable in sufficient expression levels, with only 154 differentially expressed proteins in BPBG treatment groups ($P \leq 0.5$). The BPBG conditioned media from 3 separate ASC donors were compared to those same donors grown under normal conditions, using the RayBiotech® analysis tool and heatmap clustering. There were 55 proteins that were

differentially secreted, regardless of the glass treatment: 5 proteins that were not secreted in ASCs grown under standard conditions but were secreted in all three BPBG treatments (Figure 5A), an additional 26 proteins increased their expression with all three glass treatments (Figure 5C), 20 proteins decreased with all three glass treatments (Figure 5D), and the secretion of 4 proteins were completely hampered (Figure 5B), regardless of glass treatment.

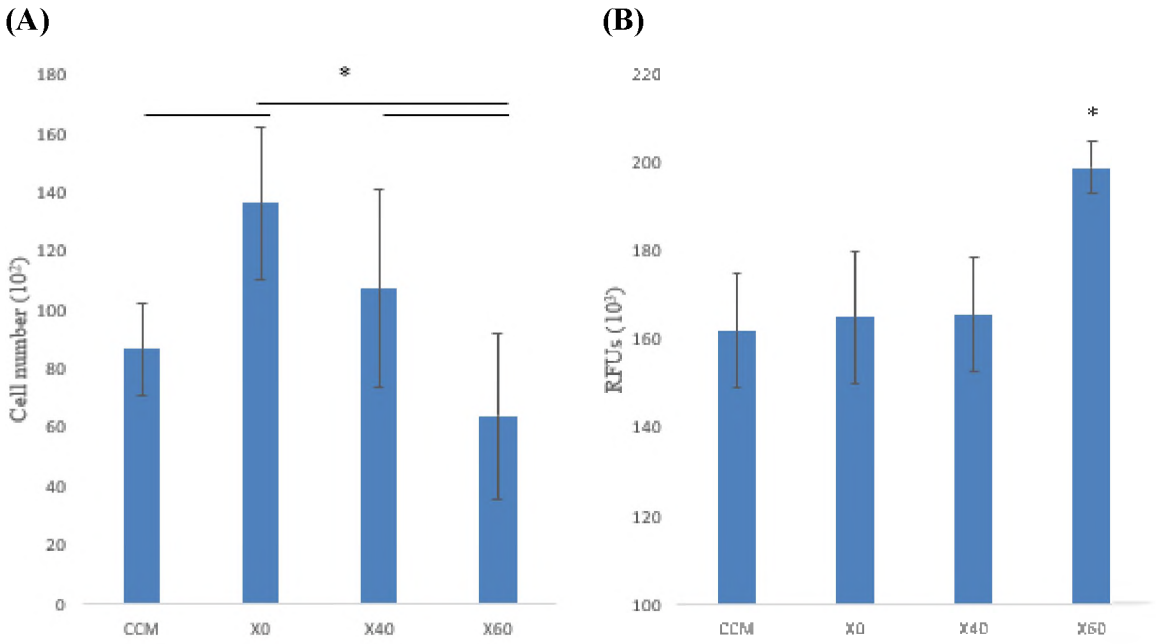

Figure 4. BPBGs affect cell migration. (A) Migration was examined by a transwell assay. ASCs were loaded onto the top inserts, while 2.5 mg/ml of glass solutions were added to the bottom. After 5 hours incubation, migrated cells were measured by CyQuant. X0 increased ASC migration. (B) ASCs were treated with glass for 24 hours under standard conditions. The resulting conditioned media was put in the bottom of a transwell with ECs added to the top. After 5 hours of incubation, migrated cells were measured by CyQuant. In both assays, three ASC donors were examined in triplicate. Error bars indicated SD (n=9); *p-value ≤0.05.

(A) Proteins promoted

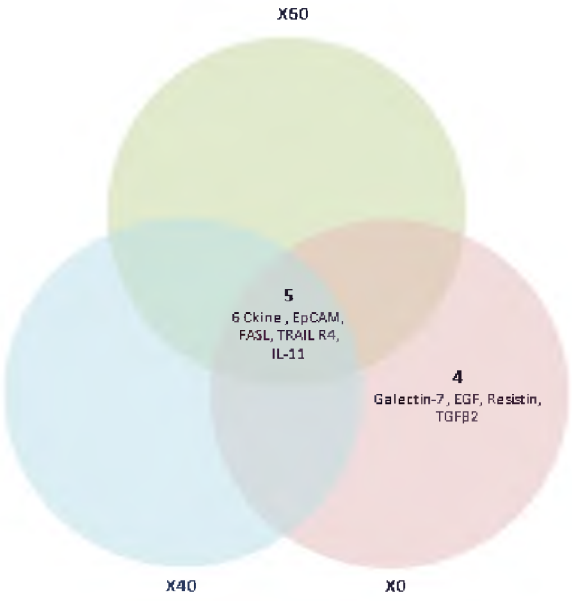

(B) Proteins inhibited

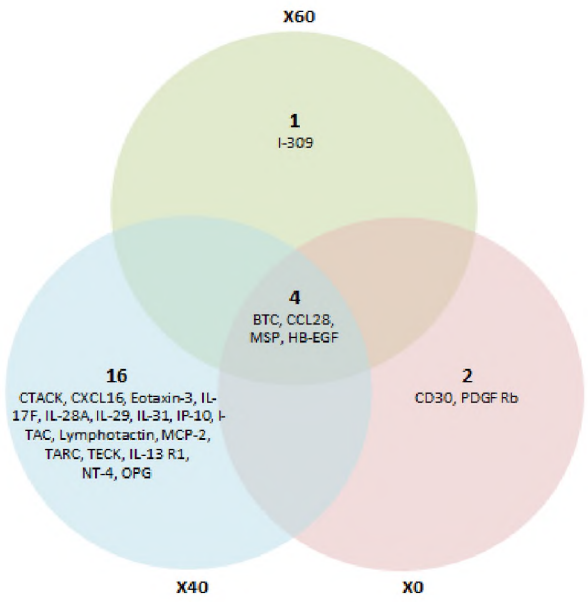

Figure 5. Effect of BPBGs on the ASCs secretory profile. Subconfluent ASCs were treated with 2.5 mg/ml of BPBG for 24 hours. Media was then collected and analyzed for secreted proteins. ASC protein secretion was promoted (A), inhibited (B), increased (C), or decreased (D) with glass treatment. All three glass compositions increased the secretion of 26 proteins (C) while promoting the secretion of 5 additional proteins that ASCs did not secrete under normal conditions (A). All three BPBGs decreased the section of 20 proteins (D) while the secretion of 4 additional proteins was completely inhibited (B).

(C) Proteins upregulated

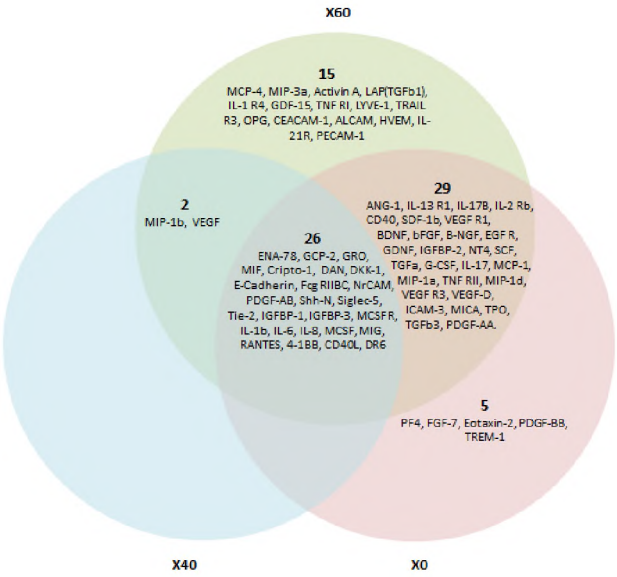

(D) Proteins downregulated

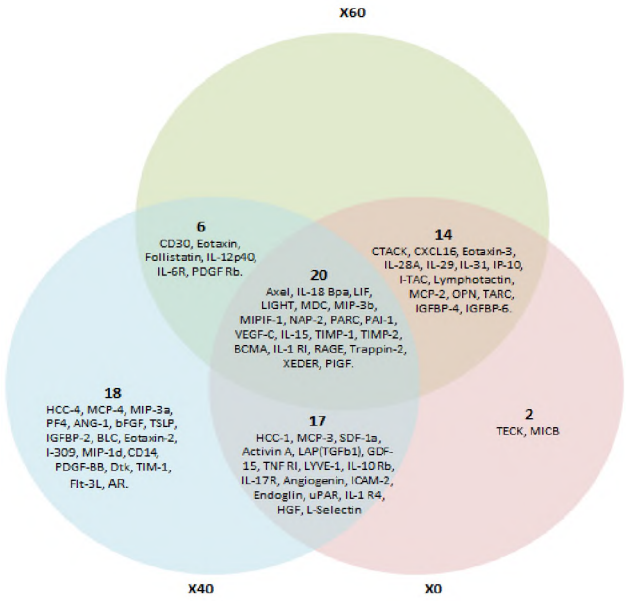

Figure 5. Effect of BPBGs on the ASCs secretory profile. Subconfluent ASCs were treated with 2.5 mg/ml of BPBG for 24 hours. Media was then collected and analyzed for secreted proteins. ASC protein secretion was promoted (A), inhibited (B), increased (C), or decreased (D) with glass treatment. All three glass compositions increased the secretion of 26 proteins (C) while promoting the secretion of 5 additional proteins that ASCs did not secrete under normal conditions (A). All three BPBGs decreased the section of 20 proteins (D) while the secretion of 4 additional proteins was completely inhibited (B). (Cont.)

There were 22 proteins that coincided with the boron concentration in our glass compositions: 2 decreased while 20 increased (Figure 6, Table 2). Figure 7 shows the differential secretion pattern unique for each glass composition represented in a hierarchal clustering heatmaps.

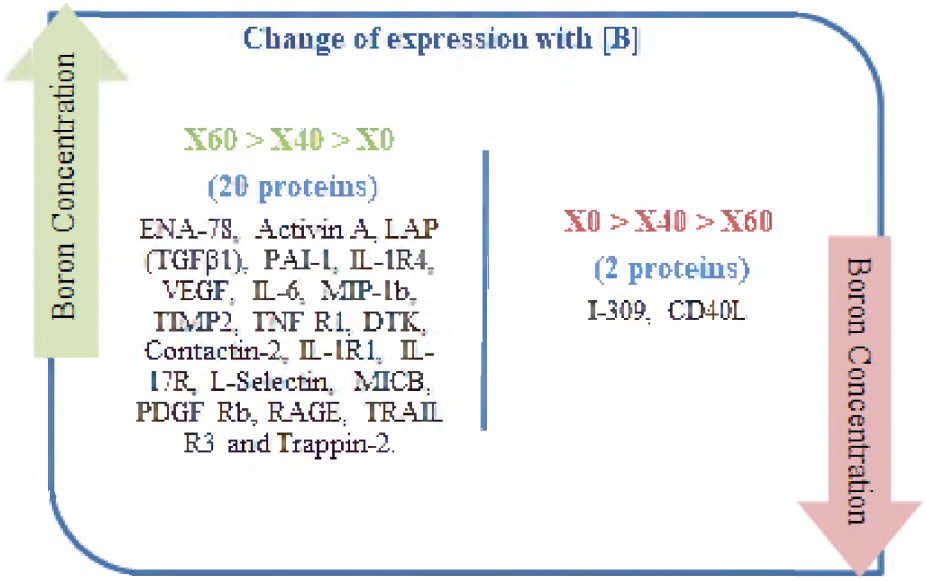

Figure 6. Boron concentration influenced ASC secretome. There were 20 proteins that increased and 2 that decreased with increasing boron in BPBG compositions. The raw data can be found in Table 2.

Table 3. Proteins secretion levels demonstrated in Fig 6, presented in pg/ml and Mean±SD. Blue color represents the highest expression.

	CCM	X0	X40	X60
ENA-78	5.72 ± 0.58	16.91 ± 0.94	34.72 ± 18.34	66.43 ± 19.25
Activin A	280.68 ± 3.43	43.34 ± 4.66	112.34 ± 40.94	725.43 ± 86.71
LAP (TGFβ1)	32.84 ± 3.69	21.13 ± 1.78	27.32 ± 2.82	39.70 ± 1.17
TNF RI	201.07 ± 8.25	185.55 ± 14.80	188.68 ± 14.05	289.75 ± 0.51
TRAIL R3	22.90 ± 7.87	19.34 ± 1.15	22.52 ± 2.56	35.79 ± 0.92
IL-1 R4	68.35 ± 53.92	2.01 ± 2.84	8.30 ± 11.74	158.44 ± 43.02
VEGF	92.27 ± 2.51	94.50 ± 3.18	137.60 ± 14.54	294.71 ± 7.60
IL-6	2701.45 ± 26.20	3118.31 ± 41.64	3865.87 ± 254.17	4109.95 ± 226.75
MIP-1b	68.36 ± 13.41	70.92 ± 4.68	92.55 ± 2.58	96.42 ± 2.91
TIMP-2	12795.45 ± 1190.17	6473.49 ± 1026.09	7645.48 ± 155.76	8481.24 ± 400.92
PAI-1	4466.23 ± 255.95	3381.66 ± 472.87	3408.96 ± 451.51	3876.75 ± 261.23
Dtk	45.79 ± 10.57	29.92 ± 40.39	37.39 ± 6.93	43.84 ± 12.14
Contactin-2	54.06 ± 25.45	34.79 ± 23.03	39.99 ± 15.39	41.34 ± 11.09
IL-1 RI	9.29 ± 0.58	1.51 ± 0.18	2.36 ± 0.29	8.00 ± 1.02
IL-17R	32.17 ± 0.49	14.40 ± 18.02	17.93 ± 1.26	30.14 ± 5.68
L-Selectin	149.13 ± 58.12	4.48 ± 6.85	10.85 ± 12.99	144.18 ± 23.18
MICB	356.25 ± 61.86	241.29 ± 140.60	322.14 ± 82.21	339.68 ± 24.50
PDGF Rb	441.62 ± 174.57	0.00	70.73 ± 99.85	149.87 ± 193.95
RAGE	7.73 ± 1.51	2.63 ± 2.20	3.02 ± 2.71	5.72 ± 1.28
Trappin-2	15.20 ± 1.92	3.47 ± 0.47	8.47 ± 2.55	11.78 ± 0.54
	Control	X0	X40	X60
I-309	1.77 ± 0.57	1.98 ± 0.00	0.05 ± 0.07	0.00
CD40L	15.91 ± 13.60	37.10 ± 13.53	36.48 ± 0.87	32.77 ± 10.19

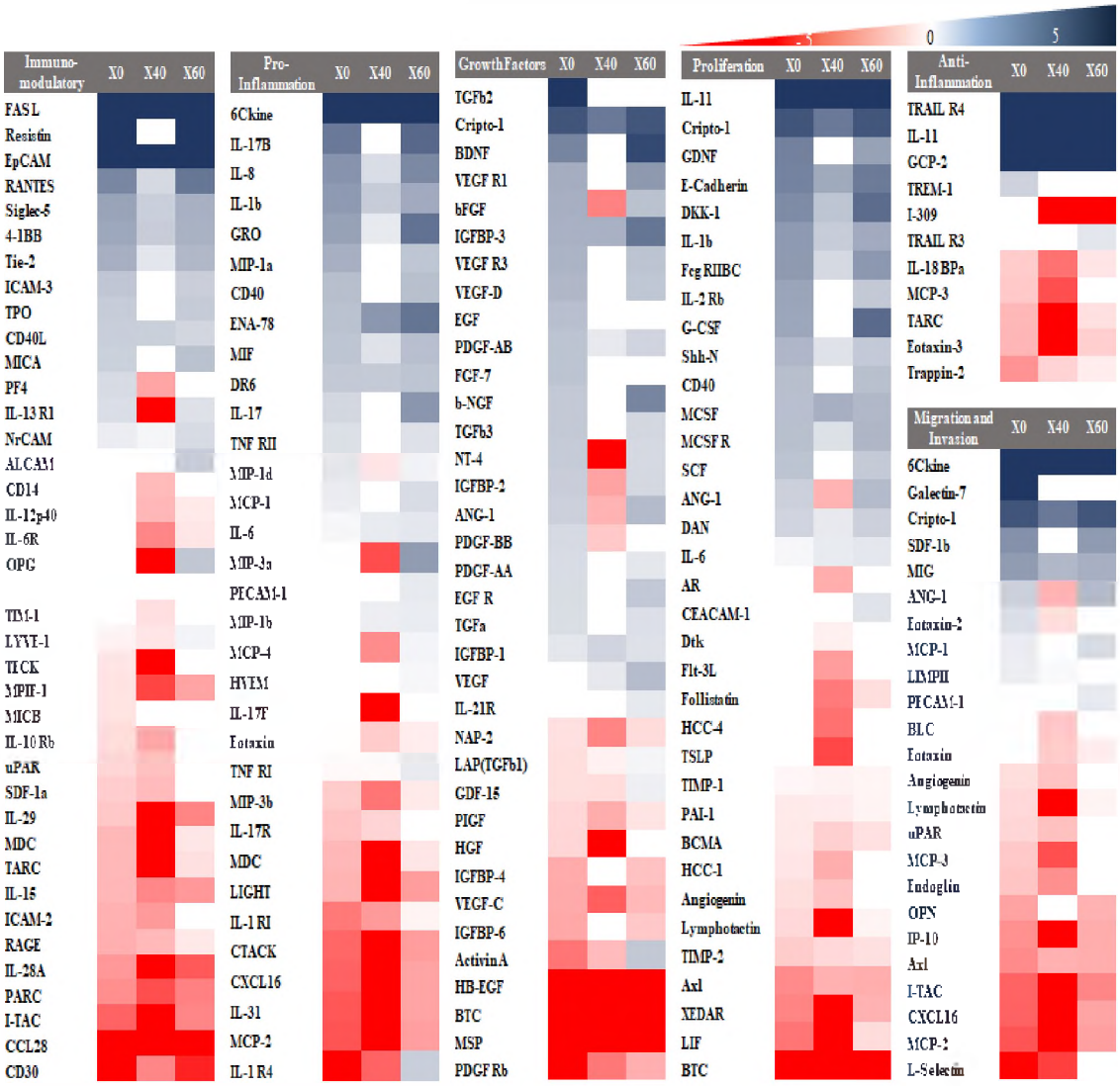

Figure 7. Representative hierarchal heatmap clustering the proteins based on their function in the body. All proteins presented are significant from the control ($p<0.5$). Log2(FC) is used in which (-5 to 5) is the range and any value above 5 represented as dark blue while any value below -5 represented as dark red color while the white color represents all the proteins that are not significant. FC represents the fold change between the samples treated with glass in relation to the control.

4. DISCUSSION

The dissolution rates and ions released into the solution are considered essential factors that determine the bioactivity of a glass [17,18,31]. When compared to silicate bioactive glasses, BBG showed to be more reactive and degrades faster in aqueous solutions [9]. As BBGs with high boron content degrades, they release boron ions into the solution creating an alkaline pH environment and thus showed high cytotoxic effects [31,32]. On the other hand, PBGs with high phosphate content, release phosphate ions into the solution creating acidic environment [33]. There has been little reported on determining the glass compositions required to dissolve in a pH neutral manner. Thus, we proved in this study that combining borate with phosphate can counter the acidic and basic effects and create a neutral pH environment which showed higher levels of cell viability. Li et al, showed similar results when silica was replaced with phosphate [22].

Although a number of studies showed the beneficial effects of the dissolution products of BGs in producing high cell viability, there is still limited investigations on the impact of the direct contact of the BGs with the cells [19,34]. Based on the limited reports, most studies showed reduced cell survival when cultured directly with the BG. A study conducted by Leu and Leach, showed low endothelial cell viability under direct contact with 45S5 BG [35]. Additionally, Qazi et al, showed similar results in which human mesenchymal stem cells (hMSCs) reduced viability by 24 hours of direct contact while showed much higher viability in indirect contact with 45S5 and 1393 BGs [19]. Interestingly, in this study, we employed a direct contact of the BPBGs with ASCs under static conditions which resulted in maintaining a cell viability over 90% for 24 hours

without pre-treating the glass. We hypothesized this result as because of the neutral pH effect of the BPBGs. Another type of pH-neutral BPBGs maintained hASCs viability for 14 days but under indirect contact [34]. This results opens the doors for further investigating the impact of the BG direct contact with the cells and for using BPBGs for *in vitro* studies.

Adipose stem cells possess an inherent ability to migrate to sites of injuries and secrete various chemokines, cytokines and growth factors enabling them to mediate the regeneration process in the body [36–38]. Hence, we evaluated the effect of the BPBGs on the ASCs migration. Our results showed that X0 attracted the highest number of ASCs than other glasses tested in a 5-hour migration assay. At 5 hours, X0 and X40 exhibited similar pH-neutral effects suggesting that the differences between the glass's migration effect is not based on the pH. Consequently, it is worth noting that X0 released the lowest amounts of calcium ions when compared to X40 and X60 glass. To which we assumed that the low concentrations of calcium released into the solution increased the ASCs migration towards the X0 glass. Calcium has long been known for their effective role in cell migration as a crucial regulators and mediators [39–41]. Our results were further proved by a previous study showed that the presence of an optimal range of calcium concentrations (3-5mM) in the solution promoted MSCs migration while the excess of calcium concentration disturbed the MSCs migration *in vitro* [42]. Based on this finding, BPBGs can be used to attract ASCs which would be beneficiary in wound healing, clinical and tissue regeneration applications.

BBG has been previously reported to be angiogenic by stimulating the *in vitro* secretion of the growth factors and proteins involved in the angiogenesis [16,43,44]. In our study, we showed that after 24 hours, only the boron-rich X60 glass increased the ability of the ASCs to be more angiogenic. Hence, we expected that the fast degradation rate of the X60 and the high release of B and Ca ions in the solution contributed in increasing the EC migration and thus become more angiogenic. The angiogenic ability of the X60 was also supported by the increased pattern of the growth factors secreted especially those that are involved in the vascularization process such as VEGF, ANG-1, b-NGF, IGFBP-3, TGFb3 and bFGF and shown in the heatmap. Furthermore, similar results was reported by majority of studies which showed the impact of boron on promoting angiogenesis and the increased expression of the angiogenic growth factors VEGF and TGFb3 when treated with boron containing BGs [16,44–47].

Most literature on bioactive glass, including BPBG, focuses on cell viability, proliferation, or differentiation of ASCs [13,34,48–50]. However, there is very little reported on the effect of BG on ASCs secretome. ASCs have a broad secretory profile of different growth factors, cytokines, and other proteins. Those secretions contribute essentially in almost all body functions and impact the body's response to injuries, healing and tissue regeneration. These secreted proteins all work in a harmony in the body to maintain its hemostasis [25,27]. Hence, it is essential to investigate the effect of any new biomaterial on the ASCs secretome to provide better understanding of the consequences of the biomaterial in the body. In this study, we showed for the first time that BPBGs can alters the ASCs secretome.

The secretory profile of the ASCs from this study revealed an interesting results that nevertheless the glass compositions, they all promoted the expression of (6-Ckine, EpCAM, FasL, TRAIL R4, and IL-4). Upon that, there were some discrepancies on the literature of whether the stem cells normally secrete those proteins. Multiple reports showed that the IL-4 is secreted normally by the stem cells [24,26,51]. In addition, it was supported from an earlier study conducted by Mazar et al. on the most studied ASC's counterpart, bone marrow mesenchymal stem cells (BMSCs) that showed a strong expression detection of FasL [52]. However, another study showed the opposite [53]. These discrepancies are most likely due to using different types of cells (ASCs, MSCs, BMSCs), along with the number of passages used (we used passages from 3-5, others used from passage 1 and 2). Furthermore, our results showed that BPBGs-treated ASCs can influence the immunomodulatory, inflammation, proliferation, migration properties of the cells. A specific patterns were observed in the heatmap presented in Figure 7, in which the boron-rich X0 glass seems to be more pro-inflammatory and angiogenic than the X0 and X40 glasses. Previous reports covering BBG mainly focused on their effect on the angiogenesis, however, the influence of boron on inflammatory responses of the cells has not gained enough attention. A recent study conducted by Zheng et al. suggested that the incorporation of boron in BGs can modulate the inflammatory response of the cells [54]. On the other hand, ASCs treated with X40 glass demonstrated an anti-proliferation and anti-migration secretion patterns which could be explained by its slow degradation rates of the Ca and P ions, an important ions contribute in cell proliferation and migration [7,15,55]. Further investigations need to be carried out on identifying the impact of the different BPBGs compositions on the ASCs secretions as well as their

functions in proliferation, migration, inflammation and immune response. Additionally, future studies need to confirm these changes *in vivo* or in 3D organoids.

As a conclusion, for better understanding the biomaterials, it is important to look at other cell processes than viability and proliferation. Secretome and extravessicles are important topics in regenerative medicine that needs to be further investigated. We have shown in this study, that different compositions of BPBGs can alter the ASCs secretions differently. Thus, it makes it possible to tailor the BGs to stimulate specific ASCs secretions and result in customizable therapies.

REFERENCES

1 Hench, L. L. The story of Bioglass®. *J. Mater. Sci. Mater. Med.* **17**, 967–978 (2006).

2. Baino, F., Fiorilli, S. & Vitale-Brovarone, C. Bioactive glass-based materials with hierarchical porosity for medical applications: Review of recent advances. *Acta Biomater.* **42**, 18–32 (2016).

3. Kaur, G. *et al.* A review of bioactive glasses: Their structure, properties, fabrication and apatite formation. *J. Biomed. Mater. Res. A* **102**, 254–274 (2014).

4. Pajares-Chamorro, N. & Chatzistavrou, X. Bioactive Glass Nanoparticles for Tissue Regeneration. *ACS Omega* **5**, 12716–12726 (2020).

5. Rahaman, M. N. *et al.* Bioactive glass in tissue engineering. *Acta Biomater.* **7**, 2355–2373 (2011).

6. Jones, J. R. Review of bioactive glass: From Hench to hybrids. *Acta Biomater.* **9**, 4457–4486 (2013).

7. Mehrabi, T., Mesgar, A. S. & Mohammadi, Z. Bioactive Glasses: A Promising Therapeutic Ion Release Strategy for Enhancing Wound Healing. *ACS Biomater. Sci. Eng.* **6**, 5399–5430 (2020).

8. Yao, A. *et al.* In Vitro Bioactive Characteristics of Borate-Based Glasses with Controllable Degradation Behavior. *J. Am. Ceram. Soc.* **90**, 303–306 (2007).

9. Fu, Q., Rahaman, M. N., Fu, H. & Liu, X. Silicate, borosilicate, and borate bioactive glass scaffolds with controllable degradation rate for bone tissue engineering applications. I. Preparation and in vitro degradation. *J. Biomed. Mater. Res. A* **95A**, 164–171 (2010).

10. Huang, W., Day, D. E., Kittiratanapiboon, K. & Rahaman, M. N. Kinetics and mechanisms of the conversion of silicate (45S5), borate, and borosilicate glasses to hydroxyapatite in dilute phosphate solutions. *J. Mater. Sci. Mater. Med.* **17**, 583–596 (2006).

11. Fu, H. *et al.* In vitro evaluation of borate-based bioactive glass scaffolds prepared by a polymer foam replication method. *Mater. Sci. Eng. C* **29**, 2275–2281 (2009).

12. Zhang, J. *et al.* Bioactive borate glass promotes the repair of radius segmental bone defects by enhancing the osteogenic differentiation of BMSCs. *Biomed. Mater.* **10**, 065011 (2015).

13. Thyparambil, N. J. *et al.* Adult stem cell response to doped bioactive borate glass. *J. Mater. Sci. Mater. Med.* **31**, 13 (2020).

14. Apdik, H., Doğan, A., Demirci, S., Aydın, S. & Şahin, F. Dose-dependent Effect of Boric Acid on Myogenic Differentiation of Human Adipose-derived Stem Cells (hADSCs). *Biol. Trace Elem. Res.* **165**, 123–130 (2015).

15. Kargozar, S., Baino, F., Hamzehlou, S., Hill, R. G. & Mozafari, M. Bioactive Glasses: Sprouting Angiogenesis in Tissue Engineering. *Trends Biotechnol.* **36**, 430–444 (2018).

16. Balasubramanian, P. *et al.* Angiogenic potential of boron-containing bioactive glasses: in vitro study. *J. Mater. Sci.* **52**, 8785–8792 (2017).

17. Hoppe, A., Güldal, N. S. & Boccaccini, A. R. A review of the biological response to ionic dissolution products from bioactive glasses and glass-ceramics. *Biomaterials* **32**, 2757–2774 (2011).

18. Jones, J. R., Sepulveda, P. & Hench, L. L. Dose-dependent behavior of bioactive glass dissolution. *J. Biomed. Mater. Res.* **58**, 720–726 (2001).

19. Qazi, T. H. *et al.* Comparison of the effects of 45S5 and 1393 bioactive glass microparticles on hMSC behavior. *J. Biomed. Mater. Res. A* **105**, 2772–2782 (2017).

20. Hohenbild, F., Arango-Ospina, M., Moghaddam, A., Boccaccini, A. R. & Westhauser, F. Preconditioning of Bioactive Glasses before Introduction to Static Cell Culture: What Is Really Necessary? *Methods Protoc.* **3**, (2020).

21. Carta, D. *et al.* The effect of composition on the structure of sodium borophosphate glasses. *J. Non-Cryst. Solids* **354**, 3671–3677 (2008).

22. Li, A. *et al.* In vitro evaluation of a novel pH neutral calcium phosphosilicate bioactive glass that does not require preconditioning prior to use. *Int. J. Appl. Glass Sci.* **8**, 403–411 (2017).

23. Bacakova, L. *et al.* Stem cells: their source, potency and use in regenerative therapies with focus on adipose-derived stem cells – a review. *Biotechnol. Adv.* **36**, 1111–1126 (2018).

24. Blaber, S. P. *et al.* Analysis of in vitro secretion profiles from adipose-derived cell populations. *J. Transl. Med.* **10**, 172 (2012).

25. Gimble, J. M. Adipose tissue derived stem cells secretome: soluble factors and their roles in regenerative medicine.

26. Kilroy, G. E. *et al.* Cytokine profile of human adipose-derived stem cells: Expression of angiogenic, hematopoietic, and pro-inflammatory factors. *J. Cell. Physiol.* **212**, 702–709 (2007).

27. Lombardi, F. *et al.* Secretome of Adipose Tissue-Derived Stem Cells (ASCs) as a Novel Trend in Chronic Non-Healing Wounds: An Overview of Experimental In Vitro and In Vivo Studies and Methodological Variables. *Int. J. Mol. Sci.* **20**, 3721 (2019).

28. Mussano, F. *et al.* Cytokine, Chemokine, and Growth Factor Profile Characterization of Undifferentiated and Osteoinduced Human Adipose-Derived Stem Cells. *Stem Cells International* vol. 2017 e6202783 https://www.hindawi.com/journals/sci/2017/6202783/ (2017).

29. ISO 10993-5:2009(en), Biological evaluation of medical devices — Part 5: Tests for in vitro cytotoxicity. https://www.iso.org/obp/ui/#iso:std:iso:10993:-5:ed-3:v1:en.

30. Baek, S. J., Kang, S. K. & Ra, J. C. In vitro migration capacity of human adipose tissue-derived mesenchymal stem cells reflects their expression of receptors for chemokines and growth factors. *Exp. Mol. Med.* **43**, 596–603 (2011).

31. Goetschius, K. L., Beuerlein, M. A., Bischoff, C. M. & Brow, R. K. Dissolution behavior of ternary alkali-alkaline earth-borate glasses in water. *J. Non-Cryst. Solids* **487**, 12–18 (2018).

32. Cheng, X., Brow, R. K. & Chen, G. The dissolution behavior in alkaline solutions of a borosilicate glass with and without P2O5. *J. Am. Ceram. Soc.* **100**, 4519–4532 (2017).

33. Ma, L., Brow, R. K. & Schlesinger, M. E. Dissolution behaviour of sodium calcium polyphosphate glasses. *Phys. Chem. Glas. - Eur. J. Glass Sci. AndTechnology Part B* **59**, 205–212 (2018).

34. Mishra, A. *et al.* In-vitro dissolution characteristics and human adipose stem cell response to novel borophosphate glasses. *J. Biomed. Mater. Res. A* **107**, 2099–2114 (2019).

35. Leu, A. & Leach, J. K. Proangiogenic Potential of a Collagen/Bioactive Glass Substrate. *Pharm Res* **25**, 1222 (2008).

36. Fu, X. *et al.* Mesenchymal Stem Cell Migration and Tissue Repair. *Cells* **8**, (2019).

37. Liu, M. *et al.* Adipose-Derived Mesenchymal Stem Cells from the Elderly Exhibit Decreased Migration and Differentiation Abilities with Senescent Properties. *Cell Transplant.* **26**, 1505–1519 (2017).

38. Lucas, B. de, Pérez, L. M. & Gálvez, B. G. Importance and regulation of adult stem cell migration. *J. Cell. Mol. Med.* **22**, 746–754 (2018).

39. Howe, A. K. Cross-talk between calcium and protein kinase A in the regulation of cell migration. *Curr. Opin. Cell Biol.* **23**, 554–561 (2011).

40. Prevarskaya, N., Skryma, R. & Shuba, Y. Calcium in tumour metastasis: new roles for known actors. *Nat. Rev. Cancer* **11**, 609–618 (2011).

41. Ridley, A. J. *et al.* Cell Migration: Integrating Signals from Front to Back. *Science* **302**, 1704–1709 (2003).

42. Aquino-Martínez, R., Angelo, A. P. & Pujol, F. V. Calcium-containing scaffolds induce bone regeneration by regulating mesenchymal stem cell differentiation and migration. *Stem Cell Res. Ther.* **8**, 265 (2017).

43. Benderdour, M. *et al.* Boron modulates extracellular matrix and TNF alpha synthesis in human fibroblasts. *Biochem. Biophys. Res. Commun.* **246**, 746–751 (1998).

44. Durand, L. A. H. *et al.* In vitro endothelial cell response to ionic dissolution products from boron-doped bioactive glass in the SiO2–CaO–P2O5–Na2O system. *J. Mater. Chem. B* **2**, 7620–7630 (2014).

45. Durand, L. A. H. *et al.* Angiogenic effects of ionic dissolution products released from a boron-doped 45S5 bioactive glass. *J. Mater. Chem. B* **3**, 1142–1148 (2015).

46. Li, K. *et al.* The enhanced angiogenic responses to ionic dissolution products from a boron-incorporated calcium silicate coating. *Mater. Sci. Eng. C* **101**, 513–520 (2019).

47. Lin, Y., Brown, R. F., Jung, S. B. & Day, D. E. Angiogenic effects of borate glass microfibers in a rodent model. *J. Biomed. Mater. Res. A* **102**, 4491–4499 (2014).

48. Vuornos, K. *et al.* Bioactive glass ions induce efficient osteogenic differentiation of human adipose stem cells encapsulated in gellan gum and collagen type I hydrogels. *Mater. Sci. Eng. C* **99**, 905–918 (2019).

49. Ojansivu, M. *et al.* The effect of S53P4-based borosilicate glasses and glass dissolution products on the osteogenic commitment of human adipose stem cells. *PLOS ONE* **13**, e0202740 (2018).

50. Ojansivu, M. *et al.* Bioactive glass induced osteogenic differentiation of human adipose stem cells is dependent on cell attachment mechanism and mitogen-activated protein kinases. *Eur. Cell. Mater.* **35**, 54–72 (2018).

51. Kyurkchiev, D. *et al.* Secretion of immunoregulatory cytokines by mesenchymal stem cells. *World J. Stem Cells* **6**, 552–570 (2014).

52. Mazar, J. *et al.* Cytotoxicity Mediated by the Fas Ligand (FasL)-activated Apoptotic Pathway in Stem Cells*. *J. Biol. Chem.* **284**, 22022–22028 (2009).

53. Ryan, J. M., Barry, F. P., Murphy, J. M. & Mahon, B. P. Mesenchymal stem cells avoid allogeneic rejection. *J. Inflamm. Lond. Engl.* **2**, 8 (2005).

54. Zheng, K. *et al.* Incorporation of Boron in Mesoporous Bioactive Glass Nanoparticles Reduces Inflammatory Response and Delays Osteogenic Differentiation. *Part. Part. Syst. Charact.* **37**, 2000054 (2020).

55. Rahmati, M. & Mozafari, M. Selective Contribution of Bioactive Glasses to Molecular and Cellular Pathways. *ACS Biomater. Sci. Eng.* **6**, 4–20 (2020).

II. THE ANGIOGENIC POTENTIAL OF PH NEUTRAL BOROPHOSPHATE BIOACTIVE GLASSES

Bradley Bromet[1], Nathaniel Blackwell[1], Nada Abokefa[1], Lesa Steen[1], Taylor Stevens[1], Parker Freudenberger[1], Rebekah Blatt[2], Richard Brow[2], Julie Semon[1]

[1] Deparment of Biological Sciences, Missouri University of Science and Technology, Rolla, MO 65409

[2] Department of Materials Engineering, Missouri University of Science and Technology, Rolla, MO 65409

ABSTRACT

Boron containing bioactive glasses have gained enormous attention over the years because of their angiogenic effects. Although, borate bioactive glasses release alkaline ions when degrade which altered the pH of the solution creating a toxic environment for the cells at some levels. Addition of phosphate ions to the glass composition have shown to counter the alkaline effect of the basic borate ions. Hence, in this study, we evaluated the effect of a series of novel borophosphate bioactive glasses (BPBGs) with different borate-to-phosphate ratios as well as doping the glass with therapeutic ions such as Cu and Co. The biological effect of this series of BPBGs was evaluated for their cytotoxicity and angiogenic effects on different types of endothelial cells in both in vitro and in vivo.

1. INTRODUCTION

The first bioactive glasses (BGs), glasses that react in the body to stimulate desired physiological responses, were developed 50 years ago by Hench[1]. These glasses,

including 45S5, were based on silicate chemistries. Since then, BGs have been developed from many different glass composition families, including those based on borate and phosphate chemistries[1,2]. Glass compositions can be modified to control the release of ions and to modify the surrounding pH[3–6]. Borate BGs have been of particular interest in applications for vascularized tissues because it has been shown that borate ions stimulate the secretion of pro-angiogenic growth factors[7–15]. Consequently, borate BGs are a promising therapy to repair tissues that require a high degree of vascularization. However, when borate BGs react in aqueous environments, the local pH of the solution, or the region near the glass surface, quickly increases due to the release of alkaline ions. The development of locally alkaline conditions promotes the formation of hydroxyapatite, a desired outcome for many biomedical applications. However, there are other situations where having locally neutral or acidic conditions around a bioactive glass would be beneficial, including the ability to study *in vitro* the effects that BGs have on cells. Because they create local alkaline conditions when first exposed to aqueous solutions, BGs are often pre-reacted before exposure to cell cultures[13,16,17], a step that complicates potential clinical applications of the glass.

A silicate BG modified with significant concentrations of phosphate was reported to create locally neutral pH conditions that increased viability of a pre-osteoblastic cell line, compared to the more conventional phosphate-free silicate BG that created locally alkaline conditions[6]. Phosphoric acid released by the dissolution of the glass neutralized the alkaline ions. We have shown that adding phosphate to borate glasses can also control the local pH conditions around BGs, from alkaline to acidic, depending on the

borate-to-phosphate ratio[39]. In the present study, we show how those local conditions affect the function of endothelial cells *in vitro* and *in vivo*.

2. MATERIALS AND METHODS

2.1. GLASS PREPARATION

Glasses with the nominal molar composition 16Na2O-24CaO-xB2O3-(60-X) P2O5 system were produced, where X = 0, 10, 20, 30, 40, 50, and 60, and several were doped with different concentrations of CuO and CoO, as indicated in Table 1. The borate bioactive glass 1393-B3 (B3)[7], with the nominal composition 6Na2O, 12K2O, 5MgO, 20 CaO, 4P2O5, 53B2O2, wt%, was also produced. Reagent grade batch materials were calcined at 300°C for at least 4 hours, and then melted at 1000-1150°C, depending on composition, for an hour in platinum crucibles. Melts were stirred on the half hour with a platinum rod, then quenched in graphite molds. Samples were annealed at 350°C for one hour then allowed to cool to room temperature and stored in a vacuum desiccator until use. Glasses were analyzed by x-ray diffraction, using a PANalytical X'Pert Multipurpose diffractometer with a Cu K-a source and a PIXcel Detector, and all compositions except the X50 composition were found to be amorphous. The X50 sample was not used in any subsequent testing.

2.2. DISSOLUTION STUDIES

Approximately 150 mg of glass particles (75-150 microns) were immersed in 50 ml of either deionized water or simulated body fluid[18] in a shaker bath at 37°C. Samples were removed periodically, dried and weighed, and solution pH was measured.

Table 1. Nominal compositions in mole percent (mol%) of the borophosphate glasses used in this study.

Glass designation	Na_2O	CaO	B_2O_3	P_2O_5	CuO	CoO
X0	16	24	-	60	-	-
X10	16	24	10	50	-	-
X20	16	24	20	40	-	-
X20Co	16	20	20	40	-	4
X20Cu	16	20	20	40	4	-
X20CuCo	16	20	20	40	2	2
X30	16	24	30	30	-	-
X40	16	24	40	20	-	-
X40Co	16	20	40	20	-	4
X40Cu	16	20	40	20	4	-
X40CuCo	16	20	40	20	2	2
X60	16	24	60	-	-	-

2.3. CELL CULTURE

Human umbilical vein endothelial cells (HUVECs, pooled donors) and adult dermal blood microvascular endothelial cells (HMVEC-d) were obtained from Lonza (Walkersville, MA). HUVECs were growing in Endothelial Cell Basal Medium-2 and HMVEC-d were grown in Endothelial Cell Basal Medium-2MV.

2.4. CELL PROLIFERATION

HUVECs were plated at 5500 cells / cm^2 in a 96-well plate and incubated at 37°C, 5% CO_2 overnight. Media was removed and glass was added at 2.5 or 10 mg/ml in endothelial medium (EM) under static conditions for 24 hours. For glass dissolution product (DP), 2.5 or 10 mg/ml of glass was added to EM and incubated at 37°C while rocking for 24 hours. The medium was then filtered to remove any residual glass and medium was added to HUVECs and incubated under static conditions for 24 hours. Wells were gently washed 3-5 times in pre-warmed PBS, and DNA was quantified with CyQuant (ThermoFisher), according to manufacturer's instructions. DNA was quantified using a fluorescent microplate reader (Fluostar optima; BMG Labtech Inc.; Durham, NC). Each experiment was performed in triplicate with a minimum of three separate ASC donors.

2.5. CELL MIGRATION

To evaluate the ability of the glass to attract ECs, migration assays were performed in 96-well transwells with 8μm pore membrane inserts (Millipore Sigma). Glass was suspended in EM at 2.5 or 10 mg/ml and 100 μl of that solution was added to

the bottom of the transwell. For glass DP, 2.5 or 10 mg/ml of glass was added to EM and incubated at 37°C while rocking for 5 hours. The solution was then filtered to remove any glass particulates, and 100 µl of that solution was added to the bottom of the transwell. On the top of the membrane insert, ~ $2x10^4$ ECs were loaded into each well insert in triplicate. After incubating 5 hours in a 37°C with 5% humidified CO2, the insert was rinsed with PBS, and the cells that had migrated to the bottom of the insert were enzymatically removed and quantified for DNA using CyQuant and a fluorescent microplate reader. Each experiment was performed in triplicate with a minimum of three separate ASC donors.

2.6. CHICK CHORIOALLANTOIC MEMBRANE (CAM)

White Leghorn chicken Spf fertile eggs (Charles River, East Roanoke, IL) were acclimated to room temperature for 4-6 hrs after delivery and then incubated at 37.5°C with constant humidity for 3 days. Eggs were cracked by gently breaking against a sterilized hex wrench and transferred into an 88 x 88 x 23 mm weigh boat. A piece of eggshell was added to the embryo to ensure normal chick development. Weigh boats with chick embryos were placed into an individual humidity chambers, which were prepared by placing Kim wipes (Kimberly-Clark Worldwide, Inc., Roswell, GA) and 100mL of Milli-Q® (Millipore Sigma, Burlington, MA) purified water inside of a 6.5 x 6.5 x 4" polypropylene container. The humidity chambers with chick embryos were placed in incubators at 37.5°C and allowed to develop 7 additional days.

2.7. BIOACTIVE GLASS ADMINISTRATION AND QUANTIFICATION

Bioactive glass was added to chick CAMs at 10 days total incubation. A sterilized 10-mm diameter poly-band ring was placed in an area on the chick embryo with no major vessels. Approximately 2.5 mg of -20 μm glass was suspended in 20 μL PBS and immediately added to the poly-band rings. Either 2 or 3 samples were placed on each egg. An overall image at 1x and a magnified image at 2x for each sample was captured on days 1 and 5 after the administration of glass using a Leica Stereo Zoom® S8 AP0 and Leica software (Leica Microsystems Inc, Buffalo Grove, IL).

Quantification of CAM images were performed using Wimasis (Córdoba, Spain). Images were digitally dived into sections to quantify observed pathologies, with scoring criteria adapted from Raga et al [19,20]. Vessels that appeared white due to a lack of blood flow were classified as "ghost" vessels. If ghost vessels were seen in at least ½ of the sections (≥ 50% of the surface area of the image), they were classified as progressive[19,20]. They were considered preliminary if identified on less than half of the sections. An accumulation of blood at the microcapillary level resulting in petechial hemorrhaging and blood droplets was classified as hyperemia. Hyperemia was classified as minimal if identified in less than ¼ of the sections, moderate in ¼ to ½ of the sections, and severe if greater than ½ of sections.

2.8. STATISTICS

Analysis was performed using Minitab® Statistical Software (State College, Pennsylvania, USA). The statistical differences among two or more groups were

determined by ANOVA, followed by post-hoc Tukey's honest significant difference for CAM assays and T-test for in vitro tests versus the respective control group.

3. RESULTS

3.1. GLASS PROPERTIES

Table 2 summarizes changes in the pH and the weight losses from glass particles immersed for 48 hrs at 37°C in either water or simulated body fluid (SBF). For samples immersed in water, there is a clear trend in solution pH, with the phosphate-rich glasses producing acidic solutions and the borate-rich glasses, including B3, producing more basic solutions. The shifts in the pH of buffered SBF are smaller after 48 hrs of reaction, although both X60 and B3 glasses produce more alkaline solutions. It is worth noting that the addition of up to 30 mol% B_2O_3 (X30) to the borate-free Na-Ca-phosphate glass (X0) reduces the dissolution rate in SBF, with a minimum in the dissolution rate for the X20 glass. The borate-rich glasses (X40, X60, and B3) dissolve much more rapidly, and the X60 glass is almost completely dissolved after 48 hours. The slower dissolution kinetics of the X10, X20, and X30 glasses help explain why these glasses had less effect on SBF pH, whereas the fast reacting, but pH neutral, X40 glass did not shift SBF pH the way the basic X60 and B3 glasses did. A discussion of the dissolution behaviors of these glasses can be found elsewhere[39].

Table 2. Change in pH and percent weight loss of glass particles (3mg/ml) after soaking in 37°C water or simulated body fluid (SBF, original pH=7.5).

Glass	Water pH (48 hrs)	SBF pH (48 hrs)	Weight Loss (SBF, 48 hrs)
X0	2.4	7.1	8%
X10	3.0	7.4	1.3%
X20	3.9	7.5	<1%
X30	6.3	7.4	3%
X40	7.1	7.0	55%
X60	9.6	8.2	90%
B3	ND	8.1	60%

3.2. HUVEC PROLIFERATION

Figure 1A shows the effects of 2.5 or 10 mg/ml glass on the proliferation of endothelial cells (ECs). At 2.5 mg/ml, the acidic and pH neutral glasses (X0, X20, and X40) did not affect HUVEC proliferation when compared to that measured for the endothelial media (EM), whereas cell proliferation was significantly lower for the two alkaline glasses (X60 and B3). In general, HUVEC proliferation was lower at 10 mg/ml, although not always significantly so. Previous studies have shown that exposing endothelial cells (ECs) to the bioactive glasses 45S5 and borate-substituted 45S5 had no influence on EC proliferation[13,21].

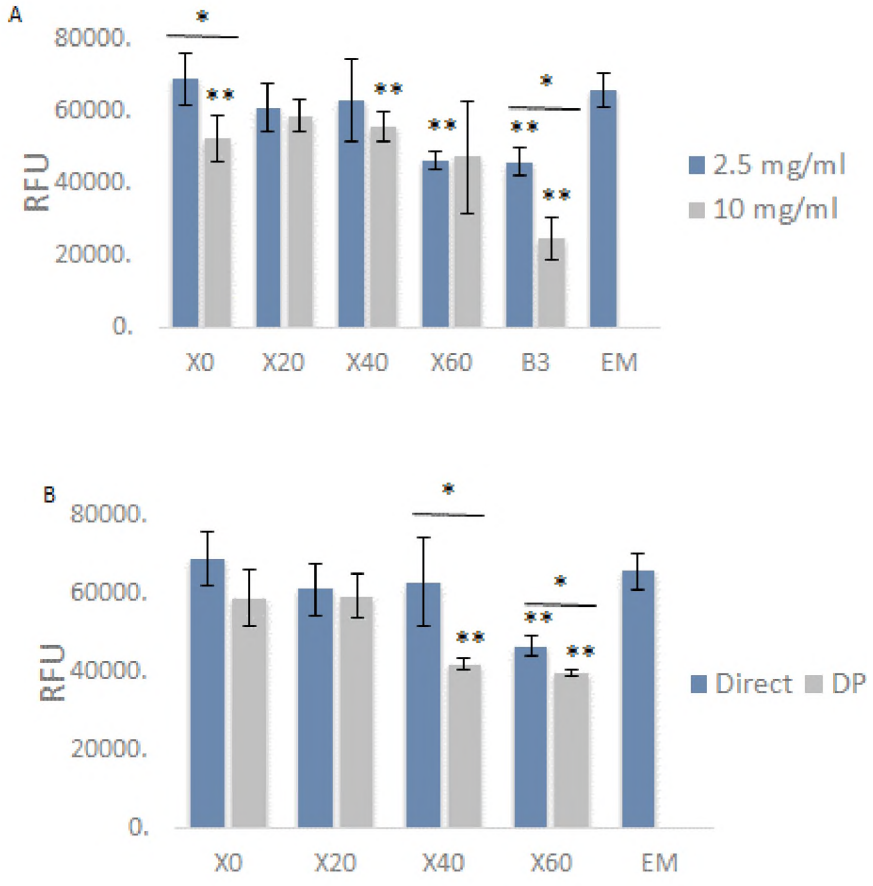

Figure 1. Borophosphate glasses did not increase proliferative of HUVECs. Bioactive glass at two different concentrations was added to HUVECs in a 96-well plate. (A) After 24-hours, cell numbers were measured by DNA content and compared to HUVECs grown under normal culture conditions in endothelial medium (EM). (B) The 24-hour dissolution product (DP) of 2.5 mg/ml bioactive glass was compared to the direct addition of glass. Mean ± SD; *$p<0.05$ and **$p<0.01$ compared to EM.

Glass particles at 2.5 mg/ml were also reacted in EM by shaking at 37°C for 24 hours, and the resulting dissolution product (DP) was then fed to HUVECs. The DP from the two most reactive glasses (X40 and X60) decreased HUVEC proliferation compared to the direct administration of each glass (Figure 1B). There were also smaller, but

statistically insignificant, decreases in cell proliferation associated with the DPs from the X0 and X20 glasses.

Two pH-neutral glasses, X20 and X40, were doped with metal cations reported to promote angiogenesis[22–24] and the effects of these glasses on HUVEC proliferation are shown in Figure 2. For both base glasses, Co additions decreased HUVEC proliferation, whereas the addition of Cu had no statistically meaningful effect. Interestingly, the CuCo combination increased HUVEC proliferation, although not in a statistically meaningful way, compared to the respective base glasses. Figure 2 also compares the effects of glass DP on HUVEC proliferation to the direct contact data. As was the case for the undoped glasses (Figure 1B), the DPs typically reduced HUVEC proliferation compared with the direct contact conditions.

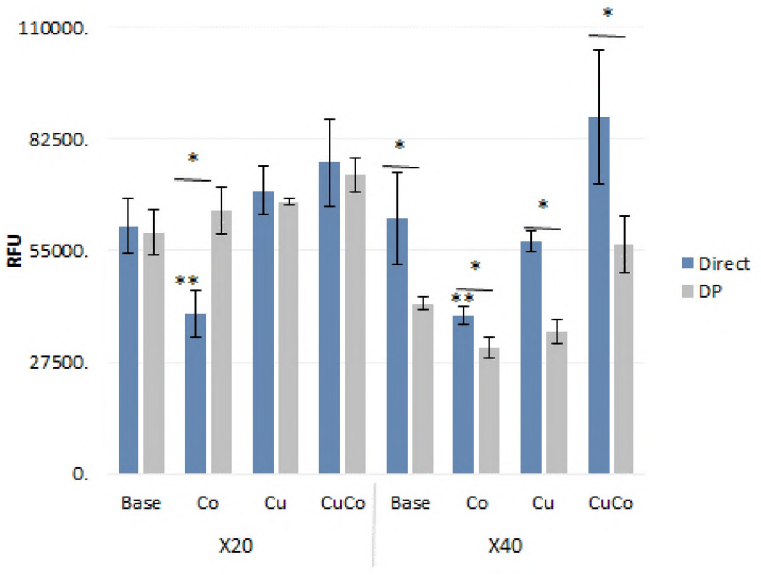

Figure 2. The dissolution product (DP) of doped glasses also did not increase HUVEC proliferation. Approximately 2.5 mg/ml of bioactive glass was degraded on a rocker at 37°C in endothelial media for 24 hours. After filtering the media, the DP was added to HUVECs in a 96-well plate and compared to the direct administration of glasses. Mean ± SD; *$p<0.05$ and **$p<0.01$ compared to respective base composition.

3.3. ENDOTHELIAL MIGRATION

Figure 3 summarizes the results of the endothelial migration tests for X20 and X40, both in direct contact and DP conditions. For both conditions, X40 was associated with statistically greater migration than was found for the EM baseline, whereas the X20 results were not statistically different from the EM results. The metal doped X40 glasses promoted greater cell migration for both direct and DP conditions than did the X20 glasses. As was found for the HUVEC proliferation experiments, endothelial migration was greater under the direct contact conditions than the DP conditions, although those results were statistically meaningful for only a few metal dopants.

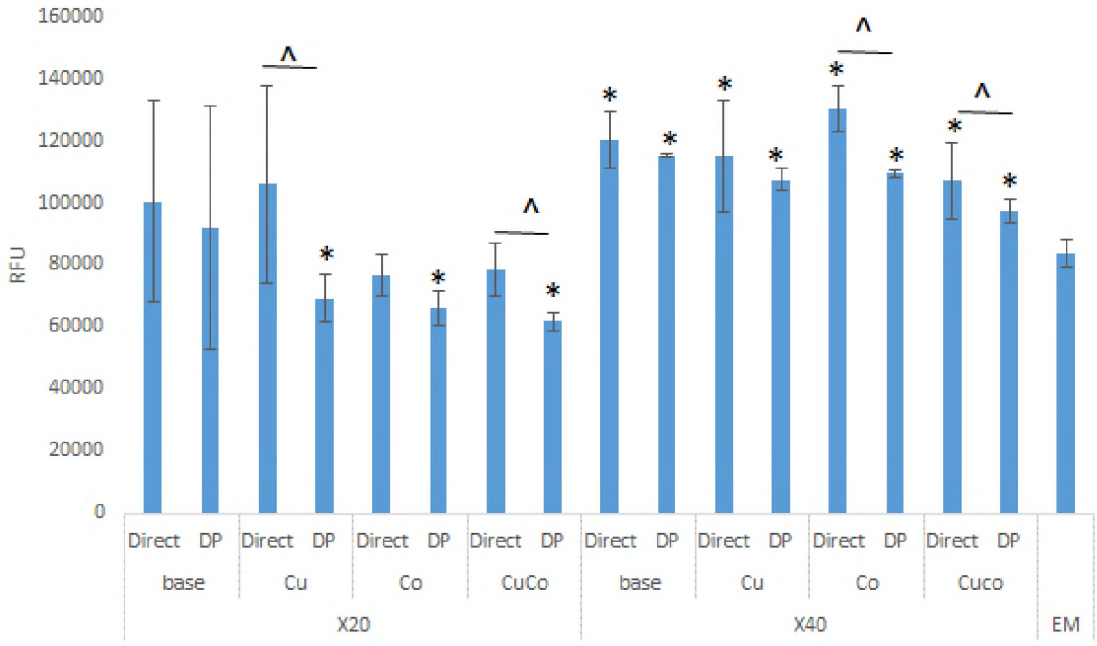

Figure 3. Borophosphate glasses attracted HUVECs. Either the dissolution product or the glass itself was added to the bottom insert of a 96-well transwell. HUVECS were added to the top of the insert and incubated for 5 hours at 37°C. HUVECs that migrated to the bottom were measured by DNA content. Mean ± SD; ^$p<0.05$ and *$p<0.01$ compared to EM.

While HUVECs are a popular source of endothelial cells, they have characteristics that are distinct compared to endothelial cells from other sources, particularly microvascular endothelial cells[25–27]. In addition, it has been shown that extracellular pH has different effects on endothelial cells acquired from different sources[22]. Because the migration of endothelial cells is critical for angiogenesis, a second type of endothelial cell, microvascular endothelial cell from the skin (HMVEC-d), was also tested in the 5-hour transwell migration assay, and those results are shown in Figure 4 for the six base glasses and the EM controls. In general, there are no statistically significant differences in HMVEC-d migration for any of the glasses in the direct contact experiments, although the X60 glasses had the lowest levels of HMVEC-d migration. As was found with other assays, the glass DPs attracted fewer cells than did the direct contact glass particles.

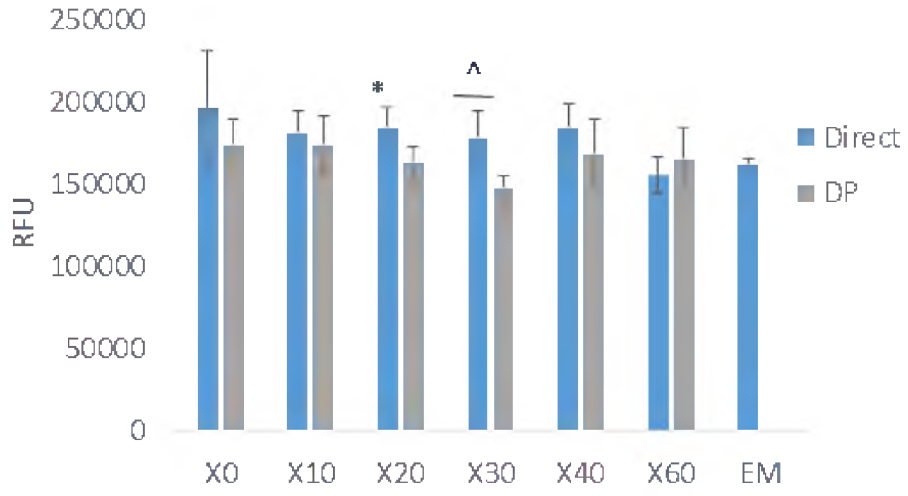

Figure 4. Borophosphate glasses stimulate HMVEC-d migration more than their dissolution product. Both glass and DP were added to the bottom insert of a 96-well transwell at two different concentrations. HMVEC-d were added to the top of the insert and incubated for 5 hours at 37°C. HMVEC-d that migrated to the bottom were measured by DNA content. Mean ± SD; ^$p<0.05$ and *$p<0.01$ compared to EM.

3.4. IN VIVO ANGIOGENESIS

The developing chick chorioallantoic membrane (CAM) is a popular model to evaluate *in vivo* angiogenic responses to biomaterials, including bioactive glass[28–31]. The developing CAM provides a large network of arterioles, venules, and capillaries that can be easily visualized and imaged. We used the CAM to investigate the *in vivo* vascular effects of BP glasses. After the eggs were incubated for 10 days, 2.5 mg/ml of bioactive glass was suspended in PBS, added to the CAM, and were imaged with a stereomicroscope 1, 3, and 5 days after administration.

Figure 5A shows representative images of the CAM on Days 1 and 5 after the administration of different BP glasses, the alkaline glass B3, and a PBS control taken at two magnifications. Figure 5B summarizes Day 1 metrics used to evaluate blood vessel formation. In general, the acidic glasses (X0, X20) had significantly lower average vessel densities and total branching points than the pH neutral (X40) and the alkaline glasses (X60 and B3), with the latter three having similar values as the PBS control. These results show that X40 and X60 are more angiogenic than X0 and X20 glasses. The trend did not continue with segment width. However, segment widths were significantly larger for the X20 and X60 glasses compared to the PBS control. X20 also had increased widths compared to X0, X40, and B3 glasses indicating an arteriogenesis formation in addition to angiogenesis formation.

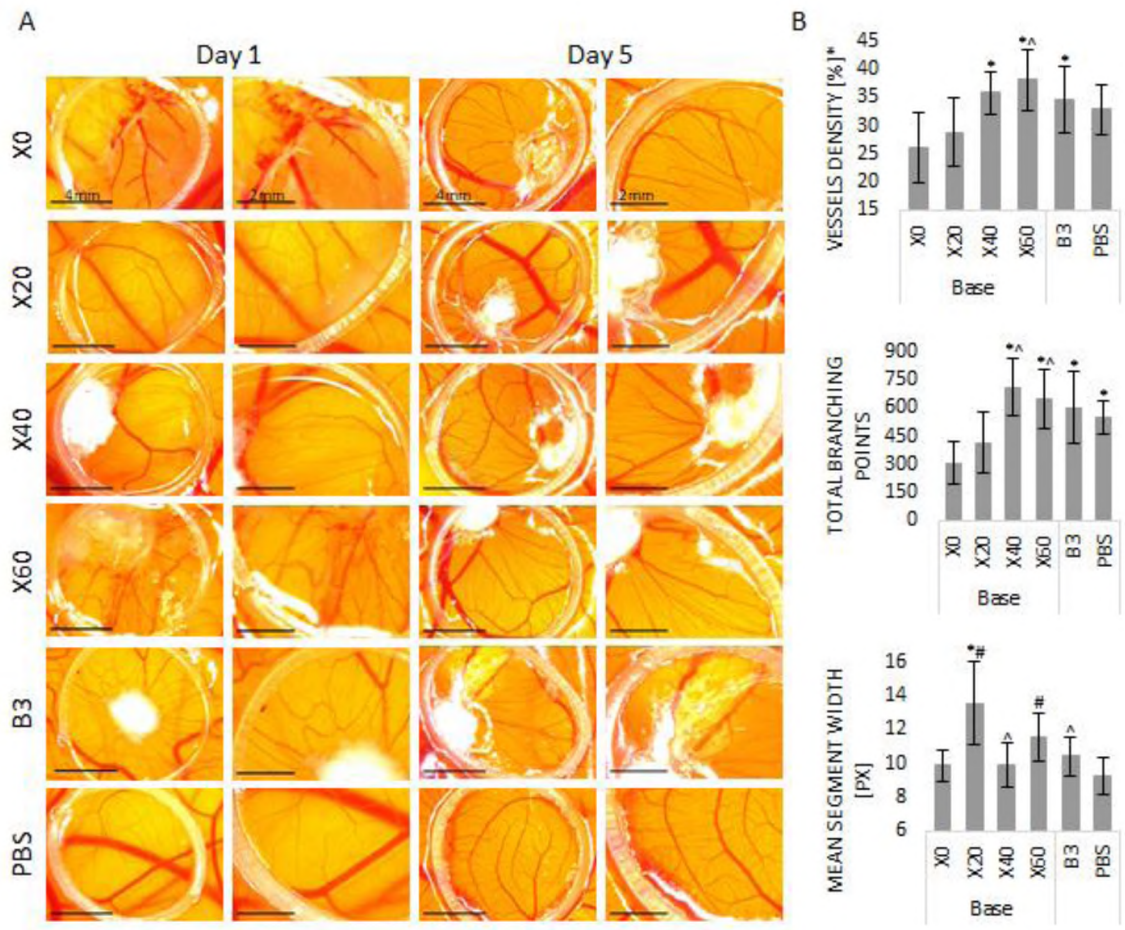

Figure 5. Angiogenesis in chick CAM. Approximately 2.5 mg of -20 µm glass was suspended in 20 µL PBS and immediately added to 10-day old chick CAMs. Image were taken on days 1 and 5 after the administration of glass (A). CAMs were evaluated by vessel density, total branching points, and vessel width at 24 hours (B). Values are mean ± SD; *p< 0.05 compared to X0, ^p< 0.05 compared to X20, and #p< 0.05 compared to PBS. Scale bar: overall image taken at 1x = 4mm, magnified image taken at 2x= 2mm.

The acidic X0 glass had an acute effect on the CAM, generating prominent, but nonuniform regions of ghost vessels (Figure 6). Ghost vessels were found to be devoid of blood flow and appeared clear under the microscope. On Day 1 after administration, 100% of the CAMs treated with X0 displayed progressive ghost vessels (Figure 6, Table 3). However, by Day 3 after administration, only 14% of CAMs treated with X0 samples

had progressive ghost vessels (defined as the presence of ghost vessels on >50% of the surface area of the CAM), whereas 43% had preliminary (<50% of treated CAM) ghost vessels. Ghost vessels were further reduced by Day 5 with only 17% of CAMs treated with X0 having preliminary ghost vessels and none having progressive ghost vessels. It is unclear to us if the reduction in ghost vessels is due to the sprouting of new vessels or revascularization of functional ghost vessels. Ghost vessels were not detected in the CAMs treated with X20 and X40 base glasses but were detected in some samples treated with X60 (Table 3). To our knowledge, this is the first time any bioactive glass has been associated with the creation of ghost vessels.

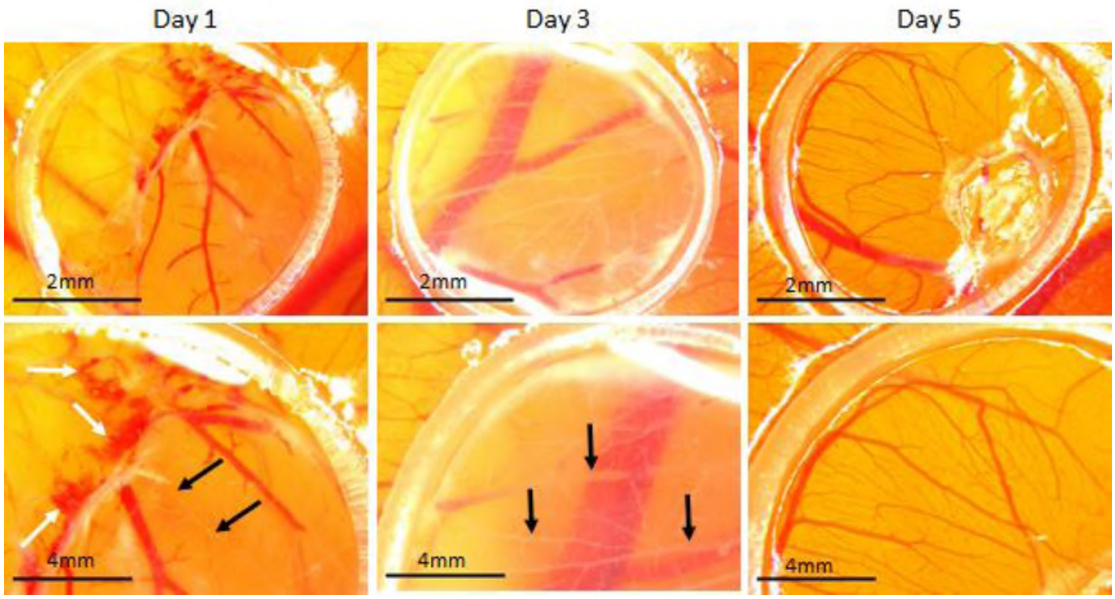

Figure 6. Histological phenomena of X0 in CAM assay. Approximately 2.5 mg of -20 µm glass was suspended in 20 µL PBS and immediately added to 10-day old chick CAMs. Images were taken on Days 1, 3, and 5 after the administration of glass. The pathologies are characterized as ghost vessels (black arrow) or hyperemia (white arrow). Scale bar: overall image taken at 1x (top row) = 4mm, magnified image taken at 2x (bottom row) = 2mm.

A similar phenomenon occurred with hyperemia, which is an increased blood flow at the microcapillary level. On Day 1 after administration, 100% of the CAMs treated with acidic X0 displayed moderate to severe hyperemia (Figure 6; Table 3). Fewer examples of hyperemia were noted for the X20 and X40 base composition treated CAMs, and somewhat more were associated with samples treated with X60 glass (Table 3). Numerous blood pools formed along the arteriole length and capillary terminals. Initially, we assumed that such increase in blood flow may have produced too much damage on the sprouting vessels, resulting in anoxia in the developing embryo. However, the survival rate of the eggs remained high throughout the study. Additionally, by Day 3, 100% of the CAMs treated with X0 had only minimal hyperemia, which then was reduced to 17% by Day 5. This indicates that the acidic X0 glass produces a burst of angio-suppression that does not compromise mortality.

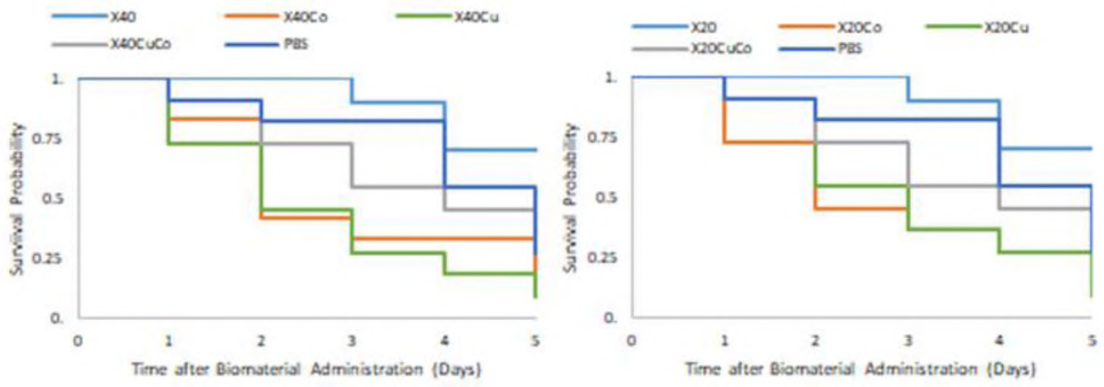

Figure 7. Kaplan-Meier survival curve of doped BP glasses. The addition of dopants to X20 and X40 series reduced the viability of chick CAMs. The combination of dopants had better survivability than single doped glasses.

Table 3: Percentages of CAMS with histological phenomenon (Day 1, 3, 5). For each day, the percentage of eggs showing severities of ghost vessels or hyperemia. Most severe pathologies were observed on Day 1 and diminished by Day 5.

		Ghost Vessels		Hyperemia		
	Dopants	Preliminary	Progressive	Minimal	Moderate	Severe
X0	Base	0, 43, 17	100, 14, 0	0, 100, 17	50, 0, 0	50, 0, 0
X20	Base	0, 0, 0	0, 0, 0	10, 0, 0	0, 0, 0	0, 0, 0
	Co	0, 0, 0	0, 0, 0	63, 0, 0	13, 0, 0	0, 0, 0
	Cu	22, 0, 0	11, 0, 0	22, 0, 0	0, 0, 0	0, 0, 0
	CuCo	30, 0, 0	0, 0, 0	60, 13, 20	30, 0, 0	0, 0, 0
X40	Base	0, 0, 0	0, 0, 0	20, 0, 0	0, 0, 0	0, 0, 0
	Co	10, 0, 0	0, 0, 0	50, 25, 25	10, 25, 25	0, 0, 0
	Cu	50, 0, 0	38, 33, 0	63, 67, 50	13, 0, 0	0, 0, 0
	CuCo	30, 0, 0	30, 0, 0	40, 0, 0	30, 0, 0	10, 0, 0
X60	Base	25, 0, 0	0, 0, 0	50, 14, 0	29, 0, 0	17, 0, 0
B3	Base	10, 0, 0	0, 0, 0	50, 0, 0	13, 0, 0	14, 0, 0

The pH neutral glasses, X20 and X40, were both doped with Co, Cu, or CuCo. The dopants decreased the viability of the chick CAMs (Figure 7). For both series, all dopants had less than 100% survivability by Day 1, < 60% by Day 3, and < 30% by Day 5. Both Co and Cu had lower survival rates than CuCo after Day 2. Furthermore, these dopants had some acute effects on the CAM with more ghost vessels and hyperemia than their respective base glasses (Figure 8; Table 3). Most of these features went away by

Day 5 after administration. Cu is noted to be angiogenic[23,24], but the amount of Cu in these glasses (4% wt CuO) may have been too much for developing vessels in the CAM, reducing viability, and may have a different effect on established vessels. The X40Cu sample agglomerated on the CAM, making overall imaging and quantification impossible. Interestingly, the X20Co glass increased the angiogenic indicators but decreased mean segment width over the X20 base composition, whereas the X40Co glass decreased angiogenic indicators and increased segment width over its base composition. For both X20 and X40 compositions, doping with CuCo increased vessel density and branching points. However, when compared to the respective base composition, X40CuCo increased mean segment width while X20CuCo was comparable.

Table 4: Summary of base glass characteristics at 24-hours. Double arrows indicate progressive / severe pathology.

	Dissolution	pH in SBF	B release (ppm)	P release (ppm)	HUVEC proliferation	HUVEC migration	HMVEC-d migration	Angiogenesis	Ghost Vessels	Hyperemia
X0	0.01	7.3	0.69	145.8	↓	NA	↑	↓	↑↑	↑↑
X20	0	7.45	2.3	0	—	—	↑	↓	—	—
X40	0.3	7.0	498	372	—	↑	↑	↑	—	—
X60	0.5	8.4	955	0	—	NA	↑	↑	↑	↑

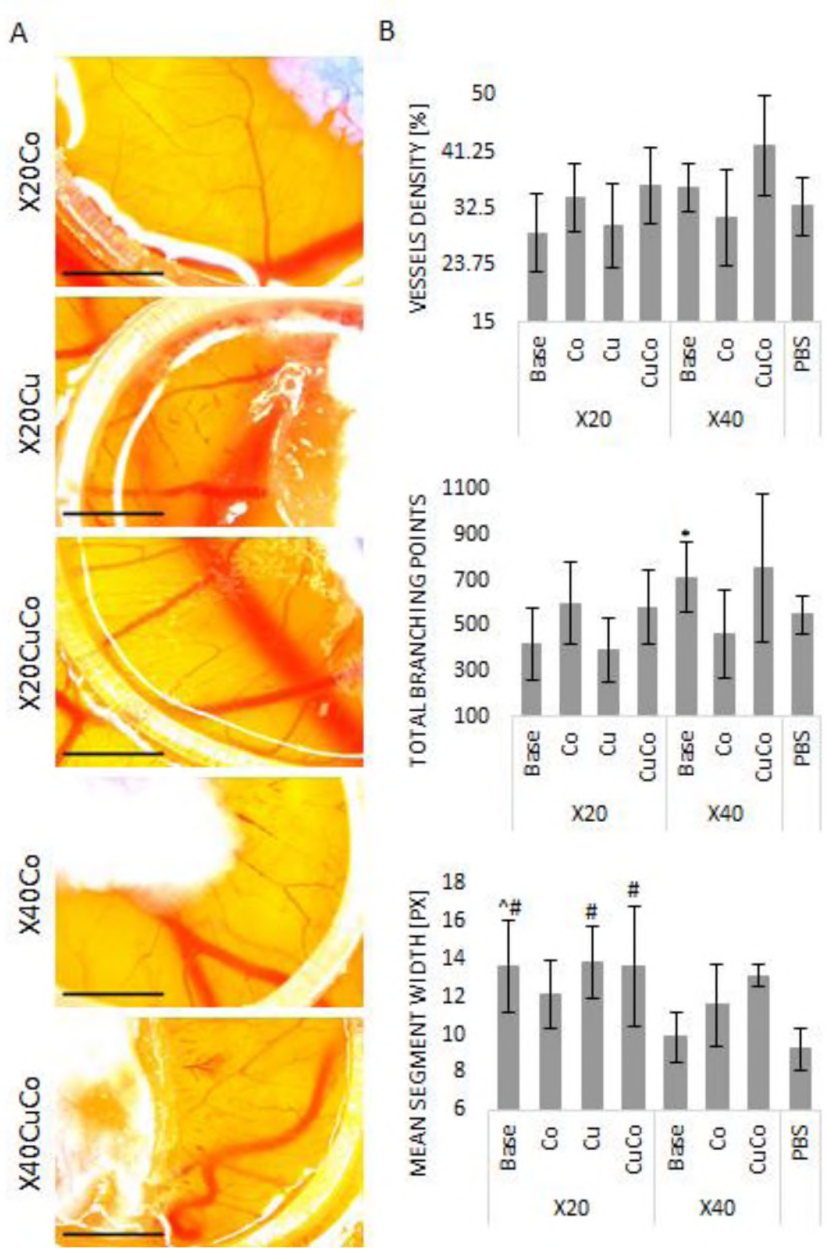

Figure 8. Angiogenesis of doped glasses in CAM assay. Approximately 2.5 mg of -20 µm doped glass was suspended in 20 µL PBS and immediately added to 10-day old chick CAMs. Image were taken 1 day after the administration of glass (A). CAMs were evaluated by vessel density, total branching points, and vessel width at 24 hours (B). Ghost vessels are excluded from these metrics. Dopants had little effect on angiogenesis compared to base glasses and the control. Values are mean ± SD; *$p < 0.01$ compared to X20 base, ^$p < 0.01$ compared to X40 base, and #$p < 0.001$ compared to PBS. Scale bar = 2mm.

4. DISCUSSION

Both Na-Ca-borate and Na-Ca phosphate glasses dissolve congruently in neutral pH solutions, releasing boric and phosphoric acid to the solution, respectively[32,33]. Boric acid is relatively weak (pKa=9.27)[34] and when it combines with the strong bases that form with the release of Na+ and Ca2+ ions, the dissolution in water of Na-Ca-borate glasses increases pH32. Phosphoric acid, on the other hand, is relatively strong (pKa=2.16)[34] and so when phosphate-rich Na-Ca-phosphate glasses dissolve in water, solution pH decreases[33]. Borophosphate glasses also dissolve congruently[39]. As shown in Table 2, phosphate-rich glasses create acidic environments, borate-rich glasses create basic environments, and the intermediate compositions can retain pH neutral environments. Similar pH-control effects have been reported for the substitution of P2O5 for SiO2 in in Na-Ca-silicate glasses[6].

In addition to altering local solution pH, the ion release rates of the X-series base glasses, vary significantly (Table 2). In SBF, X20 dissolves at a rate that is about 30 times slower than X0, which itself dissolves about 10 times slower than X40, and X40 dissolves about half as fast as X60[39]. Because these glasses dissolve congruently, the release of the constituent ions, including metal ion dopants, will vary accordingly. For example, ions are released from X40 about 350 times faster than from X20. The ability to tailor the time-release kinetics should allow biomaterial designers to use materials like these for different applications.

Angiogenesis, the process by which new blood vessels develop from pre-existing vessels, requires EC to proliferate, migrate, and form tubes[35]. Previous reports showed 45S5 and borate-substituted 45S5 did not stimulate HUVEC proliferation, but did increase endothelial migration[13].In that study, the lack of proliferation was reported to be due to insufficient concentrations of silicon in their glass, and they credited the migration to boron. Similarly, our glass series did not stimulate HUVEC proliferation, but the glass with higher boron content increased HUVEC migration.

It is interesting to note that while the X20 glass did not increase HUVEC migration (Figure 3), it did increase HMVEC-d migration (Figure 4), suggesting that local pH and ion concentrations may have different effects on different parts of the body. This coincides with results from Wesson et al who demonstrated that microvascular cells from the kidney and the heart secreted different levels of an angiogenic factor when the local pH was reduced[36].

Previous studies have reported that an acidic pH can increase angiogenesis to poorly vascularized sites under both normal and pathological conditions[35]. This may be due to an acidic extracellular environment upregulating GPR4, a proton-sensing receptor expressed on endothelial cells, or it could be the acidic extracellular environment increasing VEGF binding[21–24,37]. In this work, the acidic X0 glass produced the most ghost vessels and hyperemia on chick CAMs one day after administration. However, these features disappeared by Day 5, and the viability of the chick was unaffected throughout the experiment. Although we do not know the reasons for this, the capillary endothelium does undergo considerable morphological change in this stage of chick development, with developing vasculature having discontinuous basement membranes,

increased mitosis in days 8–10, and relatively undifferentiated endothelial cells[30]. It would be interesting to compare our results for the developing vascular network of a chick CAM to an established vascular network and evaluate if an acidic bioactive glass might have increased therapeutic applications related to angiogenesis.

Less is known about the vascular effects of an alkaline environment, like those created by X60 or B3. The earliest reports of alkaline reactions, in particular phosphatases, in vascular cells showed differing effects on capillaries compared to medium-sized arterioles, as well as differences in phosphatase activity in the capillaries of different organs[38]. Other studies showed that an alkaline agent, such as sodium bicarbonate, increased the percentage of endothelial cells expressing VEGFR-2 and provided stronger anti-cancer activity when combined with an anti-cancer drug[21]. Similar to Faes et al who witnessed an increase in mean vessel density with sodium bicarbonate treatment21, we found that CAM treated with X60 particles also increased mean vessel density (Figure 5).

An overall summary of our results for all the BP glass base compositions can be seen in Table 4. Of all the compositions tested in this study, X40, a fast-reacting, pH neutral glass, was the most angiogenic and had the least amount of pathology (ghost vessels and hyperemia) associated with the chick CAM. Consequently, X40 was further investigated by doping with Cu, Co, or CuCo, all which had previously been shown to increase angiogenesis[23,24]. We did not see an increase in angiogenesis with the Cu-doped glasses, which we had expected. The concentration of CuO may not have been optimized for developing vessels and may have different results in established vessels.

Another surprise to us was the decreased EC proliferation and migration to the DP compared to the direct glass. Except for X20Co, the DP of the doped glasses did not stimulate HUVEC proliferation as much as the direct administration of glass (Figure 2B). This may be due to the reaction rate of the glasses and phosphate precipitating out more quickly when cells are not present. These results, however, show that BP glasses have significant potential as scaffolds or for other applications since they do not require preconditioning prior to use for in vitro or in vivo studies.

5. CONCLUSIONS

There have been few investigations into creating BGs that degrade in a pH neutral manner. The angiogenic potential of novel BP glasses with a neutral pH were investigated for their angiogenic capacity in this study. The *in vitro* and *in vivo* results from this study demonstrated that these pH neutral glasses are promising candidates as angiogenic biomaterials for future use in wound healing and tissue engineering.

REFERENCES

1. Kaur, G. *et al.* A review of bioactive glasses: Their structure, properties, fabrication, and apatite formation. *J. Biomed. Mater. Res. A* **102**, 254–274 (2014).

2. Baino, F., Hamzehlou, S. & Kargozar, S. Bioactive Glasses: Where Are We and Where Are We Going? J. Funct. Biomater. 9, 25 (2018).

3. Hoppe, A., Güldal, N. S. & Boccaccini, A. R. A review of the biological response to ionic dissolution products from bioactive glasses and glass-ceramics. Biomaterials 32, 2757–2774 (2011).

4. Rahaman, M. N. et al. Bioactive glass in tissue engineering. Acta Biomater. 7, 2355–2373 (2011).

5. Kargozar, S., Baino, F., Hamzehlou, S., Hill, R. G. & Mozafari, M. Bioactive Glasses: Sprouting Angiogenesis in Tissue Engineering. Trends Biotechnol. 36, 430–444 (2018).

6. Li, A. et al. In vitro evaluation of a novel pH neutral calcium phosphosilicate bioactive glass that does not require preconditioning prior to use. Int. J. Appl. Glass Sci. 8, 403–411 (2017).

7. Lin, Y., Brown, R. F., Jung, S. B. & Day, D. E. Angiogenic effects of borate glass microfibers in a rodent model. J. Biomed. Mater. Res. A 102, 4491–4499 (2014).

8. Revolution in wound care? Inexpensive, easy-to-use cotton candy-like glass fibers appear to speed healing in initial venous stasis wound trial. The American Ceramic Society https://ceramics.org/ceramic-tech-today/revolution-in-wound-care-inexpensive-easy-to-use-cotton-candy-like-glass-fibers-appear-to-speed-healing-in-initial-venous-stasis-wound-trial (2011).

9. Balasubramanian, P., Büttner, T., Miguez Pacheco, V. & Boccaccini, A. R. Boron-containing bioactive glasses in bone and soft tissue engineering. J. Eur. Ceram. Soc. 38, 855–869 (2018).

10. Zhao, S. et al. Wound dressings composed of copper-doped borate bioactive glass microfibers stimulate angiogenesis and heal full-thickness skin defects in a rodent model. Biomaterials 53, 379–391 (2015).

11. Yang, Q., Chen, S., Shi, H., Xiao, H. & Ma, Y. In vitro study of improved wound-healing effect of bioactive borate-based glass nano-/micro-fibers. Mater. Sci. Eng. C 55, 105–117 (2015).

12. Yao, A. et al. In Vitro Bioactive Characteristics of Borate-Based Glasses with Controllable Degradation Behavior. J. Am. Ceram. Soc. 90, 303–306 (2007).

13. Durand, L. A. H. et al. In vitro endothelial cell response to ionic dissolution products from boron-doped bioactive glass in the SiO2–CaO–P2O5–Na2O system. J. Mater. Chem. B 2, 7620–7630 (2014).

14. Pizzorno, L. Nothing Boring About Boron. Integr. Med. Clin. J. 14, 35–48 (2015).

15. Nielsen, F. H. Update on human health effects of boron. J. Trace Elem. Med. Biol. 28, 383–387 (2014).

16. Ciraldo, F. E., Boccardi, E., Melli, V., Westhauser, F. & Boccaccini, A. R. Tackling bioactive glass excessive in vitro bioreactivity: Preconditioning approaches for cell culture tests. Acta Biomater. 75, 3–10 (2018).

17. El-Ghannam, A., Ducheyne, P. & Shapiro, I. M. Bioactive material template for in vitro, synthesis of bone. J. Biomed. Mater. Res. 29, 359–370 (1995).

18. Maçon, A. L. B. et al. A unified in vitro evaluation for apatite-forming ability of bioactive glasses and their variants. J. Mater. Sci. Mater. Med. 26, 115 (2015).

19. Raga, D. D., Alimboyoguen, A. B., Shen, C.-C., Herrera, A. A. & Ragasa, C. Y. Triterpenoids and an Anti-Angiogenic Sterol from Ardisia pyramidalis Cav. Pers. 94, 9 (2011).

20. Raga, D. D., Herrera, A. A., Alimboyoguen, A. B., Shen, C.-C. & Ragasa, C. Y. Angio-Suppressive Effect of Sterols from Ardisia Pyramidalis (Cav.) Pers. Pharm. Chem. J. 51, 683–689 (2017).

21. Faes, S. et al. Acidic pH reduces VEGF-mediated endothelial cell responses by downregulation of VEGFR-2; relevance for anti-angiogenic therapies. Oncotarget 7, 86026–86038 (2016).

22. Rath, S. N. et al. Bioactive Copper-Doped Glass Scaffolds Can Stimulate Endothelial Cells in Co-Culture in Combination with Mesenchymal Stem Cells. PLOS ONE 9, e113319 (2014).

23. Saghiri, M. A., Asatourian, A., Orangi, J., Sorenson, C. M. & Sheibani, N. Functional role of inorganic trace elements in angiogenesis—Part II: Cr, Si, Zn, Cu, and S. Crit. Rev. Oncol. Hematol. 96, 143–155 (2015).

24. Bose, S., Fielding, G., Tarafder, S. & Bandyopadhyay, A. Understanding of dopant-induced osteogenesis and angiogenesis in calcium phosphate ceramics. Trends Biotechnol. 31, 594–605 (2013).

25. Dib, H. et al. Proteomes of umbilical vein and microvascular endothelial cells reflect distinct biological properties and influence immune recognition. PROTEOMICS 12, 2547–2555 (2012).

26. Chi, J.-T. et al. Endothelial cell diversity revealed by global expression profiling. Proc. Natl. Acad. Sci. 100, 10623–10628 (2003).

27. Semon, J. A. et al. Integrin expression and integrin-mediated adhesion in vitro of human multipotent stromal cells (MSCs) to endothelial cells from various blood vessels. Cell Tissue Res. 341, 147–158 (2010).

28. Gorustovich, A. A. et al. Novel bioassay to evaluate biocompatibility of bioactive glass scaffolds for tissue engineering. Adv. Appl. Ceram. 107, 274–276 (2008).

29. Nowak-Sliwinska, P., Segura, T. & Iruela-Arispe, M. L. The chicken chorioallantoic membrane model in biology, medicine and bioengineering. Angiogenesis 17, 779–804 (2014).

30. Dunn, L. K. et al. Chick chorioallantoic membrane as an in vivo model to study vasoreactivity: Characterization of development-dependent hyperemia induced by epoxyeicosatrienoic acids (EETs). Anat. Rec. A. Discov. Mol. Cell. Evol. Biol. 285A, 771–780 (2005).

31. Ribatti, D. The chick embryo chorioallantoic membrane (CAM). A multifaceted experimental model. Mech. Dev. 141, 70–77 (2016).

32. Goetschius, K. L., Beuerlein, M. A., Bischoff, C. M. & Brow, R. K. Dissolution behavior of ternary alkali-alkaline earth-borate glasses in water. J. Non-Cryst. Solids 487, 12–18 (2018).

33. Ma, L., Brow, R. K., Missouri University of Science & Technology & Schlesinger, M. E. Dissolution behaviour of sodium calcium polyphosphate glasses. Phys. Chem. Glas. Eur. J. Glass Sci. Technol. Part B 59, 205–212 (2018).

34. E1: Acid Dissociation Constants at 25°C. Chemistry LibreTexts https://chem.libretexts.org/Bookshelves/Ancillary_Materials/Reference/Reference_Tables/Equilibrium_Constants/E1%3A_Acid_Dissociation_Constants_at_25C (2014).

35. Goerges, A. L. & Nugent, M. A. pH Regulates Vascular Endothelial Growth Factor Binding to Fibronectin A MECHANISM FOR CONTROL OF EXTRACELLULAR MATRIX STORAGE AND RELEASE. J. Biol. Chem. 279, 2307–2315 (2004).

36. Wesson, D. E., Simoni, J. & Green, D. F. Reduced extracellular pH increases endothelin-1 secretion by human renal microvascular endothelial cells. https://www.jci.org/articles/view/854/pdf (1998) doi:10.1172/JCI854.

37. Dong, L. et al. Acidosis Activation of the Proton-Sensing GPR4 Receptor Stimulates Vascular Endothelial Cell Inflammatory Responses Revealed by Transcriptome Analysis. PLOS ONE 8, e61991 (2013).

38. Romanul, F. C. A. & Bannister, R. G. Localized Areas of High Alkaline Phosphatase Activity in Endothelium of Arteries. Nature 195, 611–612 (1962).

39. Freudenberger, P., Kolan, K., Semon, J., Morton, A. & Brow, R. The Effect of Boron Content and Solution pH on Cellular Response in Borophosphate Glasses – Under Review. (2021).

SECTION

2. CONCLUSIONS, FUTURE DIRECTIONS AND BROADER IMPACT

2.1. CONCLUSIONS

It should be noted that only a few studies in literature focused on creating BGs that degrade in a pH neutral manner. Our collaborators created a series of pH-neutral BPBGs, and this thesis tested those glasses for biological outcomes *in vitro* and *in vivo*. These pH-neutral BPBGs maintained ASCs viability under static normal conditions and without having to be pre-reacted. Additionally, the breakdown of the glass attracted endothelial cells more than the dissolution product, further demonstrating that it is not necessary to pre-react the glass. This work also sheds light on how modification to the glass composition and pH can create either pro- or anti-inflammatory conditions, as well as pro- or anti-angiogenic conditions. Taken together, the results from these studies, will allow glass to be customized for personalized medicine.

2.2. FUTURE DIRECTIONS AND BROADER IMPACT

The work from this thesis can be further explored by:

- Further discerning how BPBGs can affect the ASC secretome. While this work treated the ASCs with BPBG for 24 hours, how would shorter or longer treatments affect ASCs? Furthermore, how long do these changes last? The answers to these questions would help us to understand how the basic science behind how these biomaterials actually works, as well as give insight to how they can be used for personalized treatments in the clinic.

- ASCs are affected by their niche, including neighboring cells and surrounding ECM. Consequently, ASCs isolated from patients with health conditions such as diabetes, Parkinson's, or multiple sclerosis, have an altered phenotype. Table 1. demonstrates the differences between ASCs from healthy and diabetic persons. One of these differences is the increased pro-inflammatory properties of ASCs from diabetics. Hence, another future direction of this work is to evaluate if BPBG alter the phenotype of ASCs from diabetics in the same manner as healthy persons. Again, this will shed light on a completely new approach to using BGs as a therapeutic agent.

Table 2.1. Differences between healthy ASCs and diabetic ASCs (dASCs).

dASCs has similar effect as healthy ASCs in:	**dASCs showed different effects in:**
• Expression of PDL-1, NOS-2, IL-10, PIGES, TGFβ-1, PDL-2, HLAG, TGS6 genes. • Glucose Production. • HeLa cell growth. • Chondrogenesis. [56,57,58,63,68,71,73]	• Expression of CD34, VEGF and MDA • Proliferation, Adipogenesis and Osteogenesis (discrepancies in the literature =, ↑, ↓) [55,56,57,58,61,62,67,72,73]
dASCs showed increase in the expression of:	**dASCs showed decrease in the expression of:**
• P16, P27, P53, MAP-2, PIGF, HGF, THBSI, INCR, NCAM1, NCAM-5 [62,65,71]. • Vimentin, Nestin, Smooth muscle actin, Fibronectin, E-Cadherin, PECAM-1, ITAGV [68]. • OCT4, Nanog, SOX-2, PAI-1, miRNA-3P & 15-5P, LC3, BECLIN1, P62 [59,62]. • Degrade fibrin [59]. • Glucose Intake [61,70].	• SOP, GSH, CAT-enzyme, FGF2, PFGF, tPA, PDGF-a, SDF-1, CXCR4, FGTR-2, PDGF-Ra, SDF-1, IGFbb, MCP-1, vWF, CD31, MMP-2, MMP-9, Ang-1, Ang-2 [55,56,60,63,66,67,73]. • Telomere length [64] • Migration to SDF-1, VEGF [72]. • CFU [64,66]. • EC tube formation/ Sprout formation [56,60,62,69].

- As previously mentioned, there is an increased interest in using medically relevant ions in BGs. These ions, when added in small amounts, are called dopants. There is controversy in literature on the effects of some ions, like B, on ASCs and other cells. Meanwhile, other ions have little to no studies on their biological functions. A future direction of this work, which I have already begun (Appendix), is to perform a meta-analysis of medically relevant ions in literature and their effects on ASCs. This will help material scientists to know what dopants to use, in what amounts, and for which applications.
- A recent article presented a novel machine learning (ML) model that has the possibility of predicting BGs dissolution behavior and resulting pH using a database of more than 1300 experimentally obtained, distinct data records. This ML model could be beneficial in future applications to design novel BGs with desired properties for the clinic [54].

Table A.1. Boron

Trace element	Ref.	Cells					Media		Protocol				Results
		Type	Species	Donor Age	Donor Sex	Passage	Basal media	Serum	Material's Form	Material's Conc.	Applications	Conditions	
Boron	1	AdMSC (Adipose tissue-Mesenchymal Stem Cells)	Rat	2-5 months	NA	Adipose tissues are collected from subcutaneous, gonadal and surrounding the kidneys.	α-MEM	15% FBS.	**For 2D application,** Boric acid (H_3BO_3) was prepared as a solution.	Cells were seeded at the density of $5x10^3$ cells/cm^2 Three different concentrations of boron were prepared (1, 10, 20 μg/ml)	Cells cultured with growth medium containing 3 different conc. of B for 24 hr.	Static Culture.	• B has not any toxic effect on AdMSCs even in the highest concentration • B promotes osteogenic differentiation of AdMSCs. • The results of Presto Blue analyses showed that the cell viability increased in each group with time. • It was remarkable that 20 μg/mL B concentration enhanced the expression of Col1A1 and RunX2at day 7 and 14.
									For 3D application, Ch scaffolds combined with hydroxyapatite (HAp) and B containing hydroxyapatite (B-HAp) (B-HAp/Ch) was prepared by freeze-drying method.	50 μL suspension of AdMSCs at a conc. of $2.5x10^5$ cells/scaffold were seeded into B-HAp/Ch scaffolds.	Cells seeded in the scaffolds were incubated in the presence of growth medium at 37°C in 5% CO_2 atmosphere for 5 days	NA	• AdMSCs expressed the typical MSC marker proteins CD29, CD90, CD54 and CD106. • Expression of the endothelial lineage and hematopoietic lineage markers CD45 and CD11b were lack of expression • There were much more ECM synthesis and collagen production in induced group when compared to unstable pellets in control group • A few numbers of AdMSCs attached onto Ch scaffolds and exhibited rounded shape, however, a high number of AdMSCs

Table A.1. Boron (cont.)

													attached onto HAp/Ch and B-HAp/Ch scaffolds. • B-HAp/Ch scaffolds affects adhesion, proliferation and osteogenic differentiation of AdMSCs. • Boron scaffolds (B-HAp/Ch) is believed to be more effective for the osteogenic differentiation of AdMSCs than Ch and HAp/Ch scaffolds. • Comparison of SEM results concluded that the most secreted ECM and calcium phosphate mineralization were observed on B-HAp/Ch scaffolds. • There was no significant difference for osteonectin expressions level between HAp/Ch and B-HAp/Ch groups at the day 14[th]. While osteopontin expressions increased on the 28th day of culture in both groups.
Boric Acid	2	hADSCs (Human Adipose derived Stem Cells)	Human	45 years old	Female	Human adipose tissue was obtained from a lipoaspirate. Cells from passage 3 were used.	DMEM	10 % FBS and 1 % PSA (Penicillin/Streptomycin/ Ampicillin)	Main stock solution of Boric acid was prepared in the culture medium concentration of 10 mg/ml (163.9 mM)	11 separate concentrations between 5 and 2000 µg/ml (5, 10, 20, 50, 100, 200, 250, 500, 700, 1000, 2000 µg/ml) of boric acid were prepared in culture medium hADSCs (passage 3) were seeded onto 96-well plates at a cell density of 3×10^3 cells/well.	Incubation periods (3 days) are 24, 48, and 72 h, 10 µL of MTS reagent in 100 µL of growth medium was added to each well, and the plate was incubated for 2 h at 37 °C	NA	• Flow cytometry results revealed that hADSCs were positive for MSCs surface antigens (CD29, CD73, CD90, CD105, and CD166) and negative for hematopoietic markers (CD34, CD45, and CD14) • Cells were positively immunostained with osteocalcin and calcium depositions, collagen II and lipid droplets to confirm the osteogenic, chondrogenic and adipogenic differentiation. • No cytotoxicity was observed for any boric acid concentrations.

Table A.1. Boron (cont.)

													• 5 and 50 µg/ml of boric acid significantly increased cell viability and did not exert any cytotoxicity. • It shows the positive MyoD, MYH, and α-SMA staining of transformed cells; 50 µg/ml boric acid application exhibited slight decrease in protein expression for MyoD and α-SMA compared to the control • Study shows that high-dose boron treatment significantly decreased the myogenic differentiation potential of hADSCs. • Results proposed that low-dose boron could be used in muscle regeneration applications.
Boron Nitride Nanotubes (BNNT)	3	Bone marrow MSCs	Rats	NA	NA	Bone marrow MSCs were obtained from bilateral femora from syngeneic rats. Both ends of the rat femora were cut away from the epiphysis.	MEME	10% FBS and 1% PSA	BNNTs used in this study were synthesized by a chemical vapor deposition method using boron and metal oxide as precursors. A certain amount of BNNTs suspension was dropped onto cover glasses treated beforehand with the piranha solution.	About 1 mL of MSCs suspension, about 10^4 cells mL^{-1} in culture medium, was poured on the BNNT layer coated plate.	The MSCs attached to the BNNT layer coated plate were cultured in 5% CO_2 at 37 °C for 7 and 14 days. The culture medium was replaced with a fresh one every 3 days.	NA	• Quantitative measurements indicated that BNNTs layer on cover glass had showed higher proteins (fibrinogen, laminin and fibronectin) adsorption ability than cover glass control. • BNNTs layer promoted proliferation, total protein and osteogenic differentiation of MSCs • The number of MSCs on BNNTs layer with 5 µg mL^{-1} concentration is the highest among the data after 14 days of culture. • MSCs on the BNNTs layer with a low BNNT content show higher ALP activity than the controls after 7 days of culture. • MSCs on the BNNTs layer showed significantly increased OCN protein concentration, a late marker of osteogenic differentiation

Table A.1. Boron (cont.)

													• For human bone marrow stromal cells (BMSCs), at low concentrations of boron (1, 10, and 100 ng mL^{-1}) increased osteogenic differentiation, and at a high concentration of boron (1000 ng mL^{-1}) inhibited proliferation of BMSCs.
Sodium pentaborate pentahydrate (NaB)	4	hADSCs	Human	NA	7 males	Fat tissue was obtained from 7 male patients treated surgically for gynecomastia. hADSCs from passages 4–6 were used in all experiments.	DMEM	10% FBS and 1% PSA	NaB were prepared in complete growth medium.	Five concentrations of NaB were tested (10, 20, 50, 100, and 150 µg/mL). Cells were seeded in 96-well-plates at a density of 5,000 cells/well	In the 2nd day, cells were treated with different concentrations of NaB. Cells were incubated with NaB for 24, 48, and 72 h.	NA	• Cells were positive for CD29, CD44, CD73, CD90, and CD105, MSC surface markers, whereas they were negative for CD14, CD34, and CD45, hematopoietic stem cell (HSC), surface markers, and for CD31, endothelial cell marker • Cells treated with NaB showed lower mRNA expression levels for adiponectin, adipocyte protein 2 (aP2), Lipoprotein lipase (LPL), CEBP α, and peroxisome proliferator-activated receptor γ (PPAR-γ), compared to the levels detected in the PC at all concentrations of NaB (20, 50, and 100 µg/mL (68, 170, and 340 µM). • None of the five NaB conc. tested was found to be toxic to hADSCs. Although, NaB increased the survival of cells. • Adipogenic differentiation capacity of hADSCs is suppressed by the NaB treatment in a dose-dependent manner
	5	hTGSCs (Human Tooth Germ Stem Cells)	Human	15 years old	NA	hTGSCs were isolated from the tooth germ of a patient.	DMEM	10% FBS and 1% PSA	NaB was dissolved in the culture medium at a 0.1 g/ml stock concentration.	13 separates NaB concentrations between (5–700 µg/ml) were prepared in culture medium	Cryopreserved cells were thawed 1 day or 6 months after each cryopreservati	Cells were cryopreserved in freezing medium containing	• Cells were proven to be positive for MSCs markers (CD29, CD73, CD90, CD105, and CD166) and negative for hematopoietic markers (CD34, CD45, and CD14).

Table A.1. Boron (cont.)

						hTGSCs at passage number 2 were used.				Cells were seeded onto 96-well plates at a conc. of $5x10^3$ cells/well followed by the addition of NaB.	on cycle for short- and long-term cryopreservation. 1×10^6 cells were cryopreserved for each freeze–thaw cycle when the cells reached 80% confluence after thawing.	20 µg/ml NaB, 20% FBS, 1% of PSA, and 5 different Me_2SO concentrations (10%, 7%, 5%, 3%, 0%)	• Concentrations higher than 200 µg/ml exerted cytotoxic effects, however, lower conc. Of NaB (20 µg/ml) shows non toxic effect and was chosen for cryopreservation experiments. • 0–3% of Me2SO (Cryopreservation) appeared to be toxic on the all freeze–thaw groups (repeated cycles and long-term freezing), whereas 5% Me2SO group displayed less toxic effects in the presence of NaB. 5% Me2SO was chosen for the differentiation experiments. • After long-term cryopreservation, hTGSCs were differentiated into the osteogenic, chondrogenic and adipogenic cell lineages to show MSC characteristics.

Table A.2. Barium

Trace element	Ref.	Cells					Media		Protocol				Results
		Type	Species	Donor Age	Donor Sex	Passage	Basal media	Serum	Material's Form	Material's Conc.	Applications	Conditions	
Barium Titanate Nano-particles (BTNPs)	6	MSCs	Rat	NA	NA	NA	DMEM	10% FBS and 1% PSA	BTNPs were purchased as a dry sample and then stabilized in an aqueous environment of non-covalent Glycol Chitosan (GC).	Six concentrations of GC-BTNPS were prepared (0, 5, 10, 20, 50 and 100 µg/ml)	MSCs were incubated with GC-BTNPs for 24, 72 and 120 h. Cells were cultured on glass coverslips (12 mm in	Static Culture	• MSCs were differentiated into adipocytes after 14 days of culture. • Viability of MSCs following exposure to increasing concentrations of barium

Table A.2. Barium (cont.)

											diameter) at a density of 15.000 cells/cm^2 Interaction of MSCs with GC-BTNPs was investigated after a 24 h incubation at increasing concentrations of nanoparticles.		titanate nanoparticles resulted excellent up to 100 µg/ml • Viability and proliferation of the MSCs were not affected by the presence of high conc. up to 100 µg/ml of glycol–chitosan coated BTNPs in the culture medium.
BTNPs with Hyper gravity Effect	7	MSCs	Rat	NA	NA	MSCs from the second passage were used in all experiments.	DMEM	10% FBS and 100 U/mL penicillin, 100 mg/mL streptomycin, and 200 mM glutamine	MSCs were trypsinized and seeded on glass slides (diameter 13 mm) 48 hours before hypergravity treatment	Both proliferating and differentiating were done at 20 µg/mL of BTNPs Cells were seeded at 10,000/cm$_2$ for tests in proliferation conditions and at 30,000/cm$_2$ for tests under osteogenic dif-ferentiation.	Cells were seeded in glass slides then provided with BTNPs (20 µg/mL) before applying the hypergravity treatment.	Swing gondola is used to support hyper gravity levels between 1g and 20g.	• Hypergravity stimulation and BTNPs administration enhance the osteogenesis of the MSCs. • Short treatment (3 hours) at 20 g combined with incubation with 20 µg/mL of BTNPs promoted the osteogenesis of MSCs • RUNX2 was significantly upregulated in 20 g-treated samples while COL1A1 transcription was significantly enhanced (1.5-fold) only in the double-stimulation 20 g + BTNPs. • ALPL was significantly upregulated (1.6-fold) when cells were synergistically stimulated with hypergravity and NPs.
BTNPs (Electro-active fibrous PLLA "Poly-L-Lactic acid"	8	BM-MSCs	Rat	NA	NA	Cells from passages 3 to 5 were used for the following experiments.	DMEM	10% FBS and 100 IU/mL PS. Media changed	BTNPs surface modification was done by using sodium citrate solution and then dispersed into the PLLA solution to form	The BTO contents were set as 1, 3, 5, 7, and 10 wt % of the PLLA	BM-MSCs were seeded onto experimental scaffolds in 12-well plates (5×10^4 cells/well)	NA	• The optimal BTNPs content in the PLLA fibrous scaffolds is at 7 wt.%. • The randomly oriented composite fibrous scaffolds significantly encouraged polygonal spreading and early

Table A.2. Barium (cont.)

scaffolds with Ferroelectric ceramic BTNPs)								every 2-3 days	BTO/PLLA solution. Then electrospinning was performed using two different collectors (plate and rolling collectors).		Cell proliferation were done at 1,3,5,7 days of culture.		osteogenic differentiation of BM-MSCs, So, it will have promising potential for bone generation applications. • The aligned composite fibrous scaffolds increased cell elongation and discouraged osteogenic differentiation of BM-MSCs.
Barium chloride and strontium chloride ($BaCl_2$+ $SrCl_2$)	[9]	BM-MSCs	Human	NA	NA	When culture dishes became near-confluent, cells were passaged and plated into 6-well culture dishes at an initial density of 25,000 cells/well.	DMEM	10% FBS and 100 U penicillin/mL, and 100 µg/mL of streptomycin.	NA	Different concentrations of BaCl2 (0.1, 0.3, or 1 mM) and SrCl2 (0.1, 0.3, and 1 mM).	Cells were plated into culture plates (150 mm in diameter) at a density of $2x10^6$. Media changes were performed twice weekly. Cell layers were fixed or harvested after 1, 3, 7, or 14 days in culture	NA	• Barium and strontium had a superior enhancing effect on cell proliferation. • Barium-like strontium is considered one of the important factors in inducing mesenchymal stem cells to differentiate into osteoblasts with further enhancement on bone formation.

Table A.3. Cobalt (cont.)

Trace element	Ref.	Cells					Media		Protocol				Results
		Type	Species	Donor Age	Donor Sex	Passage	Basal media	Serum	Material's Form	Material's Conc.	Applications	Conditions	
Cobalt Chloride ($CoCl_2$)	10	MSCs ADMSCS (Adipose MSCs) DPMSCs (Dental Pulp MSCs) UCMSCs (Umbilical cord MSCs)	Human	NA	NA	DPMSCs were obtained from healthy permanent premolars extracted during orthodontic treatment. UBMSCs were obtained from the tissue of umbilical cords of full-term pregnancies. All the cells were used between passages 4 and 7.	DMEM/F 12 Culture media changed to fresh MEM	10% FBS and 1% PS. Then changed to 2% FBS and 1% antibiotics	NA	The cells were seeded in 96-well culture plates at a density of 1×10^4 cells/well for 24 hr. The culture media changed, then cells were treated with different concentrations of $CoCl_2$ ranging from 50 to 400 μM..	The MSCs were treated with 100 μM CoCl2 for 6 h, 12 h, 24 h, and 48 h,	NA	• The highest cell viability was obtained at 100 µM of $CoCl_2$, after 24 h and 48 h in all the three MSCs tested. • The UCMSCs are more prone to chondrogenic differentiation and to nonhypertrophic chondrogenesis, compared to the DPMSCs and ADMSCs. • It was found that these cells were highly positive for CD105, CD73, and CD90 (>95%) and negative for CD34, CD19, CD45, CD14, and HLA-DR (<3%). • Densitometric analysis of protein bands showed a time-dependent upregulation of HIF-1α in DPMSCs and UCMSCs, while no significant difference was evaluated in ADMSCs. • DMSCs showed upregulation od SOX9 followed by reduction in expression after 14,21 and 28 days, and showed upregulation of VCAN after 7,14,21 and 28 days, and showed no amplification for COL2A1 and ACAN. • UCMSCs showed a time-dependent upregulation of all chondrogenic markers tested

Table A.3. Cobalt (cont.)

													(SOX9 – COL2A1 – VCAN – and ACAN). • ADMSCs showed a constant expression of SOX9 and ACAN compared to control and showed upregulation of expression for COL2A1 and ACAN.
	11	MSCs (C3H/10T 1/2 cell line)	Murine	Embryo	NA	Experiments were used from 5th to 15th passages.	DMEM	10% FBS and 1% PS Serum in culture media changed to 2% FBS and 1% antibiotics.	$CoCl_2$ dissolved in DMEM containing 2% FBS immediately before use.	Cells were seeded in 96-well culture plates at a density of 0.5×10^4 cells/100 ml in each well.	Cells were incubated in growth media for 24 hr and then incubated in growth media for 24 hr and then treated with 0.1~5 mM $CoCl_2$. For differentiation, cells were pre-incubated with 0.1 mM CoCl2 for 0, 24, or 48 h.	NA	• $CoCl_2$ did not affect the viability of MSC cells concentrations <0.25 mM while viability decreased in a dose-dependent manner at 0.5, 1, and 5 mM $CoCl_2$ • Expression of HIF-1α mRNA was significantly increased at 24 h compared to the control • RT-PCR revealed the significant up-regulation of the expression of osteogenic markers (Col I, ALP and Runx2) in CoCl2 treated group compared with control. • The expressions of osteocalcin (OCN) and osteopontin (OPN) mRNA were slightly affected by treatment of CoCl2. • In pre-incubation with CoCl2, the results indicate that treatment of CoCl2 partially enhances osteogenic differentiation and matrix mineralization on C3H/10T1/2 cells • For chondrocyte markers, SOX9 was slightly increased at 24 h of CoCl2 incubation, while the mRNA level of Aggrecan and Col 2A, the

Table A.3. Cobalt (cont.)

													downstream targets of Sox9, were significantly up-regulated in CoCl2 treated cells at 48 h of CoCl2 incubation. • Both of CoCl2 treated group significantly inhibited proliferation of cell and lipid formation compare to the control group. • For adipogenic markers, PPARγ was significantly decreased in both CoCl2 treatment groups. Also, the mRNA expression level of the downstream of PPARγ, aP2 and C/EBPα were also strongly down-regulated in treatment of CoCl2 group compared with the control • Treatment of $CoCl_2$ enhanced differentiation to osteoblasts and chondrocytes and suppressed differentiation to adipocytes.
	12	UCB-MSCs (Umbilical cord blood derived-MSCs)	Human	New-born baby	NA	Cells were isolated from umbilical cord vein of a newborn baby All experiments were performed with cells that were passaged 5–8 times.	α-MEM	10% FBS and gentamicin	$CoCl_2$ stock solution was prepared by dissolving directly in distilled water (100 mM).	$CoCl_2$ was added into the medium at 100 μM. Cells were tested with different concentrations of $CoCl_2$ (0, 0.01, 0.1, 1, 10, 100 μM).	Cells were incubated in the presence of $CoCl_2$ for the indicated times. UCB-MSCs were seeded in 96-well plates and incubated for 24 hr. The cells were treated with various concentrations of $CoCl_2$ for 72 hr.	NA	• For the effects of CoCl2 on the immunomodulatory properties of hUCB-MSCs, MLR was performed, so when CoCl2-treated hUCB-MSCs were cocultured with allogeneic hPBMCs or PHA, the proliferation and cluster formation of T cells decreased compared with that of naïve hUCB-MSCs. • CoCl2-treated hUCB-MSCs highly expressed the anti-inflammatory mediator PGE2, whereas expression levels of the proinflammatory cytokines TNF-α and IFN-γ were

Table A.3. Cobalt (cont.)

													relatively lower than those in the control group. • Treatment with CoCl2 had no effect on the morphology or viability of hUCB-MSCs. • FACS analysis showed that CoCl2-treated hUCB-MSCs expressed the MSC-specific markers CD90, CD105, CD166, and CD73, but not CD14, CD45, CD34, and HLA-DR. • Pretreatment of hUCB-MSCs with $CoCl_2$ improves the therapeutic effects of MSCs for the clinical application of allogeneic cell therapies.
Cobalt manganese ferrite nanoparticles ($Co_{0.2}Mn_{0.8}Fe_2O_4$)	13	ASCs (Adipose derived mesenchymal stromal stem cells) And Canine Mastocytoma cell line	Dog	NA	NA	MSCs were isolated from sub-cutaneous adipose tissue (2 g) collected from the dogs' tail bases.	ASCs were cultured in DMEM C2 cell line were cultured in EMEM	10% FBS and 1% PS. For C2 Cell line, 5% FBS and 1% non-essential amino acids, 50 mg/ml gentamicin, 1% L-glutamine	The preparation of CMF NP involved the following quantities of reactants: 0.1131 g of $Co(acac)_2$, 0.4455 g $Mn(acac)_2$ and 1.5651 g $Fe(acac)_3$.	C2 and ASC cells were inoculated into 24-well plates at an initial concentration $2x10^4$ per well.	Cells were incubated for 24,48 and 72 hrs. The analysis of cell morphology and growth pattern was performed on the 7th day	Static Magnetic Field	• Cobalt-manganese ferrite nanoparticles are potentially an effective tool for hyperthermic treatment of dog skin Mastocytoma. • Stimulation of ASCs with MNPs resulted in an inhibition of proliferation at all time points examined.
Calcium/ Cobalt Alginate Beads	14	ADSCs	Human	NA	NA	The hADSCs from passages 3–7 were used for further study.	DMEM	10% FBS and 1% PS	$CoCl_2$ and $CaCl_2$ were used as solutions.	Four conc. of $CoCl_2$ (10, 5, 2.5, and 1.25mM), and standard conc. of $CaCl_2$ (200mM) and all of them were encapsulated	Cells within the beads were cultured for 7, 14, and 21 days, and the medium was changed every 3-4 days.	NA	• The Co1.25 sample exhibited strong upregulation of Sox9 and versican gene expression at 14 days, however, Sox9 and versican mRNA expression levels were similar to control levels at day 21, and HIF-1 and collagen type II gene

Table A.3. Cobalt (cont.)

										in sodium alginate beads.			expression did not vary significantly over the course of the experiment • This strategy exploits the synergic actions of Co^{+2} and alginate and does not include traditional differentiation-promoting growth factors. • This study shows a novel and low-cost approach to induce in vitro chondrogenic diff. of MSCs encapsulated within alginate beads.
Micro/Nano-particles **(Iron/Nickel and Cobalt MP and NP)**	15	hASCs	Human	Average Age (43-4)	5 healthy women	All patients were in good health who have not undergone to heavy weight loss diet, non-smokers, without a history of metabolic disorders, and not receiving medications at the time of surgery. For all subsequent experiments hASCs were used at passage 5.	Cells were divided into 2 fractions each seeded in different medias: 1st fraction seeded in 1:1 DMEM/DMEM-F12 medium 2nd fraction seeded in CHANG C medium	1st fraction: 10% FBS, 2 mM L-glutamine, 1% PS, and 0.1% gentamicin 2nd fraction: 2 mM L-glutamine, 1% PS.	MPs and NPs were resuspended in fresh culture media before each treatment.	4 different concentrations of Fe, Co, and Ni MPs and NPs are used (0, 0.5, 1, 3 µg/ 200 µL)	300 cells were seeded into 96-well plates and treated after 24 h. Cells were exposed for 96 h in increasing concentrations of Fe, Co, or Ni MPs and NPs	Static conditions	• In most cases, concentration-dependent, no differences were evidenced between the two-culture media. • Fe MPs showed high cell toxicity while Ni MPs showed no effect. • Co MPs, NPs, and $CoCl_2$ elicited a dose-dependent response similar in all the three formulations • NiNPs exposure showed a cell toxicity comparable to that of CoNPs. • The experiments confirmed the cell viability for NP formulation whose cytotoxicity ranking was CoNPs > NiNPs > FeNPs, conversely, hASCs appeared more sensitive to NP exposure. • Fe MPs induced upregulation of VEGFA, IL8, IL1b and a downregulation of SOD after 96 h of exposure.

Table A.3. Cobalt (cont.)

													• Fe in all its formulation induced the expression of AP2A1, and upregulation of IL1b and BCL2. • Cobalt caused only the downregulation of interleukin 6 (IL6) expression after 96 h of exposure
Cobalt Containing Bioactive Glass (CoBG)	16	BM-MSCs	Human	NA	NA	For chondrogenic differentiation, passage 3 were used but for all other experiments, hMSCs used at passages 5–6	α-MEM	10% FBS 1 ng/μL bFGF 1% PS.	Cobalt is used in the experiment as Cobalt Bioactive Glass (CoBG)	The glass particle size used in this study was <38 μm in diameter (d= 0.9) Increasing amounts of cobalt were incorporated into the composition. The bioactive glasses are referred to as 0%CoBG, 1%CoBG, 1.5%CoBG and 2%CoBG according to their molar cobalt content or as CoBGs.	After 3 days of culturing, the medium was replaced with 1 mL of control or the various CoBG-conditioned media all containing chondrogenic supplements. The pellets were continuously cultured in the 1.5 mL microcentrifuge tubes and the medium were changed every 2–3 days.		• Exposure to 1.5%CoBG, 2%CoBG as well as the 100 μM and 200 μM CoCl2 positive control conditions led to a significant increase in the amount of HIF-1α protein compared to control medium and 0%CoBG (in order to assess whether the CoBG dissolution products mimicked hypoxia in hMSCs) • No significant differences in metabolic activity were observed after 24 h and 4 days of treating hMSCs with CoBG-conditioned media as well as 100 μM CoCl2. • After 7 days of treatment, the metabolic activity of hMSCs cultured in 2%CoBG-conditioned medium was significantly lower than in control and 0%CoBG. • Overall, metabolic activity increased over time for all conditions except for 2%CoBG which maintained its metabolic activity level from 24 h. • There were no differences in cell morphology observed

Table A.3. Cobalt (cont.)

													between conditions; however, cell density appeared to be reduced in presence of 1.5%CoBG and 2%CoBG dissolution products after 7 days of culture compared to the other conditions • hMSCs produced significantly more VEGF in presence of CoBG extracts. • The cobalt incorporation into BGs dose-dependently reduced chondrogenic differentiation of hMSCs. • In the presence of 0% CoBG dissolution products cell proliferation seemed enhanced and commitment to the chondrogenic lineage.

Table A.3. Cobalt (cont.)

Cobalt Chromium Alloys **(CoCr Alloys)**	17	MSC	Human	3 healthy donors	NA	NA	MSCs Growth Medium	NA	MSC were seeded at 6.1×10^3 cells/cm^2. CoCr were used as an alloy	MSC were incubated with 10 µM. 40 µM or 100 µM $CoCl_2$. Cells differentiated without $CoCl_2$ served as negative control.	Analysis was done at week 1, 2, 3, 4, and/or 5 **Note:** **OS-**: un-differentiated control cells, **OS+**: osteogenic differentiated cells	NA	• Treatment with 10, 40, and 100 mM CoCl2 decreased the cell number of OS- MSC in a concentration dependent manner while cell number for OS+ MSC was reduced permanently only at 100mM CoCl2. • The ALP activity was decreased in OS+ MSC for all CoCl2 concentrations at day 7. • In OS+ MSC, the expression of Runx2 was unaffected by most Co (II) concentrations and only significantly reduced in two of the three donors in the 100mM CoCl2 group at day 2. • Also, the expression of IBSP was induced up to 25fold for two of three donors at day 14 and up to 30fold for all donors at day 21 in the differentiation group without CoCl2, • The supplementation with 40mM Co (II) ions and more over 14 and 21 days reduced IBSP expression as compared to the non-supplemented group • The OCN production showed high variability in cells treated with 10 and 40mM CoCl2 and significant reduction in OCN amounts were found for 100mM CoCl2.

Table A.3. Cobalt (cont.)

CoCrMo, TiO_2-coated CoCrMo (CCMT) and Ti substrates	18	MSCs	Human	3 donors	NA	Only cells of low passage (<5) were used to ensure integrity of the results	α-MEM	10% FBS and 1% PS.	CoCrMo discs of 15 mm Ø and 1 mm thickness were used. MSCs from three donors were seeded at a density of 12.5×10^3 cells per well in Osteogenic media	Cells were examined at 7, 14, and 21 days after incubation with OM.	Media over cells changed every 3 or 4 days.	Static Conditions	• After 7 days in osteogenic culture, it was apparent that COL-I deposition was significantly enhanced on the CoCrMo surface, shown by the presence of dense collagen fibrils which were not present to the same extent on either CCMT or Ti. • After 14 days, CMT was shown to have significantly more COL-I per cell deposited compared to Ti, while not to the same level as CoCrMo. • Ti promoted the greatest amount of HA formation throughout the 3-week time course, being statistically significant over both materials at 2 weeks and CoCrMo at 3 weeks. • After 2 weeks in osteogenic culture CCMT and Ti had significantly greater calcium ion content per cell in comparison against CoCrMo, implying MSCs on these substrates are differentiating at a faster rate and producing more mineralized tissue. • Ti appeared to promote the greatest expression of vinculin at both time points and was judged to be statistically significant against CoCrMo at 24 h, while CCMT appeared to have greater vinculin expression than CoCrMo at both 3 and 24 h, although to a lesser extent than that found on Ti.

Table A.3. Cobalt (cont.)

													• Both markers of adhesion and osteogenesis were enhanced on CCMT compared to CoCrMo, implying TiO_2 coatings may be potentially influential in the future for improving the efficacy of orthopedic implants formed of nonbioactive materials such as CoCrMo.

Table A.4. Cupper

Trace element	Ref.	Cells					Media		Protocol				Results
		Type	Species	Donor Age	Donor Sex	Passage	Basal media	Serum	Material's Form	Material's Conc.	Applications	Conditions	
Cupper combined with electric field	19	ADSCs	Human	Age between 52 ± 12 years.	3 Female	ADSCs were isolated from adipose tissue samples collected from the subcutis/pelvic region or breast of female patients. Cells were isolated and characterized at passage 5–6.	DMEM/F-12 1:1	10% FBS with 1% PS and 1% glutamax.	Electrodes coated with copper and copper containing medium. Silver wire was used as a reference electrode.	A three-electrode system was used for the application of the current. The electrodes were first coated with copper, then cut to the desired size, and thus the copper coating was exposed.	Cells were magnetically stirred in a tube, and were subjected to electric current and/or copper for 1 h. ADSCs were stimulated with two different current densities with corresponding copper concentrations and with	Static ADSCs were stimulated for 1 h with copper, current or both. Copper was released to the cell suspension either abruptly or gradually via electrolysis	• Cell viability reduced measured right before and immediately after the 1 h stimulation but there was no significant difference in the cell viability between the different stimulation conditions. • By day 4, cells stimulated with 1 mA alone or Cu + 1 mA had proliferated less than the control cells or cells stimulated with Cu + 1.5 mA or copper alone. • Elongation of Cells was seen already at day 4 when the cells were exposed to current with or without the copper. • Many cells showed neuron-like morphology with branches from the cell body at the 14 days.

Table A.4. Cupper (cont.)

											copper or current alone. Cells were seeded in chamber slides for 4, 7, and 14 day	Current used was 1 or 1.5 mA applied through copper-containing electrodes or 1 mA applied through pure platinum electrodes.	• Control cells and cells stimulated with copper alone maintained their adipose-like morphology • The highest expression of beta-tubulin isotype III (a marker for immature neurons) was observed at day 7 when cells were stimulated with Cu + 1.5 mA. • The highest expression of MAP-2 (a mature neuronal marker) was observed in cells stimulated with Cu + 1.5 mA while Control cells and cells stimulated with copper alone showed no MAP-2 expression in any time points • **Summary:** only when ADSCs were stimulated with both copper and current (1 or 1.5 mA), there was a positive expression of both beta-tubulin isotype III and MAP-2. Also, the highest expressions of both antibodies were detected when the stimulation combined both copper and current. • Stimulation with electric fields combined with release of copper could provide a feasible, non-expensive, growth factor-free method for the differentiation of ADSCs toward the neuronal lineage indicated by morphological changes and upregulation of neuron-specific genes and proteins.
Metal ion (Zn, Ag & Cu) doped in hydroxyapatite Nano-coated surfaces	20	hMSCs (adipose tissue derived MSCs)	Human	NA	NA	hMSCs were used at passage 4 and 5for all experiments	MSC Basal Medium Then replaced with α-MEM	2% growth kit-low serum Then 10% FBS, 5 ng/ml of bFGF, 1% PS	Pure HAP and metal ions ceramic powders were synthesized with a wet chemical method.	NA	hMSCs were seeded in 24-multiwell plates that included coated cover slips, in 1000 L media containing $4x10^4$cells,	Static	• Cell viabilities were higher than 95% after up to 28 days on HAP-Ag, HAP-ZAg and HAPZAg-Cu surfaces. • Cell viability increased at day 1 and day 7 on all surfaces compared to the control in both OS+ and OS- groups. (OS=Osteogenic supplemented media).

Table A.4. Cupper (cont.)

HAP-Com; Hydroxyapatite Commercial. HAP-Ag; Hydroxyapatite Silver. HAP-ZAg; Hydroxyapatite -Zinc/Silver. HAP-ZAgCu; Hydroxyapatite Zinc/Silver/Copper								and 0.5% Fungizone	Cover slips coated with HAP-Com, HAP-Ag, HAP-ZAg and HAP-ZAgCu were placed into the 24 well plate.		and incubated for 1, 7, 21 and 28 days. Uncoated cover slip was used as a control surface.		• The calcium deposit on HAP-ZAgCu was the highest among all surfaces in both conditions. Also, without osteogenic inducement (OS-), calcium deposition ratio was very high on all of surfaces compared to the polystyrene surfaces. • The Nano-powders are biocompatible and have no negative effects on the hMSCs proliferation and osteoblastic differentiation in vitro. • hMSCs can differentiate to osteoblast on HAP-Com., HAP-Ag, HAP-ZAg and HAP-ZAgCu surfaces without exogenous osteogenic stimulation. • ALP activity was significantly higher in hMSCs grown on HAP-Ag, which was 20% more than the hMSCs grown on HAP-Com for OS+ group
Zn–Cu imidazole MOF coated PLLA scaffolds. (MOF= Metal-organic framework)	21	MSCs (adipose tissue-derived MSCs)	Human	NA	NA	The adipose tissue was gathered from cosmetic liposuction of 10 different volunteers. The cells were sub-cultured until passage number 5.	DMEM	10% FBS	Zn–Cu imidazole MOF particles were synthesized by dissolving powders in a solution. Then PLLA scaffolds were also synthesized .	The scaffolds were cut into 1.5 mm diameter circular pieces, then put into 24 well tissue culture plate (TCP). An initial density of 5 × 103 cells was seeded on each scaffold for assessment of cell attachment and proliferation.	The cell loaded scaffolds were refreshed with DMEM including 10% MTT solution after 24 hr. for cell adhesion and on days 1, 4, and 7 for cell proliferation assay.	Electro-spinning conditions.	• PLLA@MOF showed a smaller number of cells than pure PLLA scaffolds and TCP. • The ALP activity in all kinds of scaffolds increased from day 7 to day 14, but then reduced in the 21st day. • PLLA@MOF showed significantly highest ALP activity on the 7th and 14th day than pure PLLA scaffolds and TCP • Zn–Cu imidazole MOF coated PLLA scaffolds (PLLA@MOF) showed better osteogenesis of human adipose tissue-derived MSCs compared with pure PLLA scaffold and TCPs due to improving the surface bioactivity

Table A.4. Cupper (cont.)

Cupper	22	Bone marrow MSCs	Rat	Cells were harvested from (4 to 7 day-old) SD rats	Female	rBMSCs from the third passage were used.	DMEM-L	10% FBS and 1% antibiotic-antimycotic.	Cupper is used in the form of $CuSO_4$ 6 conc. of $CuSO_4$ were used (0, 0.5, 5, 10, 25, 50 and 100 µmol/l).	Cells were seeded into 3.5 mm dishes at 20 000 cells/dish in culture media then divided into 4 groups next day. Control group: Cells cultured in growth media Cupper group: Cells cultured in GM with $CuSO_4$ Osteo group: Cells cultured in osteogenic M. Osteo-Cu group: Cells cultured in OM+$CuSO_4$.	Cells in each group were incubated for periods of time as indicated*. rBMSCs were exposed to various conc. of CuSO4 for a total of 48 h	Static	• More than 95% of the cells were positive for expression of CD29 and CD90, while fewer than 2% expressed detectable levels of CD34 and CD45. • By the confirmation of some staining procedures, rBMSCs readily differentiated into bone, cartilage and fat cells. • Copper supplementation had no significant impact at concentrations between 0 and 5 µmol/l, but had cytotoxic effects at concentrations above 10 µmol/l. • After 3 weeks osteogenic differentiation, bone nodules became noticeable only in the Osteo group, but not in control, copper-treated and Osteo+Cu groups. • The expressions of Runx2, OSX, ALP, BMP2, OCN, OPN, Col III and Col I in the Osteo+Cu group were lower than those in the Osteo group which suggested that the expression of osteogenic differentiation-related genes had been downregulated by copper. • In the Osteo+Cu group, expression of PPARc2 and TWIST were higher compared to the Osteo group. • Copper suppressed osteogenic differentiation of rBMSCs. When the cells were cultured in osteogenic differentiation-inducing medium, they had lower expression of osteogenesis-related genes, which in turn can suppress accumulation of collagen during the bone formation process.

Table A.4. Cupper (cont.)

Cupper & Cupper-Alginate Scaffolds	23	MSCs (C57BL/6 mice) Cell line	Mice	NA	NA	MSCs at 3 passages were used in the experiment.	L-DMEM	5% FBS	Copper were added by 2 methods: as $CuSO_4$ solution and as Cu/Alg scaffolds.	5 groups with different concentrations of $CuSO_4$ were prepared: Growth medium with (1mM, 100 µM, 10 µM, & 1 µM of $CuSO_4$) and only Growth medium as a control group.	MSCs were seeded in 24-well plates with cell density of 1×10^5 cells/well and cultured with the 5 different medias of $CuSO_4$ soln for 1, 4 and 7 days. MSCs were seeded into the scaffolds at a density of 1×10^5 cells and incubated for 24 h.	Static	• When the Cu concentration is 1 mM, all cells were dead (red color). In the contrast, MSCs in the rest groups were live (green color) and showed a typical shuttle-like shape. • Cu with a concentration of 100, 10, and 1 µM had negligible toxicity at all time intervals, Also, adding 100 µM Cu enhanced the proliferation of MSCs compared to the control group. • However, after chondronduction of the MSCs, the 100 µM Cu showed an inhibitory effect on cell proliferation at day 7. • Cu could enhance MSCs chondrogenic differentiation by observing the changes to the cytoskeletons. "in the 100 and 1 µM Cu". • After 7 days of culture, the expression of Sox9 was significantly higher in the 100 µM Cu group compared to other groups. Also, Aggrecan was highly expressed in the Cu groups compared to the control group. • Also, the expression of Col-2 significantly enhanced with the increase of Cu content and the co-culture time, and a remarkably up-regulation of Col-2 expression occurred in the 100 µM Cu group at day 14 compared to other groups. • **Summary:** The adding of Cu into the chondrogenic medium exhibited a positive effect on the cartilage differentiation of MSCs including morphological change and chondrogenic genes up-regulation in vitro.

Table A.4. Cupper (cont.)

													• In vivo study showed the Alg/Cu scaffolds were better than the pure Alg scaffolds in term of the formation of new cartilage tissue.
Cupper	24	BM-MSCs	Human	Age range from 65-75 years.	Female	Cells were isolated from healthy postmenopausal women	DMEM	10% FBS	For Cell proliferation: Cupper is added in the form of cupper-histidine complex	Cu, Fe & Zn were added in 3 different concentrations to the growth medium "0.44, 2.69, 3.80 µM". 0, 5, 50 µM Cu-His is added to the culture medium for cell proliferation assay.	Cells were cultured for 14 days in different differentiation medium "Adipogenic and Osteogenic mediums" with different concs. Of Cu-His.	Static	• After 4 days, Proliferation of the cells decreased when cultured in media containing 5 or 50 µM Cu. • The addition of 5 and 50 µM Cu-His in the osteogenic medium decreased the ALP activity compared to the activity in the absence of copper; however, they pointed out that copper addition to the reaction mix didn't inhibit the enzymatic activity. • The addition of 50 µM Copper to the adipogenic differentiation medium increased the adipogenic differentiation by (1.2 – 1.4 times).
Bioactive Cupper-Doped glass scaffolds	25	BMSCs And HDMEC	Human	NA	NA	For all the experimental protocols, passage 5 were used.	DMEM/ Ham's F-12 (1:1)	10% fetal calf serum and 2 mg/L of L-glutamine	Bioactive glass scaffolds were fabricated using different CuO contents.	Cu2+ contents of 0.1 wt.% and 1 wt.% were assessed using plain 45S5 BG scaffolds as control material. The scaffold samples were divided into 3 groups based on the amount of Copper: **Group A**: for pure BG scaffolds **Group B**: for 0.1% copper-doped BG **Group C**: for 1% copper-	The samples were evaluated after 2 and 4 weeks.	Static	• In the 2D indirect analysis, the ALP expression shows no significant difference among all groups, however, only group C-2D samples show multifold higher VEGF expression compared to any other sample. Also, the osteogenic gene RUNX-2 expression was not significantly different among each other. • In the direct 3D analysis, Similar to 2D experiment, there is a basal expression of ALP in all cells without any difference among all groups. And also, the copper containing specimens displayed increased VEGF expression. • Also, in 3D analysis, Cu2+ estimated from all respective media shows significantly increased values in group C than group B and increased values in group B than group A samples.

Table A.4. Cupper (cont.)

										doped BG scaffolds. Similar groupings were done both for the **2D (indirect)** and **3D (direct seeding)** experiments.			• In 3D analysis, the live-dead assay shows all cells are alive without any significant dead cells attached to the scaffold. • Only after week 2, under the effect of Cu2+ -BG-MSC, the cells were seen to exhibit endothelial tube formation. • At week 2, there is significantly increased amount of VEGF released into the media in group IV and group V • Cu^{2+}-doped BG scaffolds exhibit no toxicity even up to 1 wt.% Cu2+ concentration • Cu^{2+}-doped BG scaffolds in combination with MSCs are superior candidates for bone tissue engineering application with enhanced angiogenic potential. • Cu^{2+} could make the best use of the two-cell system by producing VEGF from MSCs as shown in this study In addition, the whole system is cost effective for tissue engineering applications. • Cu^{2+} ions in BG scaffold act on MSCs to have high VEGF secretion into the media.

Table A.5. Cerium

Trace element	Ref.	Cells					Media		Protocol				Results
		Type	Species	Donor Age	Donor Sex	Passage	Basal media	Serum	Material's Form	Material's Conc.	Applications	Conditions	
Cerium	26	BMSCs (C57BL/6 cell line)	Mice	6 to 8-week-old	Male	Passage 3 were used.	DMEM	10% FBS, 50 U/mL penicillin and 50 mg/mL streptomycin.	NA	$CeCl_3$ at different concentrations were used (final concentrations of 0, 0.001, 1, 10 μM). Cells were seeded at the density of 1×104 cells/well in a 96-well plate	Cells were incubated with $CeCl_3$ for 24 hrs.	Static	• The cultured BMSCs were positive for CD44 (the percentage of positive cells: 99.4%) and were negative for hematopoietic lineage markers CD34 (the percentage of positive cells: 0.7%). • Ce displayed a positive effect on the BMSCs viability at lower concentrations (0.001 μM) and decreased the viability of BMSCs at higher concentrations (10 μM) for 24 hours. • After 7 days of Ce treatment, the ALP activity of BMSCs was increased at concentrations of 0.001 μM, and decreased at concentrations of 10 μM, which means that Ce promotes osteogenic differentiation of BM-MSCs • The expressions of Runx2, Satb2 and OCN were significantly up-regulated in the BMSCs treated with Ce (0.001 μM) for 7 days as compared to control group. • Ce (0.001 μM) increased the ability of BMSCs to cross the ECM • SDF-1 mRNA expression was higher in BMSCs treated with Ce, but CXCR4 mRNA expression was not significantly affected with Ce.

Table A.5. Cerium (cont.)

	27	BMSCs	12 Mice	4 to 6 weeks specific pathogen free (SPF) Kunming (KM) Mice.	Female	NA	DMEM	10% FBS, 100 U/ml penicillin, and 100 mg/ml streptomycin	NA	MSCs were seeded in 96-well tissue culture plates at the density of $4x10^6$ cells/well and incubated for 72 h. After the addition of $CeCl_3$ at different conc. (final conc. 0.0001, 0.001, 0.01, 0.1, 1, 10, and 100 μM). Cells without $CeCl_3$ treatment were used as control	Cells were incubated with the Cerium for 24, 48, and 72 hrs. For osteogenic diff., cells were incubated in OS medium supplemented with different conc. of cerium for 7, 10 and 14 days. For adipogenic diff., cells were incubated for 15, 18, and 21 days.	Static	• Ce displayed a slight positive effect on the MSC viability at conc. of 0.0001, 0.001, 0.01, and 0.1 mM, had no effect on the MSC viability at a concentration of 1mM, turned to decrease the viability of MSCs at conc. of 10 and 100mM for 1 and 2 days, but then On day 3, Ce increased the viability of MSCs at conc. of 0.0001, 0.001, 0.01, 0.1, 1, and 10 mM, but decreased the viability of MSCs at a concentration of 100 mM. • The viability of MSCs was decreased with increasing Ce concentrations. • ALP activity of MSCs treated by all conc. of Ce was increased compared with that of OS on Day 7 and 10, however, on day 14, Ce increased the ALP activity at conc. of 0.0001, 0.001, 0.01, 0.1, and 1 mM, but decreased ALP activity at conc. of 10 and 100mM. • Ce inhibited adipogenic differentiation of MSCs at all tested concentrations in which the expression of adipogenic differentiation related proteins was down-regulated by Ce. • Ce promoted the osteogenic differentiation and inhibited the adipogenic differentiation of MSCs. • Tgfb3, Tgfb1, Smad4, Bmp7, Bmp6, Bmp4, and Bmp2 genes were up-regulated when the MSCs were exposed to 0.0001 mM Ce, on the other hand, the expression of Smurf1, Smurf2, Gdf7, Gdf6,

Table A.5. Cerium (cont.)

													Gdf5, and Gdf15 was down-regulated. • Runx2, BMP2, ALP, BSP, Col I, OCN, and ERα genes were significantly up-regulated in the MSCs treated with Ce (0.0001, 0.01, and 1 mM) for 4 days as compared to OS group.
Cerium Oxide Nanoparticle (Nanoceria NC)	28	BMSCs	Rat	NA	NA	The fifth passage were used in all experiments.	DMEM	10% FBS, 100 U/ml penicillin, 100 mg/ml Streptomycin, and 200mM glutamine.	Cerium oxide nanoparticles appear as a powder of quite dispersed size distribution (5–80 nm), with a cubic crystalline structure, high purity, and a Ce3+ content of ~23%. And then diluted culture medium.	Cells were seeded in 96-wells plate at a density of 6,000/cm2 (n=6) and, after 24 h, they underwent a treatment with 0, 10, 20, 50 and 100 μg/ml of NC.	Cells were incubated with NC for 3, 6 and 10 days in expansion medium. At each time point, medium was replaced with 100 μl of the fresh medium.	Static	• NC are not harmful form MSC viability and proliferation, and a regular metabolic activity has been observed on cells loaded with different NC concentrations after 10 days, with no appreciable differences against controls. • The results showed a strong interaction between cells and NC, that are located both on the cell membrane and in the cytoplasm. • The antioxidant property of NC was examined as a potential agent of inhibition of adipogenesis in MSCs. • The results from qRT-PCR indicated a significant down-regulation of all the adipogenesis marker genes in cultures treated both with 20 μg/ml and 50 μg/ml of NC, compared with control differentiated adipocytes. • Cerium NP inhibits the adipogenesis of the MSCs.
	29	Derived neural progenitor cells	Mouse	NA	Na	NA	DMEM	5% horse serum, 10% FBS, 2 mM	The CeO_2 nanoparticles and the 20% Samarium (Sm) doped CeO_2	Cells were seeded in 48-well plates at a density of 6000 cells/cm^2 in	The following day of culturing the cells, the medium was carefully	Static	• Both CeO2 and the Sm-doped CeO2 nanoparticles are readily internalized by murine neural progenitor cells and that this was not accompanied by cell death.

Table A.5. Cerium (cont.)

		(C17.2 cell line)						glutamine, 100 U penicillin/mL, and 100 U streptomycin/mL	nanoparticles ($Sm-CeO_2$) were synthesized by a wet chemical process, and then suspended at a stock conc. of 20 mg/mL	complete DMEM medium. Five different concentrations of CeO_2 or $Sm-CeO_2$ nanoparticles were used in this experiment (5, 10, 20, 50, 100 µg/mL)	removed, and the cells were exposed to the same medium containing the different concs. Of the NP. And incubated for 48 hrs.		• The Cerium Nanoparticles inhibited the neuronal differentiation of the C17.2 Mouse cells.
	30	MSCs (C3H/10T 1/2 Cell line) EPCs are endothelial progenitor cells	Mice	NA	NA	NA	DMEM/ F12	10% FBS	CNPs with size ~5 nm was synthesized by thermal decomposition method using cerium nitrate as precursor. Scaffolds with and without CNPs were used. (prepared scaffold and scaffold@CNPs)	The scaffold without CNPs has PLLA concentrations range from 0.1% to 2.0% (w/v). The CNPs embedded scaffold (scaffold@CNPs) has ratio CNPs/PLLA (wt. %) up to 10%.	MSCs (1×10^4) were seeded on scaffold and scaffold@CNPs in 24 plate well for 1, 7, and 14 days. Each of the scaffold and scaffold@CNPs was seeded with MSCs (5×10^3) and cultured *in vitro* for 2 h.	NA	• The scaffold@CNPs provided a better microenvironment for MSCs than the scaffold without CNPs. • The osteogenic differentiation-related genes, including Col1a1, Osterix2 and Runx2, and ALP expression of MSCs seeded on scaffold and scaffold@CNPs showed no obvious difference at 14 days, which implied that the CNPs have no promotion or inhibition effect on the osteogenic differentiation of MSCs. • EPCs co-cultured with MSCs exhibited improved cell viability, as the MSCs-secreted growth factors could support the growth of EPCs. • The cell density of EPCs co-cultured with MSCs seeded on scaffold@CNPs was much higher than that of EPCs seeded on scaffold. • CNPs embedded at the scaffold and MSCs interface could promote the proliferation and inhibit the apoptosis of MSCs even though the

Table A.5. Cerium (cont.)

													nanoparticles have no effect on the osteogenic differentiation of MSCs
Cerium oxide incorporated hydroxyapatite coatings **CeO_2-HA coated**	31	BMSCs	Rat	NA	Male	BMSCs were passaged when reaching 80–90% confluence. BMSCs at passages 3–5 were used for research in this study.	DMEM	10% FBS & 1% PS	The commercial ceria powder (CeO_2) and hydroxyl-apatite powder (HA) were used in this study.	Two different powder mixtures with 10 and 30 wt. % CeO_2 were prepared and were denoted as HA-10Ce and HA-30Ce. 1ml of cell suspension supplemented with 1 mM H_2O_2 (0.1 ml) was seeded on the coating surfaces at a density of 2×10^4 cells/well	The cells were cultured for 3 and 7 days. The cell culture medium with H_2O_2 was changed every 2 days. Cells cultured on the HA coating surface without H_2O_2 treatment served as an control.	NA	• The treatment of BMSCs with H_2O_2 significantly decreased the cell viability when cultured on HA and CeO_2-incorporated HA coatings for 3 and 7 days. • With respect to BMSCs treated with H2O2, the ones cultured on the HA-30Ce coating exhibited the highest survival rate. • In vitro test revealed that the treatment of BMSCs with exogenous H_2O_2 significantly reduced the ALP activity when compared to the untreated cells. • In this study, we found that H_2O_2 reduced cell viability and induced apoptosis of BMSCs in vitro. • CeO_2 incorporation in the HA coatings enhanced the osteogenic differentiation of H_2O_2-treated BMSCs

Table A.6. Strontium

Trace element	Ref.	Cells					Media		Protocol				Results
		Type	Species	Donor Age	Donor Sex	Passage	Basal media	Serum	Material's Form	Material's Conc.	Applications	Conditions	
Strontium Chloride	32	BM-MSCs (C3H10T 1/2 cells)	Murine	NA	NA	NA	α-MEM	10% FBS, 100U/ml penicillin, 100mg/ml streptomycin, 2.5 µg/ml fungizone and 2 mM L-glutamine	Strontium chloride is used as a soluble compound	Strontium chloride concentration was expressed as strontium concentration (Sr 1.0 mM and 3.0 mM)	Strontium chloride was added into osteogenic induction medium during differentiation process of C3H10T1/2 and MSCs and incubated for 14 days. For control, MSCs were treated with solvent vehicle (DMSO, 0.1%).	Static	• At day 7, strontium at the dosage of 3.0 mM significantly increased Runx2 mRNA expression in both C3H10T1/2 cells and primary bone marrow MSCs which indicates an early osteogenic differentiation. • The middle-phase gene marker. BSP was significantly increased in MSCs instead of C3H10T1/2 cells at day 14 in response to strontium treatment. • OCN gene expression was similarly up-regulated in these two cells at day 21. • Strontium at both dosages showed little effect on ALP activity at day 7. Continuous treatment with strontium at 3.0 mM for 14 days showed significantly increased the ALP activity. • Strontium can promote the osteogenic lineage differentiation of MSCs by enhancing expression of multiple genes regulating different osteogenic stages and matrix maturation

Table A.6. Strontium (cont.)

	33	Umbilical cord MSCs	Human	NA	Female	First passage	DMEM	10% FBS and 1% antibiotic mix	NA	The cells were plated in 6 well plates at a conc. of $4*10^4$ cells/cm^2 and divided into 3 groups: Control group was cultured in DMEM only. Dexamethasone (Dex) group was cultured in osteogenic medium. and Strontium (Sr) group was cultured in osteogenic medium containing 2 mM strontium chloride.	The medium in each group was changed three times every week	2D	• Most of the cells expressed the standard MSC markers such as CD73 and CD105, whereas they did not express the hematopoietic stem markers CD34 and CD45 • The percent of ALP-positive cells in the Sr group was significantly higher than that in the Dex group after 10 days, which demonstrates that strontium enhances the osteogenic differentiation of the MSCs • The expressions of Alp, Col1a1, and Opn in the Sr group were significantly higher than those of the Dex group which suggest that the expression of osteogenesis-related genes was upregulated by strontium. • Strontium upregulated the expression of ALP, significantly increased the expression of type 1 collagen, and enhanced calcium deposition and bone nodules formation

Table A.6. Strontium (cont.)

		In vivo studies of rat calvarial defect model and transplantation of the scaffold	Sprague-Dawley rats	8-week-old	18 Female	NA	NA	NA	Collagen-Sr-HA Scaffold	The 18 female rats were evenly divided into three groups: (a) control group; (b) HA group; and (c) Sr group.	Collagen, collagen hydroxyapatite and collagen-strontium-substituted hydroxyapatite were transplanted into the control, HA, and Sr groups, respectively	3D Scaffolds	• In the HA group, the CT bone density in the defect region was increased compared with that of the control group, while in the Sr group, the bone density in the bone defect region was increased further, and the defect region area was reduced, compared with that of the HA group at 1 month after transplantation • Three months after transplantation, in the HA group, the area of the bone defect region was reduced compared with that of the control group, although the radiographic density in the defect region was still lower compared with that of the surrounding region, while in the Sr group, there was no significant bone density difference between the defect area and the surrounding region and 3D reconstruction showed no evident bone defect. • In the HA group, moderate collagen I was observed and OPN antibody was distributed evenly in the newly formed bone, and also the expression of β-Catenin showed few signals. However, in Sr group, strong collagen I signals and OPN signals were observed and β-Catenin signals were also observed strongly. • These results indicate that strontium can promote the in vivo bone formation in the calvarial defect model, can enhance the accumulation of ECM in the bone defect, and enhance the β-Catenin expression in vivo.

Table A.6. Strontium (cont.)

Strontium Ranelate	34	BMMSCs	Sprague-Dawley (SD) Rats	3 months old	Male	Cells of passage 3 were used for the following experiments.	α-MEM	10% FBS, 2 mM L-glutamine, 100 U/mL penicillin and 100 μg/mL streptomycin	Strontium ranelate consisted of $SrCl_2$ and sodium ranelate with the molar ratio of 1:10.	Conc. of strontium ranelate are expressed in terms of Sr^{2+} (mM) in this study and calcium chloride was used as a control in cell cultures.	Cells were plated in 6-well plates at a density of 5 105 cells/2 mL/well After overnight incubation, the medium was replaced with osteogenic or adipogenic medium, with or without SrR (0.1 or 1.0 mM Sr^{2+})	Static	• SrR treatment increased ALP activity but decreased OD values of Oil red O dose-dependently. • SrR decreased the proliferation, promoted osteoblastic but inhibited adipocytic differentiation of rat BMMSCs dose-dependently during 2-week treatment. • The increased osteoblastic differentiation was related to increased Cbfa1/Runx2, BSP, and OCN. • The decreased adipocytic differentiation were supported by the evidence of decreased PPARγ, aP2/ALBP, and LPL

Table A.6. Strontium (cont.)

	35	hADSCs cell line (PA20)	Human	45 years	Small fragments of subcutaneous adipose tissue biopsy from Female	PA20 cells at the 3rd passage were used.	Ham-F12 Coon's modification medium	10% FBS, 1% PS, and 1 ng/mL basic fibroblast growth factor (bFGF) was composed	NA	PA20-h5 cells were seeded in 100 mm diameter dishes at a conc. of 20,000 cells/dish and cultured for 3 days. Then the Culture medium was replaced with OM without osteogenic induction factors, containing several different conc. of Sr^{2+}: 5, 50, 100, 200, and 400 μM.	The number of cells was evaluated at 0, 3, 6, 10, 13, and 16 days	Static	• Adipogenic differentiation was not observed in the PA20-h5 line at time 0 (days), while after 35 days of adipogenic induction some cells showed intracellular vacuoles containing drops of lipids of variable shape and size • PA20-h5 line did not show ALP activity at time 0 (days), while culture in the OM up to 35 days induced an increase in the number of cells positive to ALP • Absence of significant variations of ALP, RUNX2, and DKK1 gene expression in cells cultured in GM containing 100 μM Sr2+ compared to those cultivated only in GM. • At 100 μM –400 μM concentrations, Sr2+ significantly stimulated ALP production in the PA20-h5cells, from 14 to 35 days, with maximal response being observed at 21 days with 400μM Sr2+. • At lower and higher concentrations Sr^{2+} had no significate effect on cell proliferation. • In vitro Sr^{2+} ion treatment of hADSCs enhances cell proliferation and osteogenic differentiation through expression of early and late osteoblastic biomarkers such as ALP and HA

Table A.6. Strontium (cont.)

	36	hASCs	5 Human	Average age of 35 years	NA	The cells were passaged when reach 70-80% confluence and hASCs before the third passage were used in the following study.	LG-DMEM	10% FBS, 100 mg/mL streptomycin, and 100 U/mL penicillin	NA	The effect of SrR on the osteogenic differentiation of hASCs was studied using: Sr (0, 25,100, 250, 500, 1,000, 1500, and 2000 μM) in osteogenic medium (OM).	Cells were cultured in different type of differentiation medium in addition to different concentration of SrR and incubated for 23 days.	Static	• ALP activity was significantly elevated on days 10 and 14 as indicated by ALP staining and quantitative assays. • ALP activity was suppressed at 25, 100, and 250 μM and was enhanced at 500 μM after 4, 7, and 14 days • The expression of RUNX2 was significantly reduced at 25, 100, and 250 μM SrRan, and elevated at 500 μM while the expression of COL-I and OCN was slightly upregulated at 25 μM and was significantly suppressed at 100, 250, and 500 μM. • Early osteogenic marker expression and ALP activity was increased at 500 μM SrR, but it augmented late osteogenic gene expression and increased calcium deposition at 25 μM • Low-dose SrR enhances hASC osteogenic differentiation and higher doses causes hASC apoptosis via activation of the ERK signaling pathway.
Strontium Hydroxy-apatite Scaffolds (SrHA)	37	ADMSCs	Sheep (in Vitro)	NA	NA	Passage 3 is used in the experiments	DMEM	10% FBS and 1% antibiotics	10% SrHA, Control scaffold. Hydroxyapatite (HA) scaffolds were synthesized by wet precipitation method.	SrHA and HA disc scaffolds (5 mm × 2 mm) and cylindrical implants (12 mm × 4 mm) were manually trimmed.	ADMSCs (1×104) were seeded on HA, SrHA scaffolds and maintained in osteogenic induction medium to fabricate tissue engineered scaffolds – cHA and cSrHA	2D	• Cultured sADMSCs showed the ability for the osteogenic and adipogenic differentiation by showing reddish brown calcium depositions and bright red oil globules. • Live dead staining confirmed that sADMSCs attached on HA and SrHA scaffolds were viable even after seven days of culture and no dead cells. • SrHA scaffolds exhibited an ALP activity comparable to that of the control scaffold which means that it

Table A.6. Strontium (cont.)

												enhances the osteogenic differentiation of the cells.
			(In vivo) 10 adult sheep	10-12 years old	Female	8 animals (ovariectomized OVX group) were used in the experiment while 2 served as a control	Linear incision was made on the distal one third of the lateral thigh in the OVX group, large cortical bone defect of size 12 mm × 4 mm and a press fit method has been adopted for the implantation of TE scaffolds.	Allogenic sADMSCs (1×10^4) were seeded on cylindrical HA and SrHA scaffolds and maintained in osteogenic induction medium for 7 days to fabricate TE implants.		3D	• All animals survived the implantation procedures and healing was uneventful, also there were no fibrous tissue or inflammation at the defect site, post 2 months of implantation. • A significant increase in de novo bone formation was evident in the cSrHA implanted group (Fig. 6e) since they exhibited the highest RE ratio. • Density histograms of HA and cHA implanted group indicated that bone density at the bone-implant interfaces was low compared to that of host bone, whereas in SrHA and cSrHA implanted group a comparatively improved bone density was evident, indicative of the significance of Sr incorporation in osteointegration • Strontium and osteogenically induced ADMSCs at the implant site facilitated improved osteogenesis and osteointegration towards osteoporotic bone healing.

Table A.6. Strontium (cont.)

Strontium Calcium Phosphate (SrCaPO4) and HA scaffolds	38	ADMSCs	Rabbit	NA	NA	Passage 3-4 were used in the experiment.	α-MEM	10% FBS and 200 Uml-1 of penicillin and 200 Uml-1 of streptomyc in	An in-house prepared SrCaPO4 was used for the study. HA powder was synthesized by a wet precipitation method	Porous bioactive ceramics (5 mm diameter & 5 mm thickness discs)—HA and SrCaPO4 were loaded with cells $1x10^5$ cells per scaffold	Cells were incubated in the scaffolds for 2 and 4 weeks and the media was changed twice a week.	Static	• The RADMSCs were analyzed by fluorescence activated cell sorting (FACS Aria) and showed positive expression of adhesion molecules CD105 and receptor molecule CD44 • The osteogenic differentiation (ALP activity) was found to be more prominent on SrCaPO4 than HA. • The presence of incorporated strontium has favored the differentiation and proliferation of osteoblast cells unlike HA and would easily assist in bio imaging • In vitro studies suggested SrCaPO4 as a better bone substrate than HA for further in vivo applications.
Strontium-Doped Nano-Particles (BGNPsSr)	39	hASCs	Human	NA	NA	NA	α-MEM	No supplement ations	Strontium has been doped in bioactive glass nanoparticles	Discs of both BGNPs and BGNPsSr, with an approximate weight of 100 mg and ø 4 mm, were produced through a compact and inexpensive hand driven press	The tests were carried out for 1, 3, and 7 days. hASCs were cultured with BGNPs dispersed in the medium with and without osteogenic supplements	NA	• The combination of biomaterials with stem cells has demonstrated to improve bone healing. • The nanoparticles influenced the expression levels of RUNX2 in the initial culture periods, in which a significant upregulation of RUNX2 occurred at 7 days for all culture media • The expression of type I collagen, OCN, SPP1 and COL1A1 are expressed in the first periods and downregulated in the succeeding osteoblast differentiation, being necessary for the progress of the bone cell phenotype • hASCs kept their viability levels in the presence of both nanoparticles in comparison with cells not exposed to the particles.

Table A.6. Strontium (cont.)

													• The osteogenic markers OCN and OPN were detected under all conditions, and a high protein expression up to day 14 shows bone ECM maturation • BGNPsSr formulation promoted the angiogenic phenotype of HUVECs • The upregulation of genes and the synthesis of the selected proteins were increased by both the nanoparticles without requiring osteogenic supplements, which suggest that the particles and their dissolution products are likely influencing the commitment of hASCs toward osteoblast differentiation

Table A.7. Sulfer

Trace element	Ref.	Cells					Media		Protocol				Results
		Type	Species	Donor Age	Donor Sex	Passage	Basal media	Serum	Material's Form	Material's Conc.	Applications	Conditions	
Sulfur Mustard (SM)	40	BM-MSCs	Human	10 patients were between (49 – 84) years.	NA	Passage 3 were used	α- MEM	20% FCS, 200 µM l-glutamine, 100 U/ml penicillin, 100 U/ml streptomycin)	SM were purchased and diluted for experimental approaches with growth media	The cells were treated with the vehicle control (diluted ethanol without SM) or with SM at final concentrations of 1 µM (IC_1), 10 µM (IC_5), 20 µM (IC_{10}) or 40 µM (IC_{25}) SM under a fume hood.	At 8, 24 and 48 h or 5 days after exposure to SM, cells were used for senescence, proliferation and apoptosis experiments. For DNA adduct experiments, cells were used 5 min to 48 h after SM exposure.	Static normal conditions	• When cells stained with DAPI to determine the strongest cytotoxic effect of SM which is induced by its alkylation of the DNA. a plateau of maximum fluorescence intensity was reached after 1 h of 100 µM SM incubation. That plateau stayed for about 4 h and decreased afterwards. Already 5 min after exposure the cells showed a mean fluorescence of 32.7 ± 4.1% compared to the value 1 h after exposure. • Cells were incubated for 48 h with and without SM in different sublethal concentrations (IC1-IC25). In absence of SM, 37.0 ± 1.2% of all cells were positive for Ki-67 within the nucleus which means these are proliferative cells. With increasing concentration of SM. the number of Ki-67 positive nucleus deceased to 0.8 ± 0.1% at IC25 (40 µM). • No significant changes were observed with regard to cleaved Caspase-8, PARP, p85 and AIF under exposure with all tested SM concentrations. • In the absence of SM, the MSC demonstrate nearly no senescence. Starting with exposure to low concentrations IC1 the number of senescent cells starts to increase. Using a SM concentration of 40

Table A.7. Sulfer (cont.)

													µM (IC25), most of the MSC demonstrate a senescence typical expression of ß-galactosidase. • **As a summary,** SM alkylates the DNA of the MSC. However, a large amount of DNA alkylation does not necessarily lead to apoptosis. Rather, the MSC is able to reduce and repair DNA damage.
	41	BM-MSCs	Human	14 patients were between (47 – 86) years	NA	Cells were used until passage 3.	α- MEM	20% FCS, 200 µM l-glutamine, 100 U/ml penicillin, 100 U/ml streptomycin)	SM was purchased from as an 8 M stock solution of SM in 100% ethanol.	The cells were either treated with the vehicle control (diluted ethanol without SM) or exposed with SM at concentrations of 1 lM. 10 lM. 20 lM, and 40 lM under a fume hood were incubated for 1 h. MSC from 6 independent healthy donors were poisoned with SM for one hour and afterwards cultivated for five days. A wide range of SM concentration was used to determine the inhibitory concentrations from 1% to 50% (IC1–IC50), HaCat cell	Cells were incubated with SM in different concentration and for different periods of time for different applications	Normal conditions	• In relation to HaCat cells the cultured MSC are able to tolerate a more than 40-fold increased concentration to reach the inhibitory concentration of 50%. • Using the lowest inhibitory concentration IC1 (1 lM) the number of migrated cells decreased highly significant to 54% while increasing SM concentrations the migratory activity remained stable at about 50% (IC5: 54%, IC10: 50%, IC25: 48%). • Calcification was observed under control conditions as well as under all tested SM concentrations which indicates the ability for osteogenic differentiation. • Adipocyte differentiation of MSC can be demonstrated, in which MSC transformed into adipocytes with large fat vacuoles and this process was not affected by SM exposure in all tested concentrations. • Under all tested conditions MSC were able to differentiate into functional active chondrocytes

Table A.7. Sulfer (cont.)

										culture was used as a reference cell line.			• MSC after neuronal differentiation did show the classical morphology for neurons. This morphology was not affected if the cells were incubated with SM before differentiation was induced. • **As a summary**: The presented results demonstrate a high tolerance of MSC against sulfur mustard (SM). With a 50% inhibitory concentration (IC50) of about 70 lM MSC are able to tolerate the 40-fold concentration compared with HaCat cells. •
	42	BM-MSCs	Human	10 patients were between (49 – 84) years	NA	Cells were used until passage 3.	α- MEM	20% FCS, 200 µM l-glutamine, 100 U/ml penicillin, 100 U/ml streptomycin)	SM was made purchased as pure SM (8 M) was pre-diluted in ethanol. For experiments: SM were diluted in growth media.	The cells were treated with the vehicle control (diluted ethanol without SM) or with SM at final concentrations of 1 µM (IC_1), 10 µM (IC_5), 70 µM (IC_{50}), and 570 µM (IC_{90}) under a fume hood		Normal conditions	• The secretion profile of MSC incubated for 8 h with SM was compared to the secretion profile of MSC cultured in absence of SM, concentrations 50% and 90% (IC50, IC90) were used. 49 out of 275 cytokines showed a significant changed expression under at least one of the used conditions. • Strongest decrease showed VEGF-A (−1.8-fold), GRO-a (−1.3-fold) and AREG (−1.2-fold) within the IC90 test while highest increases were obtained for GCP-2 (0.5-fold), LAP (0.2-fold) and TSH-beta (0.2-fold) • 11 of the cytokines for which a significant change was observed among SM exposure had been described in the literature as cytokines which directly or indirectly influence the migration of MSC. • In absence of SM the addition of the cytokine bFGF led to an increase in migratory activity of while that level remained

Table A.7. Sulfer (cont.)

													unchanged under presence of SM in IC1 and IC5. Only at IC50 the migratory activity was decreased by 6% whereas at IC90 an increase of 71% was observed. • GCP-2 showed a weak but constant effect to increase migratory activity under all tested conditions except the IC90. • IL-6 did not influence migration in absence of SM. In contrast migration was increased significantly in all tests after incubation with SM, and the highest was at IC5 and IC90. • IL-8(e) caused highest increase under control conditions while in absence of SM the migratory activity increased by 62%. The increase of 152% was the highest gain measured in all tests. • The related IL-8(m) showed also an increase under all conditions but much weaker than IL-8(e). • Comparable to GCP-2, MCP-1 showed just a slight but significant effect under all tested conditions. Highest increase was found at IC90 with 54%. • MIF demonstrated a negative effect under control condition which was equalized in presence of SM. • NCAM-1 showed no significant effect under any of the tested conditions. • Comparable to MIF also TIMP-1 showed none or a negative effect on the migratory activity.

Table A.7. Sulfer (cont.)

													• The effect of TIMP-2 was not uniform. Whereas the activity under IC50 and the control was slightly decreased, the migration was increased at IC5 and IC90 but remained unchanged at IC1. • VEGF led to a constant and significant increase of more than 20% except IC50 where the activity remained unchanged. • **In summary**, the secretome of MSC changes significantly under the influence of SM. There is a reduced secretion of factors that are necessary for MSC migration and increased migration of MSC can be caused by various cytokines.
	43	AD-MSCs	Human	NA	Male	Passage 3 were used	MEM	10% FBS	The studies are made on an SM-exposed male patient which had a documented encounter with SM during the Iran-Iraq war.	Our patient received 100×10^6 cells every 20 days for a total of 4 injections within a 2-month period. He was screened 7 times for evaluation of physical activities and respiratory quality MSCs were injected intravenously along with 300 ml normal saline at a maximum rate of 2×10^6 cells/minutes	We evaluated the efficacy of the injections in the patient according to the following parameters: Pulmonary function tests (PFTs) [FEV1, forced vital capacity (FVC), FEV1/FVC], total lung capacity (TLC) by body plethysmography, single-breath carbon monoxide diffusing capacity (CO diffusion), exercise performance [6-minute walk test (6MWT)] (24), Borg Scale Dyspnea Assessment (BSDA) (25), COPD Assessment Test (CAT), St. George's Respiratory Questionnaire (SGRQ) (26),		• CD markers (CD73, CD90, CD105, and CD44) demonstrated that the cultured cells were indeed ADMSCs • Karyotyping showed that the MSCs were normal and could be used for the injections. • There were no statistically significant differences observed in PFTs (FEV1, FVC, and FEV1/FVC %) for 9 months, however there were an improve after the 2nd injection. • The results indicated a reduced volume for diffusing capacity or transfer factor (TLco) of the lung for carbon monoxide and also there was no significant difference in TLC, residual volume (RV) and maximum expiratory flow (MEF) after the injections

Table A.7. Sulfer (cont.)

											and a comprehensive safety evaluation	• Systemic administration of multiple doses of MSCs appears to be safe and improve 6MWT, CAT, SGRQ, VAS, and BSDA scores in SM-exposed patients with lung injuries. •

Table A.8. Silicon

Trace element	Ref.	Cells					Media		Protocol				Results
		Type	Species	Donor Age	Donor Sex	Passage	Basal media	Serum	Material's Form	Material's Conc.	Applications	Conditions	
Silicon Ions in (Calcium Silicate)	44	HBMSCs (human bone marrow MSCs) And HUVECs were used for co-culture	Human	NA	NA	HBMSCs and HUVECs used in the study were all at passage 3.	Low glucose DMEM	10% FBS & 1% PS	CS powders were prepared by a chemical co-precipitation method. Si ion-containing media was prepared by using CS powders since CS releases ions gradually when soaked in cell culture medium.	CS extracts were diluted with DMEM by a series of gradient dilution at the ratios from 1 to 1/256 The Si-ion concentration used for this experiment was determined first with CS extracts in the concentration range from 1.75 to 14 μg mL−1	HBMSCs and HUVECs were seeded in 96-well plates at 1 × 103 cells per well for 24 h. Then, cells were treated with media containing CS extracts for different time periods.	Normal conditions	• At dilution ratios from 1/4 to 1/256 (Si-ion concentration: 0.5–29.27 μg mL−1), CS extracts showed no cytotoxicity for both HBMSCs and HUVECs, but CS extracts without dilution (CS1) showed a certain degree of cytotoxicity for both type of the cells. • The CS extracts diluted from 1/2 to 1/128 (Si-ion concentration: 0.95–59.57 μg mL−1) significantly stimulated HBMSC proliferation on day 7. • At the dilution range from 1/8 to 1/256, Si ions regulate the cell proliferation, and the bioactive Si-ion concentration for the stimulation of HBMSC proliferation is in the range between 0.95 and 59.57 μg mL−1, and that for the stimulation of

Table A.8. Silicon (cont.)

													HUVEC proliferation is in the range of 0.95–3.67 μg mL−1, which is much narrow than that for HBMSCs. • The adipogenic differentiation of HBMSCs was enhanced when cultured in osteogenic media with Si ions as compared with cells only cultured in adipogenic medium without Si ions, however under normal growth condition without adipogenic differentiation inducer, Si ions could not stimulate lipid accumulation of HBMSCs • Si ions were observed to upregulate the gene expression of PPARγ, C/EBPα, FABP4, leptin, and adiponectin in adipogenic medium, which indicated that Si ions do promote adipogenic differentiation of HBMSCs. • However, in normal growth medium, no upregulation of adipogenic gene expression was observed both with and without Si ions, suggesting that Si ions are not an inducer, and rather an enhancer of the adipogenic differentiation of HBMSCs. • The addition of Si ions in the coculture medium of HBMSC-derived adipocytes and HUVECs remarkably stimulated the capillary-like network formation, which indicated that Si ions enhanced angiogenesis of the cocultured cells. • The results also showed that Si ions also promoted VEGF secretion of monocultured adipocytes and HUVECs as compared to cells cultured without Si ions, and also showed significantly higher increase

Table A.8. Silicon (cont.)

													in secretion in cocultured cells in the presence of Si ions as compared to monocultured cells. • Si ions significantly stimulated lipid accumulation and adiponectin secretion of cocultured adipocyte. • Si ions enhanced the formation of adipose-like tissue in hydrogels with both mono- and cocultured adipocytes, and coculture group showed higher adipose tissue formation than monoculture group.
Calcium Silicate and Strontium Calcium Silicate (CS & Sr-CS)	45	hWJMSCs (human Wharton`s jelly MSCs)	Human	NA	NA	NA	DMEM	10% FBS, 100 U/mL penicillin/ 100 μg/mL streptomycin, 10−8 M dexamethasone, 2.16 g/L glycerol 2-phosphate disodium salt hydrate and 0.05 g/L L-Ascorbic acid	Calcium oxide, Silica and Strontium oxide (CaO–SiO2–SrO) powders were employed as precursor materials and were prepared in a certain way to form cement-like specimens	hWJMSCs cultured on different cements for a different period of time.		Normal conditions	• The quantitative analysis showed that the viability of hWJMSCs cultured on Sr10 was significantly higher ($p < 0.05$) than that on Sr0 (1.14 fold) and Sr5 (1.10 fold) groups after 24 h culture • The ALP activity of hWJMSCs cultured on Sr-CS cement was markedly up-regulated after 3 and 7 days • Sr-CS cements may possess higher activity in up-regulating osteogenic differentiation of hWJMSCs than the CS cement. • The Sr-CS possesses enhanced degradability in compared with the CS cements. • The ionic products of the Sr-CS possess the ability to stimulate the proliferation, osteogenic differentiation, and mineralization of hWJMSCs.

Table A.8. Silicon (cont.)

Silica NPs	46	hADSCs	Human	NA	NA	NA	DMEM	10% FBS and 1% antibiotic/antimycotic	Silica gel was prepared by a chemical reaction using hydrochloric acid and sodium silicate. washed, sterilized, and suspended in serum-free culture medium for 48 hours	Cells were cultured in a 96-well plate at 37°C in a 5% CO2 atmosphere for 1, 3, and 5 days at a density of 3,000 cells/well with DMEM (with 1% fetal bovine serum) containing silica NPs and MPs,		Normal conditions	• Silica NPs increased cell proliferation significantly, but silica MPs showed no stimulation of cell proliferation, even at day 5. • Analysis of apoptotic cells by Annexin V staining confirmed that hADSCs exposed to silica MPs undergo apoptosis (6.49%) in a 1% serum medium, however, silica NPs had no effect on apoptosis. • The silica NP medium increased the phosphorylation of ERK1/2 after 10 minutes, it has no effect on p38 phosphorylation, however, silica MP medium showed increased levels of the phosphorylated form of p38.
	47	BM-MSCs	Human	NA	NA	Fifth passage were used	α-MEM	10% FBS, L-glutamine (0.3 mg/mL), streptomycin (100 µg/mL) and penicillin (100 U/mL)	(SiO2)72 cluster was designed and used as a model of SiO2 NPs In order to compare the effect of silica and silicon clusters, a Si20 cluster as a model of silicon NPs was designed using the Gaussian 98W suite of program.	Cell therapy by catalase (CAT) sample with a conc. of 2 µM was titrated with different conc. of SiO2 NPs (1, 5, 10, 15 and 20 µM) at 298, 310 and 315 K	Different concentrations of SiO2 NPs (1, 10, 50, 100 and 200 µg/mL) were added to the cell culture medium for 24 hrs.	Normal conditions	• MTT data indicated a negligible cytotoxicity of SiO2 NPs against hMSCs up to 100 µg/mL. However, increasing the concentration of SiO2 NPs to 200 µg/mL were toxic to the cells. • After 24 hrs incubation of hMSCs with SiO2 NPs, LDH assay demonstrated a very low level of toxicity for all SiO2 NPs concentrations. • hMSCs cells exposed to different concentrations of SiO2 NPs (1, 10, 50, 100 and 200 µg/mL) for 24 hrs also revealed a significant increase in the production of ROS only at high concentrations (100 and 200 µg/mL)

Table A.8. Silicon (cont.)

Se@SiO2 Nano-composites	48	BMSCs	Sprague Dawley (SD) rats	The rats were bred and maintained under a 12/12 hr. light/dark cycle with free access to food and water. The temperature was maintained at 18–25°C, and the relative humidity was set to 40–60%.	BMSCs from passages 3–4 were used in the following experiments	DMEM/F12	10% FBS and 1% antibiotic–antimycotic	They have oxidized Se^{2-} to develop Se quantum dots, then they used the Se quantum dots to form a solid $Se@SiO_2$ nanocomposite which was then coated with poly-vinylpyrrolidone (PVP) and etched in hot water to synthesize porous Se@SiO2 nanocomposite.	BMSCs were seeded at a density of 1×104 cells per well in a flat-bottomed 96-well plate for 24 hrs at 37°C with 5% CO2. After 24 hrs, the cells were incubated with an increasing concentration of the porous Se@SiO2 nanocomposite (ranging from 0 to 180 μg/mL)	BMSCs were divided into two groups: the blank group and the Se@SiO2 group. The blank group was resuspended in serum-free DMEM/F12 medium. The Se@SiO2 group was resuspended in serum-free DMEM/F12 medium containing the porous Se@SiO2 nanocomposite at a concentration of 80 μg/mL	Normal conditions	• The results showed that the cell viability did not decrease significantly compared to the cell viability of the blank group until the concentration reached 160 μg/mL. • The results demonstrated that the porous Se@SiO2 nanocomposite promoted BMSCs migration compared to that in the blank group. • The gene expression of SDF-1 and CXCR4 in the Se@SiO2 group was increased compared to that in the blank group, suggesting that the porous Se@SiO2 nanocomposite may promote BMSCs migration through the SDF-1/CXCR4 signaling pathway. • Treatment with the porous Se@SiO2 nanocomposite decreased the level of intracellular ROS more evidently at 160 μg/mL than at 80 μg/mL. • The porous Se@SiO2 nanocomposite increased ALP activity in the Se@SiO2 group and the H2O2+Se@SiO2 group compared with that in the blank group and the H2O2 group. • The porous Se@SiO2 nanocomposite promoted the expression of Runx2, OCN, BMP-2 and Smad-1 using RT-PCR and protected the expression of Runx2, OCN, BMP-2 and Smad-1 against H2O2-induced inhibition, suggesting that the porous Se@SiO2 nanocomposite promotes osteogenic differentiation of BMSCs.

Table A.8. Silicon (cont.)

Silicon Carbide NPs combine with Nano-HA coated Anodized Titanium	49	In Vivo	24 rodents	2 months	Male	NA	NA	NA	SiC NP (1 g/L) were added to the titanium electrolyte. The electrochemical deposition procedure was completed at 27 °C for 60 min in the electrolyte with a firm voltage of 2 V. The pure HA coating was also fabricated by the same process yet without SiC sources.	Rodent osteoblast cell was a culture at 3×10^3/cm2 on TiO2, HA-coated TiO2, and SiC@HA-coated TiO2 implant. (In Vitro) Rodents were arbitrarily allocated to be embedded with TiO2, HA-coated TiO2 or SiC@HA-coated TiO2. (In Vivo)	• The cell viability in SiC@HA gathering was higher than HA, which was a lot higher than the TiO bunch at various times focuses. • Ca2+ deposition in the ECM and cell osteocalcin generation were fundamentally higher in the SiC@HA sample following a month, showing that SiC@HA advances osteogenic separation. • At about two months after the medical procedure (In Vivo), the bone region proportion (BRP) and bone-embed contact (BEC) were essentially higher around SiC@HA inserts. • At both a month and two months, the proportion of hard tissue volume to add up to volume, mean trabecular number, and mean trabecular thickness were fundamentally higher in SiC@HA-covered inserts, proposing quickened healthy osteoblast in the locale of intrigue

Table A.9. Titanium

Trace element	Ref.	Cells					Media		Protocol				Results
		Type	Species	Donor Age	Donor Sex	Passage	Basal media	Serum	Material's Form	Material's Conc.	Applications	Conditions	
Trabecular Titanium Scaffolds (Ti6Al4V)	50,51	ASCs Adipose Stem Cells	Human	NA	NA	Cells were cultured until 95% confluence then the adherent cells were trypsinized and $1x10^5$ hASCs/ 100 mm^2 tissue culture plate were seeded in flasks. These passages were repeated thrice.	DMEM F12-HAM	10% FBS, 100 U penicillin/s treptomycin, amphotericin	The trabecular titanium scaffolds are multiplanar hexagonal cell structure imitating the cell structure of the trabecular bone, and its morphology and dimension has been optimized to improve vascularization, and maximize osteo-integration	The average diameter of the cell pores used in the scaffolds is 640 µm, the structure has an average porosity of 65%. The scaffolds (Ti) used have a height of 6 mm and a diameter of 12 mm.	At confluence, the cells were trypsinized and inoculated onto each scaffold as follows: a drop of 50 µL containing $1x10^6$ cells was placed on the top of the scaffolds which were placed in 12 wells, then allowed for 2 h before the medium was added. hASCs seeded on monolayer were cultured in three different media: GM, OM, and CM, that is the GM collected from the cells/TT scaffold construct well	Static	• hASCs were positive for CD90, CD73, and CD105 surface antigens and negative for CD34 and CD45 molecules. • hASCs grown on Ti scaffolds successfully differentiated down the osteogenic lineage and expressed high levels of the bone marker AP in the presence of osteogenic medium. • The expression of type I collagen in hASCs subjected to osteogenic induction was higher at day 21 and decreased at day 28, while the expression of osteopontin and osteocalcin mRNA of hASCs grown in osteogenic medium was observed to increase from 21 to 28 days of culture. • The expression of ALP and Runx-2 of hASCs grown on TT scaffolds and Ti plates in the presence of osteogenic factors (OM) was significantly higher than that of the same cells cultured on Ti plates in the GM, both at 7 and 21 days of differentiation. • The protein deposition enhancement was particularly marked for alkaline phosphatase, type I collagen, decorin, and osteopontin when compared with the scaffold cultured with undifferentiated stem cells.

Table A.9. Titanium (cont.)

													• In this study, the ability of the hASCs to proliferate and differentiate into osteoblast-like cells and to produce a mineralized matrix when cultured on trabecular titanium scaffolds was investigated.
Titanium Particles **"Submicron commercially pure titanium (cpTi) particles"**	52	BMSCs (Bone marrow MSCs)	Human	NA	NA	Adherent cells were supplied fresh medium every 72 h and expanded for 2-3 weeks (until 75% confluence) prior to use.	DMEM/ F12 medium	10% FBS, 100 U/ml penicillin, and 100 µg/ ml streptomyc in	2 types of particles were used: cpTi particles and zirconium (IV) oxide (ZrO_2) particles.	Particle sizes of 0.939 ± 0.380 and 0.876 ± 0.540 µm for cpTi and ZrO_2.	Cells were incubated with DMEM/F12/ 10% FBS containing ZrO_2 or cpTi particles with different concentration for 24 h.	NA	• After 12 days of treatment with OS medium, BM-MSCs showed differentiating into an osteoblastic cell type, exhibiting increased gene expression of osteoblast markers AP, OC, and BSP. • Col IA2 mRNA was expressed in both treated and control, but treatment with OS medium resulted in elevated collagen type I protein production. • BSP production by OS-treated cells was not affected at low or moderate particle concentrations (50 and 500 particles/cell), while exposure to a higher particle concentration (5000 particles/cell) severely decreased BSP production. • Exposure to submicron cpTi particles for 12 days suppressed the ability of hMSCs to differentiate into a functional osteoblastic phenotype, indicated by the decreased level of BSP gene expression as well as reduced BSP and collagen type I protein production, compared to non-particulate loaded OS-treated cells. • The exposure of OS-treated cells to both particle types resulted in decreased cell numbers throughout the entire treatment period, with cpTi-loaded cultures exhibiting lower cell numbers than cells

Table A.9. Titanium (cont.)

													cultured with ZrOz at Days 6, 9, and 12.
Pure Titanium disk and Nanotube Titanium disk	[53]	DPSCs "Dental Germ Pulp Stem Cells" & ADSCs	Human	NA	NA	NA	α-MEM culture medium	20% FCS, 100 µM 2P-ascorbic acid, 2 mM L-glutamine, 100 U/ml penicillin, 100 µg/ml streptomycin	Disks of commercially pure grade-1 titanium have been used as substrate for the nanotube growth.	The disks have diameter of 30 mm with a thickness of 0.5 mm, and were arranged to show an active area of 3.8 cm^2	ADSCs and DPSCs were cultivated on two type of surface NTD and TD ADSCs and DPSCs were trypsinized upon sub-confluence and seeded on NTD and TD. The medium was changed every 3 days	Static	• **ADSC**s cultivated on NTD showed the up-regulation of bone-related genes FOSL1, RUNX2, COL1A1, ENG and the down-regulation of SP7, ALPL and SPP1 while expression of COL3A1 was the same in both cells (cultivated on NTD and TD) • **ADSC**s cultivated on NTD after 30 days of treatment, the bone-related genes FOSL1, COL3A1, COL1A1, ALPL and SPP1 were up-regulated, while SP7, ENG and RUNX2 were down-regulated • After 15 days, **DPSC**s cultivated on NTD showed the up-regulation of FOSL1 and SPP1 and the down-regulation of SP7, ENG, RUNX2, COL3A1, COL1A1 and ALPL. • NTD surface is more osteo-induced surface compared to TD, promoting the differentiation of mesenchymal stem cells in osteoblasts. • Stem cells cultivated on nanotube titanium disks showed the upregulation of bone-related genes RUNX2, FOSL1 and SPP1.

Table A.9. Titanium (cont.)

Titanium Fiber Mesh "TFM"	54	DFAT "Mature adipocyte -derived de-differentiated Fat"	White Rabbits	7-week-old	Male	After reaching confluency, cells were passaged and used for experiments	DMEM	20% FBS & 10,000 units/mL penicillin, 10,000 lg/mL streptomycin and 25 lg/mL amphoteric in B	TFM with an 87 % volumetric porosity and 50 µm fiber diameter were used as scaffold.	Prepared titanium fiber discs were shaped with a 5 mm diameter and 1.5 mm thickness.	DFAT cells seeded into the TFM were cultured in osteogenic medium for 14 days. Medium was exchanged biweekly	NA	• DFAT cells proliferated in the TFM because numerous well-spread cells were found around titanium fibers and appeared to increase in number from day 3 to 7 in SEM analysis. • DFAT cells differentiated into osteoblasts in TFM because osteocalcin and calcium as late and terminal stage markers of osteoblast differentiation, respectively, increased remarkably on day 14.
Titanium Disk	55	BMSCs "Bone marrow-derived hMSCs"	Human	NA	NA	The cells from passage 4 were used for in vitro experiments.	Culture media (PT-3001, Lonza)		Commercially pure Ti discs with a mirror-polished surface (grade 2; 8 mmϕ × 1 mm thick, referred to as Mirror) were used in the experiments.	Adhesion and differentiation of hMSCs on Ti surfaces with micron, nano, and micro/nanohybrid grid topologies created using femtosecond laser irradiation was evaluated. hMSCs were seeded on the Ti specimens at a density of 5000 cells cm^{-2} and incubated.	Adipogenic diff. was induced when cells reached 80–90% confluence with the PT-3004 medium. Osteogenic and chondrogenic diff. was induced when cells reached 100% confluence PT-3003 medium for osteogenic differentiation and PT-3002 medium for chondrogenic differentiation All were replaced every 3 days.	NA	• The micron-scale topography is beneficial for cell anchoring, while the nanometer-scale topography is beneficial for cell locomotion on the substrate. • The micro/nanohybrid grid topography strongly promoted cell adhesion. • Ti surfaces with designed grid topographies modulated multilineage differentiation, with osteogenic differentiation being strongly promoted by the nanogrid topography. • After 3D differentiation induction, a similar expression level was detected by hMSCs cultured on both Mirror and Micron for adipogenic and chondrogenic differentiation.

Table A.9. Titanium (cont.)

Titanium Nanopores	56	BMSCs	Human	The experiments were repeated with at least 3 different bone marrow cell aspirations from patients of different age, sex and origin.	NA	α-MEM	10% FCS, 2 mM of L-glutamine, 100 µg/mL of streptomycin and 100 units/mL of penicillin	Titanium surfaces with nanopores 30, 150 and 300 nm in diameter were prepared by physical vapor deposition.	The glass coverslip discs coated with a thin titanium layer were abbreviated Ti and used as controls. The membranes with nanopores coated with titanium were named Ti30, Ti150 and Ti300.	3 samples/ group were used and the experiments were reproduced at least three times. Ti30, Ti150 and Ti300 membrane discs were put into 12-well dishes, and then 500 µL cell suspensions were poured in each well. Cells were cultured on to the different substrates for 2 and 4h, and 1, 6, 12, 18 and 21 d.	Static	• Osteogenic differentiation of hMSCs cultured on nanostructured Ti (Ti nano) was investigated after 6, 12 and 21 d of culture. • hMSCs exhibited as early as day 1 a more branched cell morphology on the Ti30 surface than on other surfaces. • The most potent nanostructure for osteogenic differentiation consisted of Ti30 and Ti150 while the Ti300 had a limited effect. • Nanopores of 30 nm may promote early osteoblastic differentiation and, consequently, rapid osseointegration of titanium implants • The arrays profile led the expression of 84 genes important for cell-cell and cell-matrix interactions • 18 genes were more under expressed on Ti 30 than on the other surfaces, including 3 collagens (COL6A1, COL7A1, COL8A1), 6 integrins and 4 metalloproteases (MMP2, MMP14, MMP16 and SPG7 MMP). • In contrast, on Ti150, only 3 genes (VCAN, CTNNB1, ITGαV) were slightly under expressed compared to the other surfaces. • On Ti300, 6 genes (COL7A1, ITGα4, ITGβ5, SPG7, TIMP2 and CLEC3B) were over expressed as compared with Ti30 and Ti150 and MMP1 was expressed more than as much as on the Ti surface.

Table A.9. Titanium (cont.)

Micro-structured Titanium Substrates **"Ti Disks"**	57	MSCs	Human	NA	NA	NA	MSC Growth Medium	NA	Ti disks were prepared from 1mm thick sheets of grade 2 unalloyed Ti.	For Direct Culture: Cells were plated on the surfaces at a density of 5,000 cells/cm^2 and grown to confluence on TCPS (about 7 days). At confluence, the media were changed, and cells were incubated for 24 hours. For Indirect Culture "Co-Culture": MSCs were plated at 5,000 cells/cm^2 in 6 well plates and cultured in MSCGM. When the MG63 cells on the test surfaces were confluent, the disks were moved into cell culture inserts above the MSCs in the 6 well plates. Cells were fed using DMEM, 10% FBS, and 1% PS for an additional 12 days in the co-culture system.	NA	• Alkaline phosphatase specific activity, an early marker of osteogenic differentiation, increased two-fold on titanium surfaces when compared to TCPS. • Osteocalcin increased slightly in cultures grown on PT and SLA surfaces over basal levels but had a three-fold increase in cultures grown on modSLA surfaces. • Secreted OPG increased only in MSCs grown on the hydrophilic modSLA surfaces. • Levels of VEGF-A decreased slightly in the conditioned media of cells grown on titanium surfaces but were significantly decreased on the modSLA substrate. • RUNX2 expression was increased on titanium surfaces and significantly increased on modSLA surfaces as compared to TCPS while Osteocalcin was also significantly upregulated on modSLA surfaces. • After 12 days in the Co-culture system, MSC cell number significantly decreased in cultures exposed to osteoblasts on titanium surfaces • The surface microstructure and surface energy are able to direct MSCs toward an osteoblast lineage. • Using the co-culture model, that differentiated osteoblasts on implant surfaces create a sufficient environment for osteogenic differentiation of the surrounding MSCs.

Table A.10. Yttrium

Trace element	Ref.	Cells					Media		Protocol				Results
		Type	Species	Donor Age	Donor Sex	Passage	Basal media	Serum	Material's Form	Material's Conc.	Applications	Conditions	
Yttrium-Stabilized Zirconia (YSZ) Scaffolds	58	hMSCs "Bone marrow MSCs"	Human	NA	NA	The cells were harvested at approximately 80–90% confluence for further subcultures.	α-MEM	10% FBS, 2 mM L-glutamine, 0.2 mM ascorbic acid, 100 U/mL penicillin, and 100 mg/mL streptomycin.	Yttrium is used in this experiment as YSZ-PVP fibers.	Ceramic scaffolds were seeded at a density of 2×10^4 cells/cm^2 and cultured in an incubator for up to 14 days in OM and in both BM and MM for 28 days. The culture medium was refreshed every 2 days. BM= Basal Medium OM= Osteogenic medium MM= supplemented osteogenic medium to support the osteogenic diff.		NA	• All investigated scaffolds showed a high rate of viable cells, which indicates no cytotoxic effects derived from the developed YSZ nanofibrillar scaffolds. • The nanofibers mat offered a very low density, in the range of 0.06–0.09 g/cm3. • Bulk YSZ scaffolds had a significantly higher metabolic activity than all nanofibrous scaffolds, which could be due to the higher differentiation of hMSCs on nanofibrous scaffolds compared to bulk YSZ. • ALP activity increased between day 7 and day 14 in OM and was significantly enhanced for CO annealed scaffolds. • Gene expression of RUNX2 was significantly higher for CO and MW annealed scaffolds compared to bulk YSZ in both culture media. • RUNX2 stimulates other downstream osteo-related genes such as osteopontin (OPN), osteocalcin (OCN), bone sialoprotein (BSP), and type I collagen. • The osteogenic differentiation and mineralization of seeded human

Table A.10. Yttrium (cont.)

													mesenchymal stromal cells were supported by the nanofibrous structure of YSZ scaffolds, in contrast to the well-known bioinert behavior of bulk YSZ.
Tetragonal Zirconia Polycrystal (YTZP) Scaffolds	59	hADMSC	Human	NA	NA	Passage 4 is used in the experiment.	DMEM / F12	NA	Scaffold samples used were taken from Y-TZP	Y-TZP have grooves and holes in their rod section with a Y-TZP size (Ø = 2.9mm, P = 3mm).	Y-TZPSs were put into 24 culture wells (M24) with $2x10^6$ cells (200 µL/well) And then incubated for 1 hr. Tubes were rocked to mix cells with the suspensions and Y-TZPSs. The cell-coated Y-TZPSs then were ready in the next 3 days for SEM	Dynamic	• MSCs on the expressions of CD 90, CD 73 and CD 105 were above 95%, while they on CD 14, CD 19, CD34, CD 45 and HLA-DR were below 2%. • Results of the Toxicity Test on Y-TZPSs in 96M revealed that Y-TZPSs was not toxic to hADMSC • Y-TZPSs- hADMSCs as a biomaterial had high biocompatibility for osseointgrated acceleration of implantation.
Hydroxy-apatite (HA) doped with either Cadmium (Cd), Zinc (Zn), Magnesium (Mg), or Yttrium (Y)	60	Osteoblasts	Rat	NA	NA	Osteoblasts at population numbers 2–4 were used in the experiments.	DMEM	10% FBS	Undoped HA and HA doped with various concs. (2–7 mol%) of select elements [Cd, Zn, Mg, or Y] were prepared via the "cake-method" according to wet chemistry techniques.	NA	Osteoblasts (3500 cells/cm^2) were seeded per substrate glass, undoped HA as well as on HA doped with 2 mol% of either, Cd, Zn, Mg, or Y and allowed to adhere for 4hrs.	NA	• Compared with glass (reference substrate), osteoblast adhesion was significantly ($p < 0.01$) greater on undoped HA. • Significantly ($p < 0.01$) greater amount of albumin, laminin, and fibronectin adsorbed onto undoped HA than onto HA doped with 2 mol% of either Cd, Zn, Mg, or Y. in fact no albumin, laminin, and fibronectin were detected on HA doped with either Cd, Zn, Mg, or Y. • Compared with undoped HA, osteoblast adhesion was significantly ($p < 0.05$) greater on HA doped with 2 mol% of either cadmium, zinc, or magnesium and

Table A.10. Yttrium (cont.)

													was the greatest on HA doped with 2 mol% yttrium. • A significantly ($p < 0.01$) greater amount of calcium adsorbed on HA doped with 2 mol% Y than on undoped HA as well as on HA doped with either Cd, Zn, or Mg. • The present study demonstrated, for the first time, enhanced osteoblast adhesion on HA doped with Y
Nano-structured Calcium Phosphate (nCaP) on Magnesium–Yttrium alloy substrates	61	BMSCs	Sprague –Dawley Rat	19 day-olds	Male	Cells were harvested from the femur and tibia. NA	DMEM	10% FBS & 1% PS	Pure (99.9 %) Mg 250 µm thick sheets and Magnesium-4 wt.% Yttrium (MgY) alloy were used in this study.	The pure Mg and MgY sheets of 250 µm thick were then cut into 10x10 mm squares for coating deposition and cell culture.	When the BMSCs reached 90 % confluency, they were and seeded at a density of 10,000 cells/cm^2 onto the nCaP-coated and non-coated Mg and MgY samples in a 12 well (PSTC) plate and incubated for 24hr.	Static	• The majority of BMSCs showed morphological changes when cultured with Mg and MgY samples as compared with the cells only control without any samples. • When placed in a rabbit model, CaP-coated Mg alloy implants showed enhanced new bone growth around the implant and exhibited increased osteoconductivity and osteogenesis compared to non-coated Mg alloys. "They didn't say how, and it was mainly engineering analysis for surface topography and adhesion"

Table A.10. Yttrium (cont.)

Magnesium Yttrium Alloys	62	BMSCs	Goat	NA	Female	Once the cells reached 80–90% confluence, they were detached passed to subculture. Cells from the 2nd passage were used in this experiment	DMEM	10% FBS & 1% PS	Mg- 4 wt. % Y (MgY) alloy was prepared by melting Mg with 4 wt. % Y.	The as-cast MgY alloy ingot was cut into 250 μm thick discs. The as produced MgY alloy discs had thermal oxide layers on their surfaces and were called MgY_O in this study.	Cells were seeded directly onto MgY_O and MgY_P samples at a density of 40,000 cells/cm^2 and incubated for 24 hrs. Bioactive glass was used as a positive control The cell cultures experiments were performed in triplicate.	Static	• The BMSCs cultured on bioactive glass had an elongated, spindle like morphology. • The most cell adhesion was observed on the surface of bioactive glass and the least cell adhesion on MgY_O. • The in vitro BMSC culture results showed that MgY_P was superior to MgY_O as a substrate for cell adhesion. • MgY_O degraded more slowly than MgY_P in DI water because MgY_O began with a protective thermal oxide layer • The photographs of degradation over time showed that degradation of MgY_O samples in DMEM began around the edges and progressed inwards.
Magnesium, Argentum, Yttrium Alloy **Mg-Ag-Y alloys**	63	MSCs for the *in-vitro* experiments.	Human	NA	NA	NA	NA	NA	Mg-Ag-Y alloys, composed of 1 wt. % Ag and 1 wt. % Y, were prepared.	The cell viability was assessed after 24, 48, and 72 h of in vitro culture under the influence of aqueous extract of Mg-Ag-Y alloys		NA	• The quantity of cells in the Mg-Ag-Y alloys group were significantly better than that of +ve control group and there was no statistical difference between the various level of Mg-Ag-Y alloys extract group and the negative control group. • Cell toxicity test indicated no cytotoxic effect, and the alloy and its degradation products do not show toxicity to experimental animals

Table A.10. Yttrium (cont.)

		NA	36 Sprague Dawley rats for the *in-vivo* experiments	NA	NA	All rats were randomly separated into 3 groups according to implant materials: **GP. A**: Mg-1Ag-1Y, **GP. B**: Pure-Mg, and **GP.C**: stainless steel, SS.	NA	NA	NA	NA	Holes (Ø1.5x4 mm) were drilled around the left distal femora and the rod samples were perpendicularly implanted into metaphysis of the rat femora. The rats were sacrificed 6 weeks.	NA	• During the whole research, all rats survived, and the serum Mg^{2+} ions concentration was fluctuated around the normal range, which was 0.96–1.55 mmol/L in Mg-Ag-Y alloy, 0.88–1.31 mmol/L in pure-Mg, and 0.93–1.27 mmol/L in SS group • Mg-Ag-Y alloy, composed of 1 wt. % Ag and 1 wt. % Y, occupied better elastic moduli, tensile and compressive stress than pure Mg

Table A.11. Gallium

Trace element	Ref.	Cells					Media		Protocol				Results
		Type	Species	Donor Age	Donor Sex	Passage	Basal media	Serum	Material's Form	Material's Conc.	Applications	Conditions	
Hydroxy-apatite Nanophase Co-doped with Gallium, Magnesium and Carbonate	64	ASCs	Human	NA	NA	NA	α-MEM	10% FBS & 1% PA	Doped HA materials were obtained by adding gallium nitrate ($Ga(NO_3)_3$, & magnesium chloride ($MgCl_2$) in the alkaline suspension, whereas calcium bicarbonate ($NaHCO_3$, was dropped with the phosphoric acid solution	3 different gallium-doped apatite (GaHAs) were prepared, with nominal X_{Ga} (where X_{Ga} is the molar ratio Ga/Ca) equal to 0.025, 0.05, and 0.1. Also, two different multi-substituted materials were prepared with X_{Ga}= 0.25 and 0.5, X_{Mg}= 0.1 (where X_{Mg} is the molar ratio Mg/Ca) and X_{CO}= 0.1 (where $X_{CO}3$ is the molar ratio CO3/PO4)	24hrs. after the cell seeding, 2 different conc. (50 and 500 μg/mL) of nanoparticles (Ga-HA-2, Ga-MCHA-2, and HA) were added and the cells left in culture for 14 days.	NA	• Enhancement in cell proliferation induced by the presence of Ga, in detail Ga-MCHA-2 at the highest concentration starting from day 3 with respect to HA group. • The results show no changes in cell morphology induced by the presence of the foreign ions Ga, Mg and CO3 in the apatite structure. • The ALP activity was up-regulated by the presence of the highest concentration of Ga-MCHA-2 only at day 14 with respect to Ga-HA-2 and HA used as control group. • The doping with gallium was effective in inducing antibacterial effect against some bacterial strains, without reducing the viability of human cells

Table A.11. Gallium (cont.)

Gallium Nitride (GaN) Nanopores	65	hMSCs	Human	NA	NA	hMSCs used in the experiments were at passage 3–7.	MSCGM	NA	The GaN films were grown on c-plane sapphire substrate using a 2-step growth procedure. While the nonporous GaN films were fabricated by electrochemical etching.	In our experiments, the doping concentration of GaN was fixed at $5x10^{18}$ cm^{-3}.	Cells were cultured both on plain GaN films and nanoporous GaN films with different pore sizes. 2000 cells were seeded in each hole. The whole devices were incubated for 4 hrs. and 24 hrs.	NA	• GaN films with nanopores of 30 nm most effectively supported osteogenic differentiation • hMSCs on GaN films with 30 nm nanopores (26% porosity) showed the largest spreading area, while those on GaN films with 80 nm nanopores (60% porosity) showed the largest elongation.
Ga-containing phosphate glasses (GPGs)	66	BMSCs	Mouse	NA	NA	Passage 5 is used in the experiment	H-DMEM	10% FBS	The β-TCP powders (d_{50} = 3.0 μm) and GPGs powders (d_{50} = 5.4 μm) were obtained by solid-phase reaction and melt-quenching method	Three different GPGs (GPG1, GPG2, and GPG3) powders were prepared *The honeycomb bio ceramic scaffolds without GPGs additive were named as TCP, and those with GPGs additives were designated as TCP-GPGs; that is, the scaffolds with GPG1, GPG2, and GPG3 additives were designated as TCP-GPG1, TCP-GPG2, & TCP-GPG3*	The Cells were seeded into the 96-well plate with a density of $2×10^3$ cells per well. After incubation for 1 day, the media were replaced by the bio ceramic extracts and incubated for 3-14 days.	NA	• For the cells treated with the extracts of TCP, TCP-GPG1, and TCP-GPG2, the cells highly elongated and completely spread, however, very few cells were present in the TCPGPG3 extract, and most cells did not fully spread. • After culturing for 3 and 5 days, the best cell proliferation was shown in TCP-GPG1, followed by TCP-GPG2. The cell number in TCP-GPG3 extract was significantly lower than TCP extract. • At the 7th and 14th days, the mBMSCs cultured in the TCP-GPGs extracts showed obviously lower ALP activity than those in the TCP extract. • Compared with TCP extract, the mBMSCs cultured in TCP-GPGs extracts expressed distinctively lower level of Col I, Runx2, and OPN and as for the mBMSCs treated with TCP-GPGs extracts containing greater amount of Ga (TCP-GPG1 < TCP-GPG2 < TCP-

Table A.11. Gallium (cont.)

													GPG3), lower expressions of Col I, OPN, and Runx2 were detected (TCP-GPG1 > TCP-GPG2 > TCP-GPG3) • The OCN expression of cells in TCP-GPG1 and TCP-GPG2 extracts was significantly higher than that in TCP and TCP-GPG3 extracts. • The cells treated by TCP-GPGs extracts showed remarkable decrease in expressions of NFATc1, cathepsin, TRAP, and c-Fos.

REFERENCES

1. Akdere, Ö. E., Shikhaliyeva, İ. & Gümüşderelioğlu, M. Boron mediated 2D and 3D cultures of adipose derived mesenchymal stem cells. *Cytotechnology* **71**, 611–622 (2019).

2. Apdik, H., Doğan, A., Demirci, S., Aydın, S. & Şahin, F. Dose-dependent Effect of Boric Acid on Myogenic Differentiation of Human Adipose-derived Stem Cells (hADSCs). *Biol. Trace Elem. Res.* **165**, 123–130 (2015).

3. Li, X. *et al.* Boron nitride nanotube-enhanced osteogenic differentiation of mesenchymal stem cells. *J. Biomed. Mater. Res. B Appl. Biomater.* **104**, 323–329 (2016).

4. Abdik, E. A., Abdik, H., Taşlı, P. N., Deniz, A. A. H. & Şahin, F. Suppressive Role of Boron on Adipogenic Differentiation and Fat Deposition in Human Mesenchymal Stem Cells. *Biol. Trace Elem. Res.* **188**, 384–392 (2019).

5. Demirci, S., Doğan, A., Şişli, B. & Sahin, F. Boron increases the cell viability of mesenchymal stem cells after long-term cryopreservation. *Cryobiology* **68**, 139–146 (2014).

6. Ciofani, G. *et al.* Effects of barium titanate nanoparticles on proliferation and differentiation of rat mesenchymal stem cells. *Colloids Surf. B Biointerfaces* **102**, 312–320 (2013).

7. Rocca, A. *et al.* Barium titanate nanoparticles and hypergravity stimulation improve differentiation of mesenchymal stem cells into osteoblasts. *Int. J. Nanomedicine* **10**, 433–445 (2015).

8. Li, Y. *et al.* Electroactive BaTiO3 nanoparticle-functionalized fibrous scaffolds enhance osteogenic differentiation of mesenchymal stem cells. *Int. J. Nanomedicine* **12**, 4007–4018 (2017).

9. Ahn), (Ki Hoon *et al.* Barium Stimulates the Expression of Osteogenic Genes in Human Mesenchymal Stem Cells into Osteoblasts in vitro. 대한폐경학회지 **17**, 81–87 (2011).

10. Teti, G. *et al.* The Hypoxia-Mimetic Agent Cobalt Chloride Differently Affects Human Mesenchymal Stem Cells in Their Chondrogenic Potential. *Stem Cells International* https://www.hindawi.com/journals/sci/2018/3237253/ (2018) doi:10.1155/2018/3237253.

11. Yoo, H. I., Moon, Y. H. & Kim, M. S. Effects of CoCl2 on multi-lineage differentiation of C3H/10T1/2 mesenchymal stem cells. *Korean J. Physiol. Pharmacol. Off. J. Korean Physiol. Soc. Korean Soc. Pharmacol.* **20**, 53–62 (2016).

12. Kwak, J. *et al.* Cobalt Chloride Enhances the Anti-Inflammatory Potency of Human Umbilical Cord Blood-Derived Mesenchymal Stem Cells through the ERK-HIF-1α-MicroRNA-146a-Mediated Signaling Pathway. *Stem Cells Int.* **2018**, (2018).

13. Marycz, K. *et al.* The Effect of Co0.2Mn0.8Fe2O4 Ferrite Nanoparticles on the C2 Canine Mastocytoma Cell Line and Adipose-Derived Mesenchymal Stromal Stem Cells (ASCs) Cultured Under a Static Magnetic Field: Possible Implications in the Treatment of Dog Mastocytoma. *Cell. Mol. Bioeng.* **10**, 209–222 (2017).

14. Focaroli, S., Teti, G., Salvatore, V., Orienti, I. & Falconi, M. Calcium/Cobalt Alginate Beads as Functional Scaffolds for Cartilage Tissue Engineering. *Stem Cells Int.* **2016**, (2016).

15. Palombella, S. *et al.* Effects of Metal Micro and Nano-Particles on hASCs: An In Vitro Model. *Nanomaterials* **7**, (2017).

16. Littmann, E. *et al.* Cobalt-containing bioactive glasses reduce human mesenchymal stem cell chondrogenic differentiation despite HIF-1α stabilisation. *J. Eur. Ceram. Soc.* **38**, 877–886 (2018).

17. Schröck, K. *et al.* Co(II)-mediated effects of plain and plasma immersion ion implanted cobalt-chromium alloys on the osteogenic differentiation of human mesenchymal stem cells. *J. Orthop. Res.* **33**, 325–333 (2015).

18. Logan, N. *et al.* TiO2-coated CoCrMo: Improving the osteogenic differentiation and adhesion of mesenchymal stem cells in vitro. *J. Biomed. Mater. Res. A* **103**, 1208–1217 (2015).

19. Jaatinen, L., Salemi, S., Miettinen, S., Hyttinen, J. & Eberli, D. The Combination of Electric Current and Copper Promotes Neuronal Differentiation of Adipose-Derived Stem Cells. *Ann. Biomed. Eng.* **43**, 1014–1023 (2015).

20. Bostancioglu, R. B. *et al.* Adhesion profile and differentiation capacity of human adipose tissue derived mesenchymal stem cells grown on metal ion (Zn, Ag and Cu) doped hydroxyapatite nano-coated surfaces. *Colloids Surf. B Biointerfaces* **155**, 415–428 (2017).

21. Telgerd, M. D. *et al.* Enhanced osteogenic differentiation of mesenchymal stem cells on metal–organic framework based on copper, zinc, and imidazole coated poly-l-lactic acid nanofiber scaffolds. *J. Biomed. Mater. Res. A* **107**, 1841–1848 (2019).

22. Li, S. *et al.* Inhibition of osteogenic differentiation of mesenchymal stem cells by copper supplementation. *Cell Prolif.* **47**, 81–90 (2014).

23. Xu, C. *et al.* Promotion of chondrogenic differentiation of mesenchymal stem cells by copper: Implications for new cartilage repair biomaterials. *Mater. Sci. Eng. C* **93**, 106–114 (2018).

24. Rodríguez, J. P., Ríos, S. & González, M. Modulation of the proliferation and differentiation of human mesenchymal stem cells by copper. *J. Cell. Biochem.* **85**, 92–100 (2002).

25. Rath, S. N. *et al.* Bioactive Copper-Doped Glass Scaffolds Can Stimulate Endothelial Cells in Co-Culture in Combination with Mesenchymal Stem Cells. *PLOS ONE* **9**, e113319 (2014).

26. Hu, Y., Du, Y., Jiang, H. & Jiang, G.-S. Cerium promotes bone marrow stromal cells migration and osteogenic differentiation via Smad1/5/8 signaling pathway. *Int. J. Clin. Exp. Pathol.* **7**, 5369–5378 (2014).

27. Liu, D.-D., Zhang, J.-C., Zhang, Q., Wang, S.-X. & Yang, M.-S. TGF-β/BMP signaling pathway is involved in cerium-promoted osteogenic differentiation of mesenchymal stem cells. *J. Cell. Biochem.* **114**, 1105–1114 (2013).

28. Rocca, A., Mattoli, V., Mazzolai, B. & Ciofani, G. Cerium Oxide Nanoparticles Inhibit Adipogenesis in Rat Mesenchymal Stem Cells: Potential Therapeutic Implications. *Pharm. Res.* **31**, 2952–2962 (2014).

29. Gliga, A. R. *et al.* Cerium oxide nanoparticles inhibit differentiation of neural stem cells. *Sci. Rep.* **7**, 1–20 (2017).

30. Xiang, J. *et al.* Cerium Oxide Nanoparticle Modified Scaffold Interface Enhances Vascularization of Bone Grafts by Activating Calcium Channel of Mesenchymal Stem Cells. *ACS Appl. Mater. Interfaces* **8**, 4489–4499 (2016).

31. Li, K. *et al.* Incorporation of Cerium Oxide into Hydroxyapatite Coating Protects Bone Marrow Stromal Cells Against H2O2-Induced Inhibition of Osteogenic Differentiation. *Biol. Trace Elem. Res.* **182**, 91–104 (2018).

32. Peng, S. *et al.* Strontium Promotes Osteogenic Differentiation of Mesenchymal Stem Cells Through the Ras/MAPK Signaling Pathway. *Cell. Physiol. Biochem.* **23**, 165–174 (2009).

33. Yang, F. *et al.* Strontium Enhances Osteogenic Differentiation of Mesenchymal Stem Cells and In Vivo Bone Formation by Activating Wnt/Catenin Signaling. *STEM CELLS* **29**, 981–991 (2011).

34. Li, Y. *et al.* Effects of strontium on proliferation and differentiation of rat bone marrow mesenchymal stem cells. *Biochem. Biophys. Res. Commun.* **418**, 725–730 (2012).

35. Nardone, V. *et al.* In Vitro Effects of Strontium on Proliferation and Osteoinduction of Human Preadipocytes. *Stem Cells International* https://www.hindawi.com/journals/sci/2015/871863/ (2015) doi:10.1155/2015/871863.

36. Aimaiti, A. *et al.* Low-dose strontium stimulates osteogenesis but high-dose doses cause apoptosis in human adipose-derived stem cells via regulation of the ERK1/2 signaling pathway. *Stem Cell Res. Ther.* **8**, 282 (2017).

37. Chandran, S. *et al.* Strontium Hydroxyapatite scaffolds engineered with stem cells aid osteointegration and osteogenesis in osteoporotic sheep model. *Colloids Surf. B Biointerfaces* **163**, 346–354 (2018).

38. Mohan, B. G., Suresh Babu, S., Varma, H. K. & John, A. In vitro evaluation of bioactive strontium-based ceramic with rabbit adipose-derived stem cells for bone tissue regeneration. *J. Mater. Sci. Mater. Med.* **24**, 2831–2844 (2013).

39. Leite, Á. J., Gonçalves, A. I., Rodrigues, M. T., Gomes, M. E. & Mano, J. F. Strontium-Doped Bioactive Glass Nanoparticles in Osteogenic Commitment. *ACS Appl. Mater. Interfaces* **10**, 23311–23320 (2018).

40. Schmidt, A., Steinritz, D., Rothmiller, S., Thiermann, H. & Scherer, A. M. Effects of sulfur mustard on mesenchymal stem cells. *Toxicol. Lett.* **293**, 98–104 (2018).

41. Schmidt, A., Scherer, M., Thiermann, H. & Steinritz, D. Mesenchymal stem cells are highly resistant to sulfur mustard. *Chem. Biol. Interact.* **206**, 505–511 (2013).

42. Schreier, C. *et al.* Mobilization of human mesenchymal stem cells through different cytokines and growth factors after their immobilization by sulfur mustard. *Toxicol. Lett.* **293**, 105–111 (2018).

43. Nejad-Moghaddam, A. *et al.* Adipose-Derived Mesenchymal Stem Cells for Treatment of Airway Injuries in A Patient after Long-Term Exposure to Sulfur Mustard. *Cell J. Yakhteh* **19**, 117–126 (2017).

44. Wang, X. *et al.* Silicon-Enhanced Adipogenesis and Angiogenesis for Vascularized Adipose Tissue Engineering. *Adv. Sci.* **5**, (2018).

45. Huang, T.-H. *et al.* Substitutions of strontium in bioactive calcium silicate bone cements stimulate osteogenic differentiation in human mesenchymal stem cells. *J. Mater. Sci. Mater. Med.* **30**, 68 (2019).

46. Kim, K. J. *et al.* Silica nanoparticles increase human adipose tissue-derived stem cell proliferation through ERK1/2 activation. *Int. J. Nanomedicine* **10**, 2261–2272 (2015).

47. Mousavi, M. *et al.* The interaction of silica nanoparticles with catalase and human mesenchymal stem cells: biophysical, theoretical and cellular studies. *Int. J. Nanomedicine* **14**, 5355–5368 (2019).

48. Li, C. *et al.* Porous Se@SiO2 nanocomposite promotes migration and osteogenic differentiation of rat bone marrow mesenchymal stem cell to accelerate bone fracture healing in a rat model. *Int. J. Nanomedicine* **14**, 3845–3860 (2019).

49. Li, T., Li, X.-L., Hu, S.-X. & Wu, J. Enhanced osteoporotic effect of silicon carbide nanoparticles combine with nano-hydroxyapatite coated anodized titanium implant on healthy bone regeneration in femoral fracture. *J. Photochem. Photobiol. B* **197**, 111515 (2019).

50. Gastaldi, G. *et al.* Human adipose-derived stem cells (hASCs) proliferate and differentiate in osteoblast-like cells on trabecular titanium scaffolds. *J. Biomed. Mater. Res. A* **94A**, 790–799 (2010).

51. Benazzo, F. *et al.* Trabecular titanium can induce in vitro osteogenic differentiation of human adipose derived stem cells without osteogenic factors. *J. Biomed. Mater. Res. A* **102**, 2061–2071 (2014).

52. Wang, M. L. *et al.* Titanium particles suppress expression of osteoblastic phenotype in human mesenchymal stem cells. *J. Orthop. Res.* **20**, 1175–1184 (2002).

53. Pozio, A., Palmieri, A., Girardi, A., Cura, F. & Carinci, F. Titanium nanotubes stimulate osteoblast differentiation of stem cells from pulp and adipose tissue. *Dent. Res. J.* **9**, S169–S174 (2012).

54. Kishimoto, N. *et al.* Dedifferentiated fat cells differentiate into osteoblasts in titanium fiber mesh. *Cytotechnology* **65**, 15–22 (2013).

55. Chen, P. *et al.* Adhesion and differentiation behaviors of mesenchymal stem cells on titanium with micrometer and nanometer-scale grid patterns produced by femtosecond laser irradiation. *J. Biomed. Mater. Res. A* **106**, 2735–2743 (2018).

56. Lavenus, S. *et al.* Adhesion and osteogenic differentiation of human mesenchymal stem cells on titanium nanopores. *Eur. Cell. Mater.* **22**, 84–96; discussion 96 (2011).

57. Olivares-Navarrete, R. *et al.* Direct and indirect effects of microstructured titanium substrates on the induction of mesenchymal stem cell differentiation towards the osteoblast lineage. *Biomaterials* **31**, 2728–2735 (2010).

58. Cadafalch Gazquez, G. *et al.* Flexible Yttrium-Stabilized Zirconia Nanofibers Offer Bioactive Cues for Osteogenic Differentiation of Human Mesenchymal Stromal Cells. *ACS Nano* **10**, 5789–5799 (2016).

59. Rachman, A. *et al.* Biocompatibility of Yttria-Tetragonal Zirconia Polycrystal Seeded with Human Adipose Derived Mesenchymal Stem Cell. *Acta Inform. Medica* **26**, 249–253 (2018).

60. Webster, T. J., Ergun, C., Doremus, R. H. & Bizios, R. Hydroxylapatite with substituted magnesium, zinc, cadmium, and yttrium. II. Mechanisms of osteoblast adhesion. *J. Biomed. Mater. Res.* **59**, 312–317 (2002).

61. Iskandar, M. E., Aslani, A., Tian, Q. & Liu, H. Nanostructured calcium phosphate coatings on magnesium alloys: characterization and cytocompatibility with mesenchymal stem cells. *J. Mater. Sci. Mater. Med.* **26**, 189 (2015).

62. Johnson, I., Perchy, D. & Liu, H. In vitro evaluation of the surface effects on magnesium-yttrium alloy degradation and mesenchymal stem cell adhesion. *J. Biomed. Mater. Res. A* **100A**, 477–485 (2012).

63. Yu, K. *et al.* In vitro and in vivo evaluation of novel biodegradable Mg-Ag-Y alloys for use as resorbable bone fixation implant. *J. Biomed. Mater. Res. A* **106**, 2059–2069 (2018).

64. Ballardini, A. *et al.* New hydroxyapatite nanophases with enhanced osteogenic and anti-bacterial activity. *J. Biomed. Mater. Res. A* **106**, 521–530 (2018).

65. Han, L. *et al.* Single-Crystalline, Nanoporous Gallium Nitride Films With Fine Tuning of Pore Size for Stem Cell Engineering. *J. Nanotechnol. Eng. Med.* **5**, 0410041–0410049 (2014).

66. He, F. *et al.* Modification of honeycomb bioceramic scaffolds for bone regeneration under the condition of excessive bone resorption. *J. Biomed. Mater. Res. A* **107**, 1314–1323 (2019).

BIBLIOGRAPHY

1. Baino, F., Fiorilli, S. & Vitale-Brovarone, C. Bioactive glass-based materials with hierarchical porosity for medical applications: Review of recent advances. *Acta Biomater.* **42**, 18–32 (2016).

2. Boccaccini, A. R., Brauer, D. S. & Hupa, L. *Bioactive Glasses: Fundamentals, Technology and Applications*. (Royal Society of Chemistry, 2016).

3. Hench, L. L. The story of Bioglass®. *J. Mater. Sci. Mater. Med.* **17**, 967–978 (2006).

4. Jones, J. R. Review of bioactive glass: From Hench to hybrids. *Acta Biomater.* **9**, 4457–4486 (2013).

5. Baino, F., Hamzehlou, S. & Kargozar, S. Bioactive Glasses: Where Are We and Where Are We Going? *J. Funct. Biomater.* **9**, (2018).

6. Bi, L. *et al.* Effect of bioactive borate glass microstructure on bone regeneration, angiogenesis, and hydroxyapatite conversion in a rat calvarial defect model. *Acta Biomater.* **9**, 8015–8026 (2013).

7. Fu, H. *et al.* In vitro evaluation of borate-based bioactive glass scaffolds prepared by a polymer foam replication method. *Mater. Sci. Eng. C* **29**, 2275–2281 (2009).

8. Fu, Q., Rahaman, M. N., Fu, H. & Liu, X. Silicate, borosilicate, and borate bioactive glass scaffolds with controllable degradation rate for bone tissue engineering applications. I. Preparation and in vitro degradation. *J. Biomed. Mater. Res. A* **95A**, 164–171 (2010).

9. Yao, A. *et al.* In Vitro Bioactive Characteristics of Borate-Based Glasses with Controllable Degradation Behavior. *J. Am. Ceram. Soc.* **90**, 303–306 (2007).

10. Zhang, J. *et al.* Bioactive borate glass promotes the repair of radius segmental bone defects by enhancing the osteogenic differentiation of BMSCs. *Biomed. Mater.* **10**, 065011 (2015).

11. Thyparambil, N. J. *et al.* Adult stem cell response to doped bioactive borate glass. *J. Mater. Sci. Mater. Med.* **31**, 13 (2020).

12. Hoppe, A., Güldal, N. S. & Boccaccini, A. R. A review of the biological response to ionic dissolution products from bioactive glasses and glass-ceramics. *Biomaterials* **32**, 2757–2774 (2011).

13. Jones, J. R., Sepulveda, P. & Hench, L. L. Dose-dependent behavior of bioactive glass dissolution. *J. Biomed. Mater. Res.* **58**, 720–726 (2001).

14. Hohenbild, F., Arango-Ospina, M., Moghaddam, A., Boccaccini, A. R. & Westhauser, F. Preconditioning of Bioactive Glasses before Introduction to Static Cell Culture: What Is Really Necessary? *Methods Protoc.* **3**, (2020).

15. Lakhkar, N. J. *et al.* Bone formation controlled by biologically relevant inorganic ions: Role and controlled delivery from phosphate-based glasses. *Adv. Drug Deliv. Rev.* **65**, 405–420 (2013).

16. Saranti, A., Koutselas, I. & Karakassides, M. A. Bioactive glasses in the system CaO–B2O3–P2O5: Preparation, structural study and in vitro evaluation. *J. Non-Cryst. Solids* **352**, 390–398 (2006).

17. Li, A. *et al.* In vitro evaluation of a novel pH neutral calcium phosphosilicate bioactive glass that does not require preconditioning prior to use. *Int. J. Appl. Glass Sci.* **8**, 403–411 (2017).

18. Zhang, Y. & Santos, J. D. Crystallization and microstructure analysis of calcium phosphate-based glass ceramics for biomedical applications. *J. Non-Cryst. Solids* **272**, 14–21 (2000).

19. Massera, J. *et al.* Processing and characterization of novel borophosphate glasses and fibers for medical applications. *J. Non-Cryst. Solids* **425**, 52–60 (2015).

20. Mishra, A. *et al.* In-vitro dissolution characteristics and human adipose stem cell response to novel borophosphate glasses. *J. Biomed. Mater. Res. A* **107**, 2099–2114 (2019).

21. Gimble Jeffrey M., Katz Adam J., & Bunnell Bruce A. Adipose-Derived Stem Cells for Regenerative Medicine. *Circ. Res.* **100**, 1249–1260 (2007).

22. Skalnaya, M. G. & Skalny, A. V. ESSENTIAL TRACE ELEMENTS IN HUMAN HEALTH: A PHYSICIAN'S VIEW. 224.

23. Caplan, A. I. Adult mesenchymal stem cells for tissue engineering versus regenerative medicine. *J. Cell. Physiol.* **213**, 341–347 (2007).

24. Gimble, J. M., Bunnell, B. A., Chiu, E. S. & Guilak, F. Concise Review: Adipose-Derived Stromal Vascular Fraction Cells and Stem Cells: Let's Not Get Lost in Translation. *STEM CELLS* **29**, 749–754 (2011).

25. Sabol, R. A. *et al.* Therapeutic Potential of Adipose Stem Cells. in 1–11 (Springer US). doi:10.1007/5584_2018_248.

26. Uccelli, A., Moretta, L. & Pistoia, V. Mesenchymal stem cells in health and disease. *Nat. Rev. Immunol.* **8**, 726–736 (2008).

27. Blaber, S. P. *et al.* Analysis of in vitro secretion profiles from adipose-derived cell populations. *J. Transl. Med.* **10**, 172 (2012).

28. Kilroy, G. E. *et al.* Cytokine profile of human adipose-derived stem cells: Expression of angiogenic, hematopoietic, and pro-inflammatory factors. *J. Cell. Physiol.* **212**, 702–709 (2007).

29. Lombardi, F. *et al.* Secretome of Adipose Tissue-Derived Stem Cells (ASCs) as a Novel Trend in Chronic Non-Healing Wounds: An Overview of Experimental In Vitro and In Vivo Studies and Methodological Variables. *Int. J. Mol. Sci.* **20**, 3721 (2019).

30. Al-Ghadban, S. & Bunnell, B. A. Adipose Tissue-Derived Stem Cells: Immunomodulatory Effects and Therapeutic Potential. *Physiology* **35**, 125–133 (2020).

31. Chacón-Martínez, C. A., Koester, J. & Wickström, S. A. Signaling in the stem cell niche: regulating cell fate, function and plasticity. *Development* **145**, (2018).

32. Chi, J.-T. *et al.* Endothelial cell diversity revealed by global expression profiling. *Proc. Natl. Acad. Sci.* **100**, 10623–10628 (2003).

33. Lovett, M., Lee, K., Edwards, A. & Kaplan, D. L. Vascularization Strategies for Tissue Engineering. *Tissue Eng. Part B Rev.* **15**, 353–370 (2009).

34. Balasubramanian, P. *et al.* Angiogenic potential of boron-containing bioactive glasses: in vitro study. *J. Mater. Sci.* **52**, 8785–8792 (2017).

35. Kaur, G. *et al.* A review of bioactive glasses: Their structure, properties, fabrication and apatite formation. *J. Biomed. Mater. Res. A* **102**, 254–274 (2014).

36. Pajares-Chamorro, N. & Chatzistavrou, X. Bioactive Glass Nanoparticles for Tissue Regeneration. *ACS Omega* **5**, 12716–12726 (2020).

37. Rahaman, M. N. *et al.* Bioactive glass in tissue engineering. *Acta Biomater.* **7**, 2355–2373 (2011).

38. Mehrabi, T., Mesgar, A. S. & Mohammadi, Z. Bioactive Glasses: A Promising Therapeutic Ion Release Strategy for Enhancing Wound Healing. *ACS Biomater. Sci. Eng.* **6**, 5399–5430 (2020).

39. Huang, W., Day, D. E., Kittiratanapiboon, K. & Rahaman, M. N. Kinetics and mechanisms of the conversion of silicate (45S5), borate, and borosilicate glasses to hydroxyapatite in dilute phosphate solutions. *J. Mater. Sci. Mater. Med.* **17**, 583–596 (2006).

40. Apdik, H., Doğan, A., Demirci, S., Aydın, S. & Şahin, F. Dose-dependent Effect of Boric Acid on Myogenic Differentiation of Human Adipose-derived Stem Cells (hADSCs). *Biol. Trace Elem. Res.* **165**, 123–130 (2015).

41. Kargozar, S., Baino, F., Hamzehlou, S., Hill, R. G. & Mozafari, M. Bioactive Glasses: Sprouting Angiogenesis in Tissue Engineering. *Trends Biotechnol.* **36**, 430–444 (2018).

42. Qazi, T. H. *et al.* Comparison of the effects of 45S5 and 1393 bioactive glass microparticles on hMSC behavior. *J. Biomed. Mater. Res. A* **105**, 2772–2782 (2017).

43. Carta, D. *et al.* The effect of composition on the structure of sodium borophosphate glasses. *J. Non-Cryst. Solids* **354**, 3671–3677 (2008).

44. Bacakova, L. *et al.* Stem cells: their source, potency and use in regenerative therapies with focus on adipose-derived stem cells – a review. *Biotechnol. Adv.* **36**, 1111–1126 (2018).

45. Gimble, J. M. Adipose tissue derived stem cells secretome: soluble factors and their roles in regenerative medicine.

46. Mussano, F. *et al.* Cytokine, Chemokine, and Growth Factor Profile Characterization of Undifferentiated and Osteoinduced Human Adipose-Derived Stem Cells. *Stem Cells International* vol. 2017 e6202783 https://www.hindawi.com/journals/sci/2017/6202783/ (2017).

47. ISO 10993-5:2009(en), Biological evaluation of medical devices — Part 5: Tests for in vitro cytotoxicity. https://www.iso.org/obp/ui/#iso:std:iso:10993:-5:ed-3:v1:en.

48. Baek, S. J., Kang, S. K. & Ra, J. C. In vitro migration capacity of human adipose tissue-derived mesenchymal stem cells reflects their expression of receptors for chemokines and growth factors. *Exp. Mol. Med.* **43**, 596–603 (2011).

49. Vuornos, K. *et al.* Bioactive glass ions induce efficient osteogenic differentiation of human adipose stem cells encapsulated in gellan gum and collagen type I hydrogels. *Mater. Sci. Eng. C* **99**, 905–918 (2019).

50. Ojansivu, M. *et al.* The effect of S53P4-based borosilicate glasses and glass dissolution products on the osteogenic commitment of human adipose stem cells. *PLOS ONE* **13**, e0202740 (2018).

51. Ojansivu, M. *et al.* Bioactive glass induced osteogenic differentiation of human adipose stem cells is dependent on cell attachment mechanism and mitogen-activated protein kinases. *Eur. Cell. Mater.* **35**, 54–72 (2018).

52. Thyparambil, N. J. *et al.* Bioactive borate glass triggers phenotypic changes in adipose stem cells. *J. Mater. Sci. Mater. Med.* **31**, 35 (2020).

53. Lucas, B. de, Pérez, L. M. & Gálvez, B. G. Importance and regulation of adult stem cell migration. *J. Cell. Mol. Med.* **22**, 746–754 (2018).

54. Han, T., Stone-Weiss, N., Huang, J., Goel, A. & Kumar, A. Machine learning as a tool to design glasses with controlled dissolution for healthcare applications. *Acta Biomater.* (2020) doi:10.1016/j.actbio.2020.02.037.

55. Policha, Aleksandra, et al. "Endothelial differentiation of diabetic adipose-derived stem cells." journal of surgical research 192.2 (2014): 656-663.

56. Mathew, Suja Ann, and Ramesh Bhonde. "Mesenchymal stromal cells isolated from gestationally diabetic human placenta exhibit insulin resistance, decreased clonogenicity and angiogenesis." Placenta 59 (2017): 1-8.

57. Cheng, Nai-Chen, et al. "High glucose-induced reactive oxygen species generation promotes stemness in human adipose-derived stem cells." Cytotherapy 18.3 (2016): 371-383.

58. Dentelli, Patrizia, et al. "A diabetic milieu promotes OCT4 and NANOG production in human visceral-derived adipose stem cells." Diabetologia 56.1 (2013): 173-184.

59. Acosta, Lourdes, et al. "Adipose mesenchymal stromal cells isolated from type 2 diabetic patients display reduced fibrinolytic activity." Diabetes 62.12 (2013): 4266-4269.

60. Rennert, Robert C., et al. "Diabetes impairs the angiogenic potential of adipose-derived stem cells by selectively depleting cellular subpopulations." Stem cell research & therapy 5.3 (2014): 79.

61. Minteer, Danielle Marie, et al. "Analysis of type II diabetes mellitus adipose-derived stem cells for tissue engineering applications." Journal of tissue engineering 6 (2015): 2041731415579215.

62. Dzhoyashvili, Nina A., et al. "Disturbed angiogenic activity of adipose-derived stromal cells obtained from patients with coronary artery disease and diabetes mellitus type 2." Journal of translational medicine 12.1 (2014): 337.

63. Yaochite, Juliana Navarro Ueda, et al. "Multipotent mesenchymal stromal cells from patients with newly diagnosed type 1 diabetes mellitus exhibit preserved in vitro and in vivo immunomodulatory properties." Stem cell research & therapy 7.1 (2016): 14.

64. Hajer, Gideon R., Timon W. van Haeften, and Frank LJ Visseren. "Adipose tissue dysfunction in obesity, diabetes, and vascular diseases." European heart journal 29.24 (2008): 2959-2971.

65. Gu, Ja Hea, et al. "Neovascular potential of adipose-derived stromal cells (ASCs) from diabetic patients." Wound Repair and Regeneration 20.2 (2012): 243-252.

66. Mahmoud, Marwa, et al. "Impact of diabetes mellitus on human mesenchymal stromal cell biology and functionality: Implications for autologous transplantation." Stem Cell Reviews and Reports 15.2 (2019): 194-217.

67. Ali, Fatima, Fehmina Aziz, and Nadia Wajid. "Effect of type 2 diabetic serum on the behavior of Wharton's jelly-derived mesenchymal stem cells in vitro." Chronic diseases and translational medicine 3.2 (2017): 105-111.

68. Phadnis, Smruti M., et al. "Mesenchymal stem cells derived from bone marrow of diabetic patients portrait unique markers influenced by the diabetic microenvironment." The review of diabetic studies: RDS 6.4 (2009): 260.

69. Rezabakhsh, Aysa, et al. "Type 2 diabetes inhibited human mesenchymal stem cells angiogenic response by over-activity of the autophagic pathway." Journal of cellular biochemistry 118.6 (2017): 1518-1530.

70. Hankamolsiri, Weerawan, et al. "The effects of high glucose on adipogenic and osteogenic differentiation of gestational tissue-derived MSCs." Stem cells international 2016 (2016).

71. Wajid, Nadia, et al. "The effect of gestational diabetes on proliferation capacity and viability of human umbilical cord-derived stromal cells." Cell and tissue banking 16.3 (2015): 389-397.

72. Cronk, Stephen M., et al. "Adipose-derived stem cells from diabetic mice show impaired vascular stabilization in a murine model of diabetic retinopathy." Stem cells translational medicine 4.5 (2015): 459-467.

73. Cianfarani, Francesca, et al. "Diabetes impairs adipose tissue–derived stem cell function and efficiency in promoting wound healing." Wound repair and regeneration 21.4 (2013): 545-553.Han, T., Stone-Weiss, N., Huang, J., Goel, A. & Kumar, A. Machine learning as a tool to design glasses with controlled dissolution for healthcare applications. *Acta Biomater.* (2020) doi:10.1016/j.actbio.2020.02.037.

VITA

Nada Abokefa earned her Bachelor's in Biotechnology/Biomolecular chemistry from Faculty of Science, Cairo University, Egypt in May 2018. She worked on Trans-Differentiation of Adipose-Derived Stem Cells in her graduation project. She joined Missouri University of Science and Technology in Fall 2019 for her master's degree. Nada worked as a graduate teaching assistant for the comparative vertebrate anatomy, microbiology, and cell biology labs. She received the graduate research funding award from the biological science department at Missouri S&T in the spring of 2020. She received her master's degree in Applied and Environmental Biology from Missouri University of Science and Technology in May 2021.